

ผลของกรดอัลฟาไลโปอิกและสารประกอบเชิงซ้อนของกรดอัลฟาไลโปอิกกับโพลีโรแทกแซนส์

ในการป้องกันการทำลายดีเอ็นเอโดยซิสพลาติน และกลไกการเหนี่ยวนำการตาย

แบบอะพอพโทติกในเซลล์มะเร็งปอดของคน



นางสาว จิรพันธ์ ม่วงเจริญ

สถาบันวิทยบริการ

วิทยานิพนธ์นี้เป็นส่วนหนึ่งของการศึกษาตามหลักสูตรปริญญาวิทยาศาสตรดุษฎีบัณฑิต

สาขาวิชาเทคโนโลยีสารสนเทศ

คณะเภสัชศาสตร์ จุฬาลงกรณ์มหาวิทยาลัย

ปีการศึกษา 2549

ลิขสิทธิ์ของจุฬาลงกรณ์มหาวิทยาลัย

**PROTECTIVE EFFECTS OF  $\alpha$ -LIPOIC ACID AND  
ITS POLYROTAXANES COMPLEXES AGAINST CISPLATIN INDUCED  
DNA DAMAGE AND ITS APOPTOTIC MECHANISM INDUCING  
IN HUMAN LUNG EPITHERIAL CANCER CELLS**



Miss Jirapan Moungjaroen

สถาบันวิทยบริการ  
A Dissertation Submitted in Partial Fulfillment of the Requirements  
for the Degree of Doctor of Philosophy Program in Pharmaceutical Technology

Faculty of Pharmaceutical Sciences

Chulalongkorn University

Academic Year 2006

Copyright of Chulalongkorn University

Thesis Title            PROTECTIVE EFFECTS OF  $\alpha$ -LIPOIC ACID AND ITS  
POLYROTAXANES COMPLEXES AGAINST CISPLATIN  
INDUCED DNA DAMAGE AND ITS APOPTOTIC  
MECHANISM INDUCING IN HUMAN LUNG  
EPITHELIAL CANCER CELLS

By                            Miss Jirapan Mounjaroen


Field of study            Pharmaceutical Technology

Thesis Advisor           Associate Professor Ubonthip Nimmannit, Ph.D.

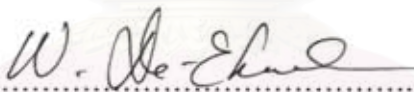
Thesis Co-advisor      Professor Patrick S. Callery, Ph.D.  
Associate Professor Vimolmas Lipipun, Ph.D.


---

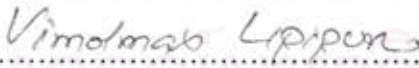
Accepted by the Faculty of Pharmaceutical Sciences, Chulalongkorn  
University in Partial Fulfillment of the Requirements for the Doctor's Degree


 ..... Dean of the Faculty of Pharmaceutical Sciences  
(Associate Professor Pornpen Pramyothin, Ph.D.)

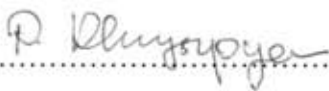
#### THESIS COMMITTEE

 ..... Chairman  
(Associate Professor Wanchai De-Eknamkul, Ph.D.)

 ..... Thesis Advisor  
(Associate Professor Ubonthip Nimmannit, Ph.D.)

 ..... Thesis Co-advisor  
(Associate Professor Vimolmas Lipipun, Ph.D. )

 ..... Member  
(Associate Professor Parkpoom Tengamnuay, Ph.D.)

 ..... Member  
(Prapaipat Klungsupaya, Ph.D. )

จิรพันธ์ ม่วงเจริญ: ผลของกรดอัลฟาไลโปอิกและสารประกอบเชิงซ้อนของกรดอัลฟาไลโปอิกกับโพลีโรแทกแซนส์ในการป้องกันการทำลายดีเอ็นเอโดยซิสพลาติน และกลไกการเหนี่ยวนำการตายแบบอะพอพโตติกในเซลล์มะเร็งปอดของคน (PROTECTIVE EFFECTS OF  $\alpha$ -LIPOIC ACID AND ITS POLYROTAXANES COMPLEXES AGAINST CISPLATIN INDUCED DNA DAMAGE AND ITS APOPTOTIC MECHANISM INDUCING IN HUMAN LUNG EPITHELIAL CANCER CELLS). อ. ที่ปรึกษา: รศ.ดร. อุบลทิพย์ นิมมานนิตย์, อ.ที่ปรึกษาร่วม: ศ.ดร. Patrick S Callery, รศ. ดร. วิมลมาศ ลิปิพันธ์, 168 หน้า.

กรดอัลฟาไลโปอิกเป็นสารต่อต้านอนุมูลอิสระที่เกิดขึ้นเองตามธรรมชาติพบในไมโตคอนเดรียของพืชและมนุษย์ กรดอัลฟาไลโปอิกสกัดได้จากผักปวยเล้ง (*Spinacea oleracea*) นำมาเตรียมเป็นสารประกอบเชิงซ้อนกับโพลีโรแทกแซนส์เพื่อเพิ่มการซึมผ่านผิวหนังและป้องกันการทำลายดีเอ็นเอ ในการศึกษาที่ใช้ดีเอ็นเอสายคู่ เซลล์มะเร็งปอด H-460 และเซลล์ไฟโบรบลาสต์ของผิวหนัง ผลการวิจัยพบว่ากรดไลโปอิกสามารถป้องกันการถูกทำลายของดีเอ็นเอสายคู่ได้และป้องกันการเกิดสารประกอบดีเอ็นเอ แพลททินัมซึ่งเป็นสาเหตุสำคัญของการเกิดความเป็นพิษต่อเซลล์ นอกจากนี้กรดอัลฟาไลโปอิกสามารถซ่อมแซมดีเอ็นเอที่ถูกทำลายให้กลับคืนสู่สภาพเดิมได้ดีกว่าสารต้านอนุมูลอิสระอื่นๆ เพื่อเพิ่มประสิทธิภาพในการซึมผ่านผิวหนังชั้นสตราตัมคอร์เนียมของกรดอัลฟาไลโปอิกจึงได้พัฒนากรดอัลฟาไลโปอิกให้อยู่ในรูปของสารประกอบเชิงซ้อนกรดอัลฟาไลโปอิกโพลีโรแทกแซนส์ และสารประกอบเชิงซ้อนกรดอัลฟาไลโปอิกโพลีโรแทกแซนส์คลอโรเรสเดอรอล ศึกษาเปรียบเทียบการซึมผ่านผิวหนังชั้นสตราตัมคอร์เนียมมนุษย์ของกรดอัลฟาไลโปอิกนอกร่างโดยใช้ฟรานซ์ดีฟิวชันเซลล์ พบว่าโพลีโรแทกแซนส์เพิ่มความสามารถในการซึมผ่านผิวหนังของกรดไลโปอิกได้ดีกว่าสารละลายกรดไลโปอิก และโพลีโรแทกแซนส์คลอโรเรสเดอรอลเพิ่มการซึมผ่านของกรดอัลฟาไลโปอิกมากกว่าเมื่อเปรียบเทียบกับโพลีโรแทกแซนส์ ผลการศึกษาความเป็นพิษในเซลล์ไฟโบรบลาสต์พบว่าสารประกอบเชิงซ้อนกรดอัลฟาไลโปอิกโพลีโรแทกแซนส์และสารประกอบเชิงซ้อนกรดอัลฟาไลโปอิกโพลีโรแทกแซนส์คลอโรเรสเดอรอลไม่ก่อให้เกิดความเป็นพิษต่อเซลล์ อีกทั้งยังสามารถช่วยในการเจริญเติบโตของเซลล์อีกด้วย สูตรตำรับทั้งสองที่ได้ถูกพัฒนาขึ้นจึงมีความเหมาะสมที่จะนำไปใช้ในผลิตภัณฑ์ภายนอกสำหรับผิวหนัง เพื่อช่วยเพิ่มการซึมผ่านของกรดอัลฟาไลโปอิกเข้าสู่ผิวหนัง ในการศึกษาผลของกรดอัลฟาไลโปอิกพบว่ากรดอัลฟาไลโปอิกยังทำหน้าที่เป็นโปรออกซิแดนซ์ เหนี่ยวนำให้เกิดการสร้างอนุมูลอิสระ และกระตุ้นการทำงานของแคสเปส 9 เป็นสาเหตุให้เกิดการลดลงของโปรตีน Bcl-2 ในไมโตคอนเดรีย และทำให้เกิดการตายแบบอะพอพโตซิสของเซลล์มะเร็ง H-460 อีกด้วย ดังนั้นกรดอัลฟาไลโปอิกจึงมีบทบาทใหม่ที่พบว่าเป็นโปรออกซิแดนซ์ในการทำให้เกิดการตายแบบอะพอพโตซิสในการรักษาโรคมะเร็ง

ลายมือชื่อนิสิต.....

สาขาวิชาเทคโนโลยีเภสัชกรรมนานาชาติ

ลายมือชื่ออาจารย์ที่ปรึกษา.....

ปีการศึกษา 2549

ลายมือชื่ออาจารย์ที่ปรึกษาร่วม.....



#4476951933: MAJOR PHARMACEUTICAL TECHNOLOGY (INTERNATIONAL) PROGRAM  
KEY WORD: LIPOIC ACID/ PROOXIDANT/ POLYROTAXANES/ DNA/ CISPLATIN

**JIRAPAN MOUNGJAROEN: PROTECTIVE EFFECTS OF  $\alpha$ -LIPOIC ACID AND ITS POLYROTAXANES COMPLEXES AGAINST CISPLATIN INDUCED DNA DAMAGE AND ITS APOPTOTIC MECHANISM INDUCING IN HUMAN LUNG EPITHELIAL CANCER CELLS, THESIS ADVISOR: ASSOC. PROF. UBONTHIP NIMMANNIT, Ph.D. THESIS COADVISOR: PROF. PATRIC S. CALLERY, Ph. D., ASSOC. PROF. VIMOLMAS LIPIPUN, Ph.D. 168 pp.**

$\alpha$ -Lipoic acid(LA) is a naturally-occurring antioxidant found in mitochondria of plant and human being. Thai spinach (*Spinacea oleracea*) was selected to extract natural LA. It formed complex with polyrotaxanes (PRx) to deliver and enhance the permeation through the skin to prevent DNA damage. Double strand DNA (dsDNA), human lung cancer H-460 cells and skin fibroblast cells were used in this study. The result showed that LA could protect the DNA damage and prevent the formation of DNA-platinum adducts those inducing cytotoxicity. Moreover, it had high efficacy to recover the DNA damage when compared with other antioxidants. For enhancing the topical absorption of LA, PRx and cholesterol modified PRx complexes were developed. The *ex-vivo* permeation study was investigated using the stratum corneum (SC) as a model membrane in Franze diffusion cell. LA-PRx complex enhance the permeation of LA through the SC when compared with LA solution. The cholesterol modified PRx gave the better permeation of free LA than LA-PRx complex. Both delivery systems were not toxic to fibroblast cells and they could stimulate the cell growth. Together, cholesterol modified PRx and even PRx might be a good approach for creating new biodegradable systems for topical application in term of enhancing the penetration through the skin. Studying the effect of LA in cancer cell, LA was found to be prooxidant by an induction of mitochondrial reactive oxygen species (ROS) generation and a concomitant increase in apoptosis in human lung epithelial cancer H-460 cells. The mechanism to induce the apoptosis of LA was found to be mediated through the mitochondrial death pathway which requires caspase-9 activation. Inhibition of caspase activity by pan-caspase inhibitor (z-VAD-fmk) or caspase-9-specific inhibitor (z-LEHD-fmk) completely inhibited the apoptotic effect of LA. ROS inducing from LA activated the caspase-9 cascade and caused the downregulation of mitochondrial Bcl-2 protein through peroxide-dependent proteasomal degradation. Furthermore a novel prooxidant role of LA in apoptosis induction may be exploited for the treatment of cancer and related apoptosis disorders.

Field of study Pharmaceutical Technology    Student's signature..... *Jirapan Mungjaroen*  
Academic year 2006                                    Advisor's signature..... *Ubonthip Nimmannit*  
Co-advisor's signature..... *Vimolmas Lipipun*

## ACKNOWLEDGEMENTS

My sincere and heartfelt thanks to my advisor, Associate Professor Ubonthip Nimmannit, my co-advisor Associate Professor Vimolmas Lipipun and Professor Dr. Patrick S. Callery who, from the very first day of my study in Pharmaceutical Technology program have given me the invaluable advice, supervision, encouragement throughout this study.

I would like to express my deep appreciate to Professor Yongyuth Rojanasakul of the Department of Pharmaceutical Sciences, West Virginia University, for giving a chance to perform experiments at West Virginia University, USA. His excellent advice, guidance, encouragement, understanding and prompt action which have made this study a reality in time, are highly regarded and appreciated.

I am very much indebted to Professor Dr. Yui Nohibuki, Dr. Touru Ooya and Dr Wanpen Tachaboonyakiat for their valuable knowledge and suggestion when I was in Japan. Their kindness and helpfulness are also appreciated.

I would like to thank to the staffs of the Department of Pharmaceutical Sciences; West Virginia University, the School of Material Science; Japan Advance Institute of Science and Technology and Pharmaceutical Technology Program, Chulalongkorn University.

I am very much obliged and honored to the members of the Thesis Committee for their supportive attitude, constructive criticisms and for their invaluable discussions over my dissertation.

It would not be completed without expressing my heartfelt gratitude to my parents for their love, understanding, moral support and tremendous encouragement throughout my life.

Finally, my deep appreciation goes to my friends, all the faculty members in the Pharmaceutical Technology (International) Program and other people, whose names have not been mentioned, for helping me in anyway during the time of my study.

The present work was partly supported by the Royal Golden Jubilee Program, Thailand Research Fund 5.Q.CU.45/A.1, NIH Grant HL-071545 and Jasso Short-Term Student Exchange Promotion Program (Inbound) Scholarship.

## CONTENTS

	PAGE
ABSTRACT (THAI).....	iv
ABSTRACT (ENGLISH).....	v
ACKNOWLEDGEMENTS .....	vi
CONTENTS.....	vii
LIST OF TABLES.....	xi
LIST OF FIGURES.....	xiv
LIST OF ABBREVIATIONS.....	xviii
CHAPTER	
I INTRODUCTION.....	1
II LITERATURE REVIEWS.....	6
1. Reactive oxygen species and oxidative stress.....	6
2. Antioxidants.....	7
3. $\alpha$ -Lipoic acid.....	9
4. <i>Spinacea oleracea</i> .....	15
5. Skin.....	15
6. Delivery system.....	17
7. Polyrotaxanes.....	17
8. Deoxyribonucleic acid.....	19
9. Cancer.....	21
10. Apoptosis.....	21
11. The Bcl-2 family.....	28
12. Cisplatin.....	30
13. Electrospray ionization mass spectrometry.....	32

	PAGE
III MATERIALS AND METHODS .....	34
1. Extraction of LA from <i>Spinacea oleracea</i> .....	38
2. DHLA synthesis .....	38
3. HPLC assay .....	39
4. LA – PRx complex and cholesterol modified-LA –PRx complex synthesis .....	40
5. Characterization .....	42
6. Penetration study .....	43
7. Cytotoxicity assay .....	44
8. The effect of LA, LA-PRx complex and cholesterol modified LA-PRx complex on cell growth .....	45
9. The effect of LA, DHLA, LA-PRx complex, cholesterol modified LA-PRx complex on DNA-Damage .....	46
10. Apoptosis assay of human epithelial lung cancer H-460 cells .....	49
11. LA and DHLA induce caspase activation .....	51
12. LA and DHLA induce ROS generation .....	51
13. Responsibility of mitochondrial ROS on LA-induced apoptosis .....	52
14. The effect of antioxidant and Bcl-2 overexpression on LA-Induced apoptosis and ROS generation .....	53
IV RESULTS AND DISCUSSION .....	55
1. Extraction of LA from <i>Spinacea oleracea</i> .....	55
2. DHLA synthesis .....	55
3. HPLC assay .....	55
4. LA – PRx complex and cholesterol modified-LA –PRx complex synthesis .....	59
5. Characterization .....	64
6. Penetration study .....	67



	PAGE
IV RESULTS AND DISCUSSION (cont.).....	
7. Cytotoxicity assay.....	70
8. The effect of LA, LA-PRx complex and cholesterol modified LA-PRx complex on cell growth.....	70
9. The effect of LA, DHLA, LA-PRx complex, cholesterol modified LA-PRx complex on DNA-Damage.....	71
10. The apoptosis assay of human epithelial lung cancer H-460 cells.....	96
11. LA and DHLA induce caspase activation.....	101
12. LA and DHLA induce ROS generation.....	103
13. Responsibility of mitochondrial ROS on LA-induced apoptosis.....	103
14. The effect of antioxidant and Bcl-2 overexpression on LA-Induced apoptosis and ROS generation.....	105
V CONCLUSIONS.....	111
1. The extraction of LA from Thai spinach ( <i>Spinacea oleracea</i> ).....	111
2. The synthesis of DHLA.....	111
3. Characterization of LA, DHLA and DNA-platinum adducts using ESI-MS and dHPLC.....	111
4. Novel biodegradable PRx and cholesterol modified PRx enhanced the penetration of LA.....	112
5. LA and DHLA protect against DNA damage inducing by cisplatin.....	113
6. The effect of LA and DHLA on PT induced apoptosis in H-460 cells.....	114
7. The efficacy of LA, LA-PRx complex and cholesterol modified LA-PRx complex on DNA damage protection.....	114

	PAGE
V CONCLUSIONS(cont.).....	
8. ROS mediate caspase activation and apoptosis induced by LA in human lung epithelial cancer cells through Bcl-2 down-regulation.....	115
REFERENCES.....	118
APPENDICES.....	132
APPENDIX A.....	133
APPENDIX B.....	138
APPENDIX C.....	160
VITA.....	168



สถาบันวิทยบริการ  
จุฬาลงกรณ์มหาวิทยาลัย

## LIST OF TABLES

TABLE	PAGE
1. Characteristic of LA and DHLA.....	11
2. Differences between apoptosis and necrosis.....	22
3. Human diseases associated with disordered apoptosis.....	28
4. Accuracy and intraday precision of LA assayed by HPLC method.....	57
5. Precision (%CV) data of LA assayed by the HPLC method.....	58
6. Linear regression analysis parameters for quantification of LA.....	58
7. The theoretical m/z of DNA-platinum adducts for each charge.....	75
8. The theoretical m/z of ssDNA and duplex undecamer DNA at different charge.....	82
9. Accuracy data of LA assayed by HPLC method.....	139
10. Precision data of LA by HPLC method.....	140
11. Linearity data of LA assayed by HPLC method.....	141
12. LOD and LOQ data of LA assayed by the HPLC method.....	142
13. Linearity data of LA assayed by UV/VIS spectrometer at 208 nm.....	142
14. The amount of LA in PRx or cholesterol modified PRx analyzed by UV/VIS spectrometer at 208 nm.....	143
15. The cumulative amount of LA from LA solution.....	143
16. The cumulative amount, flux and rate constant (k) of LA from LA solution.....	144
17. The cumulative amount of LA from LA-PRx complex.....	145
18. The cumulative amount, flux and rate constant (k) of LA from LA-PRx complex.....	146
19. The cumulative amount of LA from cholesterol modified LA-PRx complex.....	147
20. The cumulative amount, flux and rate constant (k) of LA from cholesterol modified LA-PRx complex.....	148

TABLE	PAGE
21. The cytotoxicity of LA ,PRx-LA and cholesterol modified LA-PRx complex to human skin fibroblast.....	149
22. The effect of LA, PRx-LA and cholesterol modified LA-PRx to cell growth.....	149
23. The percentage of apoptotic H-460 cells induced by LA and DHLA treatment.....	150
24. Caspase activities of H460 cells after treatment with LA or DHLA analyzed by fluorometric assays.....	150
25. The percentage of apoptotic H-460 cells after treated with LA or DHLA in the presence or absence of caspase-9 inhibitor or pan-caspase inhibitor.....	151
26. Effects of antioxidants on LA- and DHLA-induced apoptosis and ROS generation.....	151
27. The relative fluorescence intensity of DCF and DHE over non-treated control after treatment of LA or DHLA.....	152
28. Effects of antioxidants on LA- and DHLA-induced DCF and DHE fluorescence intensities.....	152
29. Effects of DPI and ROT on LA-induced apoptosis in H-460 cells.....	153
30. Effects of DPI and ROT on LA-induced ROS in H-460 cells.....	153
31. Effects of GPx and SOD overexpression on LA-induced apoptosis in H-460 cells.....	154
32. Effects of GPx and SOD overexpression on LA-induced ROS generation in H-460 cells.....	154
33. Bcl-2 overexpression inhibits LA-induced apoptosis in H-460 cells.....	155
34. Effect of LA on Bcl-2 expression in H-460 cells after treated with LA for various times.....	155
35. Effect of LA on Bcl-2 expression in H-460 cells after treated with LA for various doses.....	156



TABLE	PAGE
36. Effect of LA on Bcl-2 expression of H-460 cells in the presence or absence of LAC.....	156
37. Effect of antioxidants on Bcl-2 expression in H-460 cells.....	157
38. Effect of GPx and SOD overexpression on Bcl-2 expression in H-460 cells.....	157
39. The protective effect of LA and DHLA to prevent the damage of DNA from cisplatin determined by dHPLC.....	158
40. The protective effect of LA at the different concentration to prevent the damage of DNA from cisplatin analyzed by dHPLC.....	158
41. The protective effect of DHLA at the different concentration to prevent the damage of DNA from cisplatin analyzed by dHPLC.....	159
42. The protective effect of LA, LA-PRx complex and cholesterol modified LA-PRx complex to prevent the damage of DNA from cisplatin analyzed by dHPLC.....	159

## LIST OF FIGURES

FIGURE	PAGE
1. The structure of LA and its reduced form, DHLA.....	10
2. Polyrotaxanes structure.....	18
3. Apoptosis process.....	24
4. Apoptosis pathway.....	27
5. The chromatogram of standard LA from Sigma and LA from <i>Spinacea oleracea</i> .....	56
6. The calibration curve of LA.....	59
7. The synthetic procedure of PRx.....	60
8. The synthetic procedure of cholesterol modified PRx.....	61
9. The reaction between $\alpha$ -CD in PRx and cholesterol.....	61
10. The synthetic procedure of LA-PRx complex.....	62
11. The synthetic procedure of cholesterol modified LA-PRx complex.....	63
12. The reaction between $\alpha$ -CD in PRx and LA.....	63
13. The mass spectrum of LA.....	64
14. The mass spectrum of DHLA.....	65
15. $^1\text{H-NMR}$ spectrum of PRx and cholesterol modified PRx in DMSO-d <sub>6</sub> .....	66
16. The calibration curve of LA in PRx.....	67
17. The cumulative amount of LA from LA solution, LA-PRx complex and cholesterol modified LA-PRx complex.....	69
18. Fluxes of LA through human SC from LA solution and LA-PRx complex and cholesterol modified LA-PRx complex.....	69
19. Cell viability of human skin fibroblast after treatment with LA, LA-PRx complex and cholesterol modified LA-PRx complex.....	70
20. Cell growth assay of skin fibroblast after incubated with LA, LA-PRx or cholesterol modified LA-PRx complex.....	71

FIGURE	PAGE
21. Peak of dsDNA alone or dsDNA incubated with different molar ratios of PT (1:1, 1:5 and 1:10) at 37 °C for 24 h.....	72
22. The percent of dsDNA (Dickerson dodecamer) reduction alone and dsDNA to cisplatin (PT) in the different molar ratios (1:1, 1:5 and 1:10) after the incubation at 37°C for 1, 2 3, 4 and 24 h.....	72
23. The mass spectra of dsDNA (Dickerson dodecamer).....	74
24. MS spectra of dsDNA-platinum adducts and ssDNA-platinum adducts.....	77
25. The percent of dsDNA in the system contained LA, dsDNA and cisplatin (PT) after incubation at 37 °C for 24 h.....	79
26. The percent of dsDNA in the system containing DHLA, dsDNA and cisplatin(PT) after incubation 24 h.....	79
27. Mass spectra of dsDNA (Dickerson dodecamer) and adducts of system containing dsDNA, cisplatin (PT) and LA , DHLA or acetic acid.....	81
28. The full scan mass spectra of ssDNA MW 3279 and ssDNA MW3399.....	84
29. Mass spectra of duplex undecamer DNA MW 6678.....	87
30. Full scan mass spectra of undecamer DNA showed the DNA-adduct formation protection efficacy of LA and DHLA.....	89
31. Cisplatin(PT) reduced the amount of dsDNA heteroduplex undecamer when studying by dHPLC.....	91
32. The structure of LA-platinum adduct and the ammonium adduct of platinum-LA.....	92
33. The protection effect of different sulfur-containing compound and chelating agent to DNA in the system containing cisplatin.....	94
34. The recovery efficacies of different treatment in cisplatin induced DNA damage after 4 h.....	95

FIGURE	PAGE
35. The protection effect of LA solution, LA-PRx complex and cholesterol modified LA-PRx complex on DNA damage.....	96
36. Cisplatin(PT) induced H-460 cells apoptosis in dose-dependent manner.....	97
37. The effect of LA to cisplatin(PT) induced apoptosis in H-460 cells.....	98
38. LA and DHLA induce apoptosis in H-460 cells, Fluorescence micrographs of treated cells and LA or DHLA induced caspase activity in H-460 cells.....	100
39. Effects of antioxidants on LA- and DHLA-induced apoptosis and ROS generation.....	102
40. Effects of DPI and ROT on LA-induced apoptosis and ROS generation.....	104
41. Effects of GPx and SOD overexpression on LA-induced apoptosis and ROS generation.....	106
42. Bcl-2 protein overexpression of Bcl-2 transfection cell inhibits LA-induced apoptosis.....	108
43. Effect of LA exposure time on Bcl-2 expression.....	109
44. Effect of antioxidants on Bcl-2 expression.....	110
45. GPx and SOD overexpression of H-460 cells.....	161
46. Bcl-2 overexpression of H-460 cells.....	161
47. Effect of LA on Bcl-2 expression.....	162
48. Effect of antioxidants on Bcl-2 expression.....	163
49. The mass spectra of dsDNA (Dickerson dodecamer).....	164
50. MS spectra of dsDNA-platinum adducts.....	164
51. Mass spectra of dsDNA and adducts of system containing dsDNA, cisplatin and LA or DHLA.....	165
52. Mass spectra of duplex undecamer DNA MW 6678 recorded at m/z 1668.5 and 1336.7 for -4 and -5 ion.....	166
53. Mass spectra of duplex undecamer DNA-platinum adduct.....	166



FIGURE	PAGE
54. Full scan mass spectra of undecamer DNA showed the DNA-adduct formation protection efficacy of LA.....	167
55. Full scan mass spectra of undecamer DNA showed the DNA-adduct formation protection efficacy of DHLA.....	167



สถาบันวิทยบริการ  
จุฬาลงกรณ์มหาวิทยาลัย

## LIST OF ABBREVIATIONS

$\mu\text{g}$	=	microgram (s)
$\mu\text{L}$	=	microliter (s)
$\mu\text{m}$	=	micrometer
$\mu\text{mole}$	=	micromole
%	=	percentage
$^{\circ}\text{C}$	=	degree Celsius (centigrade)
AA	=	acetic acid
AIF	=	apoptosis inducing factor
AMC	=	amino-4-methyl coumarin
Apaf-1	=	the initiating apoptosis protease activating factor 1
As	=	arsenic
ATP	=	adenosine triphosphate
Bcl-2	=	an anti-apoptotic protein in Bcl-2 family
BH	=	Bcl-2 homology
CD	=	cyclodextrin (s)
$\text{Cd}^{2+}$	=	cadmium ion
CE	=	collision energy
c-FLIP	=	cellular FLICE-like inhibitory protein
$\text{Co}^{2+}$	=	cobalt ion
$\text{CO}_2$	=	carbon dioxide
COOH	=	carboxylic group
$\text{Cu}^{2+}$	=	copper ion
CV	=	coefficient of variation
Cys	=	cysteine
d	=	day
da	=	dalton

DCC	=	dicyclohexylcarbodiimide
DCF-DA	=	2', 7' -dichlorodihydrofluorescein diacetate
DcR	=	decoy receptors
DD	=	Dickerson dodecamer
DHE	=	dihydroethidium bromide
DHLA	=	dihydrolipoic acid
dHPLC	=	denatured high-performance liquid chromatography
DIEA	=	Diisopropylethylamine
DISC	=	death inducing signaling complex
DMF	=	dimethylformamide
DMSO	=	Dimethyl sulfoxide
DNA	=	deoxyribonucleic acid
DPI	=	diphenylene iodonium
ds	=	double strand
DSC	=	differential scanning calorimetry
DTT	=	dithioerythiol
EDTA	=	ethylene diamine tetraacetic acid
ESI	=	electrospray ionization
et al.	=	et alii, and others
EtOAc	=	ethyl acetate
EtOH	=	ethanol
FADD	=	Fas-associated death domain
Fas	=	Fas receptor
FasL	=	Fas ligand
Fe <sup>2+</sup>	=	ferrous ion
Fe <sup>3+</sup>	=	ferric ion
FLIP	=	FLICE-inhibitory protein
g	=	gram
GPx	=	glutathione peroxidase overexpressed cells
GSH	=	glutathione

GR	=	glutathione reductase
GTK	=	glutamine transaminase K
h	=	hour
HCl	=	hydrochloric acid
HDL	=	high density lipoprotein
HEPES	=	4-(2-hydroxyethyl)-1-piperazine ethanesulfonic acid
Hg <sup>2+</sup>	=	mercury ion
HIV	=	human immunodeficiency virus
HOBT	=	N-Hydroxybenzotriazole
HOCl	=	hypochlorous acid
HPLC	=	high-performance liquid chromatography
H <sub>2</sub> O <sub>2</sub>	=	hydrogen peroxide
IAP	=	inhibitor of apoptosis
IETD-AMC	=	Ile-Glu-Thr-Asp (7-amino-4-trifluoromethyl coumarin)
IFN-γ	=	interferon gamma
IL-1β	=	interlukin-1-beta
kg	=	kilogram (s)
LA	=	α-lipoic acid
LAC	=	lactacystin
LC-MS	=	liquid chromatography mass spectrometry
LEHD-AMC	=	N-acetyl-Leu-Glu-His-Asp-AFC (7-amino-4-trifluoromethyl coumarin)
lipoDH	=	lipoyl dehydrogenase
LOO•	=	lipid peroxide
MAPK	=	mitogen-activated protein kinase
MeOH	=	methanol
mg	=	milligram (s)
min	=	minute (s)
mL	=	milliliter



mM	=	millimolar
mm	=	millimeter (s)
Mn <sup>2+</sup>	=	manganese ion
MnTBAP	=	Mn(III)tetrakis (4-benzoic acid) porphyrin
MS	=	Mass spectrometry
MW	=	molecular weight
m/z	=	mass per ion
N	=	normal
NaBH <sub>4</sub>	=	sodium borohydride
NAC	=	N-acetylcysteine
NaCl	=	sodium chloride
NAD <sup>+</sup>	=	nicotinamide adenosine dinucleotide
NADH	=	reduced nicotinamide adenosine dinucleotide
NADPH	=	reduced nicotinamide adenosine dinucleotide phosphate
NaF	=	sodium fluoride
NaHCO <sub>3</sub>	=	sodium bicarbonate
NaOH	=	sodium hydroxide
NF-kB	=	Nuclear Factor kB
NH <sub>3</sub>	=	ammonia
NHDF	=	normal human dermal fibroblast cells
Ni <sup>2+</sup>	=	nickel ion
nM	=	nanomolar
NMR	=	nuclear magnetic resonance
<sup>1</sup> O <sub>2</sub>	=	singlet oxygen
O <sub>2</sub> <sup>•-</sup>	=	superoxide radical
OH <sup>•</sup>	=	hydroxyl radical
8-OH-G	=	8 hydroxy guanine
ONOO <sup>-</sup>	=	peroxynitrite
PAGE	=	polyacrylamide gel electrophoresis

Pb <sup>2+</sup>	=	lead ion
PBS	=	phosphate-buffered saline
PEG	=	poly (ethylene glycol)
PLP	=	pyridoxal 5β-phosphate
pH	=	the negative logarithm of hydrogen ion concentration
PRx	=	polyrotaxanes
Pt	=	Platinum
PT	=	cisplatin
PTP	=	mitochondrial permeability transition pore
PVDF	=	polyvinylidene fluoride
r <sup>2</sup>	=	coefficient of determination
RNA	=	ribonucleic acid
RPMI	=	Roswell Park Memorial Institute's medium
ROS	=	reactive oxygen species
ROT	=	rotenone
SC	=	stratum coreum
SDS-PAGE	=	sodium dodecyl sulfate-polyacrylamide gel electrophoresis

สถาบันวิทยบริการ  
จุฬาลงกรณ์มหาวิทยาลัย

SEM	=	standard effort of mean
SH	=	sulhydriyl group
SOD	=	superoxide dismutase
SRB	=	sulphorhodamine B
ss	=	single strand
TBST	=	Tris-buffered saline, 0.1 % Tween 20
TCR	=	T-cell receptor
TEAA	=	triethylammonium acetate
TNFR	=	tumor necrosis factor receptor; TNFR-associated factor-2,
TRAF-2		
TNF	=	tumor necrosis factor
TNF- $\alpha$	=	tumor necrosis factor alpha
TRADD	=	TNF receptor associated death domain
TRAF-2	=	TNFR-associated factor-2,
TRAIL	=	TNF-related apoptosis-inducing ligand
UV	=	ultraviolet
v	=	volt
z-LEHD-fmk	=	benzyloxycarbonyl-Leu-Glu(OMe)-His-Asp(OMe)- fluoromethyl ketone
Zn <sup>2+</sup>	=	zinc ion
z-VAD-fmk	=	benzyloxycarbonyl-Val-Ala-Asp-(OMe) fluoromethyl ketone

สถาบันวิทยบริการ  
จุฬาลงกรณ์มหาวิทยาลัย

## CHAPTER I

### INTRODUCTION

Cisplatin or cis-diamminedichloroplatinum(II) is a potent antitumor drug. It has been approved as anti-cancer drug in the USA since 1979. The clinical application of cisplatin has increased enormously. It has become the leading and most widely used anticancer drug. Complete remissions are obtained for testicular cancers in more than 85% of all treated patients, whereas high efficacy in the treatment of ovarian and bladder cancer and considerable activity in osteogenic sarcoma, head and neck cancer, endometrial and cervical cancer as well as non—small cell lung cancer have been reported (Reedijk and Lohman, 1985; Osman et al., 2000) Cisplatin-based combination chemotherapy regimens are also currently used as front-line therapy in these treatments.

The therapeutic effects of cisplatin are significantly improved by dose escalation. However, high-dose therapy with cisplatin is limited by its cumulative ototoxicity, hepatotoxicity, nephrotoxicity and neurotoxicity (Vickers et al., 2004; Koc et al., 2005; McDonald et al., 2005; Sastry and Kellie, 2005). All of these toxicity occur after the damage of DNA (Vickers et al., 2004; McDonald et al., 2005). The acute nephrotoxicity observed is consistent with the concentration-dependent binding of platinum to sulfhydryl groups in the renal tubules. Platinum (II) compound has high affinity to sulfur (Borch and Pleasants, 1979) and the platinum anticancer drugs kinetically prefer sulfur over nitrogen donors (Deubel, 2004). A large number of sulfur-containing compounds such as procainamide, diethyldithiocarbamate, N-methyl-D-glucaminedithio carbamate, methimazole, sulfathiazole and amifostine have been shown to reduce the nephrotoxicity of cisplatin without inhibiting its antitumor effect (Borch and Pleasants, 1979; Jones et al., 1992; Yee et al., 1994; Korst et al, 1998; Osman et al., 2000).

$\alpha$ -Lipoic acid (LA) or thioctic acid is an interesting small sulfur-containing antioxidant. It is a naturally-occurring essential co-enzyme in mitochondrial multi-enzyme complexes catalyzing the oxidative decarboxylation of  $\alpha$ -keto acids such as



pyruvate,  $\alpha$ -ketoglutarate, and branched-chain  $\alpha$ -keto acid (Packer et al., 1995; Bilaska and Wlodek, 2005). It is of great interest because of its superior ability compared to other antioxidants. Most antioxidants preferentially minimize the damage caused by either fat or water soluble reactive oxygen species (ROS). In contrast, LA can protect against both fat and water soluble ROS. Therefore, it is able to defend against ROS both inside and outside cells. LA has been shown to combat oxidative stress by quenching a variety of intracellular reactive oxygen species (ROS) (Suzuki et al., 1991; Bilaska and Wlodek, 2005). In addition to ROS scavenging, LA has also been shown to be involved in the recycling of other cellular antioxidants including vitamins C and E, and glutathione (Biewenga et al., 1997). Different from other antioxidants, the reduced form of LA, dihydrolipoic acid (DHLA), also possesses the ability to scavenge ROS and chelates the metal ions. LA has been demonstrated to be effective in preventing pathology in various experimental models in which ROS have been implicated, such as ischemia-reperfusion injury (Coombes et al., 2000), diabetes (Kocak and Karasu, 2002), diabetic neuropathy (Vincent et al., 2005; Vincent et al., 2005), neurodegeneration (Pirlich et al., 2002), hypertension (El Midaoui and de Champlain, 2002; Midaoui et al., 2003), radiation injury (Demir et al., 2005), and HIV activation (Patrick, 2000). LA is present in all kinds of prokaryotic and eukaryotic cells. It is also synthesized in mammalian cells (Glantzounis et al., 2006). Food derived from tissue with a high metabolic activity has a high LA content (Herbert and Guest, 1975). LA also was found in vegetable such as potato, spinach and tomato as well (Herbert and Guest, 1975). Natural LA has the antioxidant efficacy higher than synthetic LA. Unlike natural LA, synthetic LA contains a 50/50 mixture of two forms (enantiomers) called (R)-LA and (S)-LA. Both (R)- and (S)-forms of LA are isomers—essentially mirror-image molecular formulas, with the atomic arrangements reversed (Biewenga et al., 1997). Only the R-enantiomer of LA is biologically active. To study the effect of natural LA, spinach (*Spinacea oleracea*) was selected as the source of LA. The extraction and purification of LA were developed.

The delivery system of LA was developed to enhance the penetration and the DNA damage protection activity. Very few delivery systems of LA i.e. chitosan polymer (Bernkop-Schnurch et al., 2004) and solid-lipid nanoparticles (SLN) (Souto

et al., 2005) was studied in the previous works. Polyrotaxanes (PRx) is an interesting novel nanotechnology which is selected to deliver LA. PRx is the complexation of cyclodextrins (CDs) threaded onto polyethylene glycol (PEG). They form PRx by non-covalent-bond molecular interaction. The ability to penetration of PRx is depending on the molecular weight of PEG and the conditions of the terminal capping reaction. The most striking feature of these PRx is supramolecular dissociation triggered by terminal hydrolysis: once either of the terminals is cleaved via the hydrolysis, all the CDs are dethreaded from the PEG chain at once (Yui and Ooya, 2004). This characteristic, therefore, may be considered promising as a new style of biodegradable polymer for use as the carrier for improving the penetration and the efficacy of LA. It is capable of including phospholipids especially phosphatidylcholine and sphingomyelin, so PRx may affect the permeability of drugs through the skin via the interaction with these components of the skin, leading to reversible imbalance of bilayer and increase membrane fluidity (Wataru et al., 1996). Cholesterol has been shown to improve cell proliferation and control the degradation rate of PRx (Tachaboonyakiat et al., 2004). Therefore, it seems to be interesting to introduce cholesterol into PRx. LA complexes with PRx and LA complexes with cholesterol modified PRx were developed and the permeation was investigated to compare between LA alone and both in the form of PRx complexes. For prediction of the *in vitro* absorption through the skin, diffusion of LA in the modified Franz diffusion cell was studied using excised human stratum corneum (SC) as the membrane.

Not only antioxidant activity, but LA also has been reported to possess prooxidant activities (Dicter et al., 2002; Cakatay et al., 2005). For examples, LA dose dependently increases intramuscular ROS production and stimulates glucose uptake into adipocytes by increasing intracellular oxidant levels (Dicter et al., 2002). In cancer cells, ROS also are well recognized for playing a crucial dual role as both deleterious and beneficial species in tumor cells. The “two-faced” character of ROS is substantiated by growing body of evidence that ROS within cells act as secondary messengers in intracellular signaling cascades, which induce and maintain the oncogenic phenotype of cancer cells, however, ROS can induce cellular senescence and apoptosis, a physiological model of cell death, in which the cell itself executes the

program for its own demise and subsequent removal, is an active field of research worldwide by scientists engaged in the search for cancer chemopreventive agents (Takahashi et al., 2004). This mechanism can therefore function as anti-tumourigenic species as well (Wu et al., 2005).

As mention above, LA has been reported to act both as a pro- and anti-oxidant. The investigation of LA, prooxidant activity also has been studied. In transformed human colon cancer HT29 cells, LA was shown to increase mitochondrial respiration and superoxide anion ( $O_2^{\cdot-}$ ) generation with a concomitant increase in apoptosis (Wenzel et al., 2005), the effects that were not observed in normal non-transformed colonocytes. Likewise, LA was shown to induce apoptosis of several tumor cell lines including Jurkat, FaDu, and Ki-v-Ras-transformed mesenchymal cells with minimal effect on non-transformed cell lines (van de Mark et al., 2003). LA also potentiated Fas-mediated apoptosis of human leukemic T-cells through redox regulation without having an effect on peripheral blood monocytes from healthy humans (Sen et al., 1999). These studies support the potential utility of LA as an anticancer agent and the role of ROS in cancer cell death by LA. Because of its therapeutic potential and the widespread use of LA as a nutritional supplement including the existing in vegetables and meat (Packer et al., 1997) that are consumed by humans on a daily basis, the apoptosis activity and the underlying mechanisms of action of LA have to be determined. This research examined the mechanism and specific pathway of apoptosis that activated by LA in human lung epithelial cancer cell H-460.

In conclusion, the purposes of this study were as follows:

1. To develop the extraction of LA from *Spinacea oleracea*.
2. To synthesize LA-PRx complex and cholesterol modified LA-PRx complex for enhancing the penetration of LA through the SC.
3. To evaluate the protection effect of LA from cisplatin induced DNA damage.
4. To compare the DNA damage protection activity among LA solution, LA-PRx complex and cholesterol modified LA-PRx complex.
5. To compare the permeation ability of LA, LA-PRx complex and cholesterol modified LA-PRx complex through the SC.
6. To study the mechanism of apoptosis that activated by LA.

Clarification of DNA damage protection effect of LA, the molecular mechanisms responsible for this inducing apoptosis, including the development of the novel delivery system PRx may lead to the improvement of the treatment for the diseases and the pathology involved in DNA damage and apoptosis disorder.



สถาบันวิทยบริการ  
จุฬาลงกรณ์มหาวิทยาลัย

## CHAPTER II

### LITERATURE REVIEWS

#### 1. Reactive oxygen species (ROS) and oxidative stress

The functioning of living systems depends on the energy. Aerobic organisms derive their energy from the oxidation of fuel molecules such as glucose and fatty acids. In oxidation, electrons are removed from these molecules and subsequently transferred in a chain of reactions to other molecules until they finally reach their ultimate electron acceptor:  $O_2$ . Oxidative stress often originates from improper control of this reduction of  $O_2$ .

An important molecule in the oxidative stress is molecular oxygen,  $O_2$ . In its ground state,  $O_2$  has two unpaired electrons in its antibonding  $\pi^*$  molecular orbital. More reactive forms of oxygen are the singlet oxygen ( $^1O_2$ ). If the electron is added to  $O_2$ , the product is superoxide radical ( $O_2^{\bullet-}$ ), with only one unpaired electron. Consequently, addition of one more electron will give a nonradical species, the peroxide ion ( $O_2^{2-}$ ) which forms the presence of the protons,  $H_2O_2$  (Biewenga et al., 1997).

Some transition metals can participate in the chain of  $O_2$  reduction. Oxidized metals, such  $Fe^{3+}$  and  $Cu^{2+}$ , catalyze electron transfer from one oxygen species to another. Reduced metal ions, such  $Fe^{2+}$  and  $Cu^+$ , can donate one electron and thus start a whole sequence of reactions. An example is the Fenton reaction in which the very reactive hydroxyl radical ( $\bullet OH$ ) is formed. Traces of  $Fe^{3+}$  might be able to react further with  $H_2O_2$ , although this is very slow at physiological pH. The overall sum of these reactions is the iron-catalyzed decomposition of hydrogen peroxide.

In aerobic organisms, almost all steps in the reduction of  $O_2$  are catalyzed by metals. Mostly, the reactivity of the metals is controlled by in co-operating the metal in an enzyme. Examples of such enzymes are superoxide dismutase (SOD), catalase and cytochromes. Dissociated from their protein environments, metals take part in other, often unwanted, secondary reactions. The protein environment of SOD prevents



the metal-catalyzed reaction between  $O_2^{\bullet-}$  and  $H_2O_2$ , but unbound iron or copper induces hydroxyl radical (OH $\cdot$ ) formation.

The generation of reactive oxygen radicals in mammalian cells profoundly damages biomolecules such as DNA, proteins and lipids and affects numerous critical cellular functions. One method of overcoming oxidative damage is degradation and renewal. A second method is repair, which may be particularly important for proteins with a low turnover rate. In the proteins, amino acid residues such as tryptophan, histidine, tyrosine, cysteine and methionine are susceptible to oxidation. Whereas some oxidants (e.g., ozone,  $O_2^{\bullet-}$  /OH $\cdot$ ) destroy the residues at random, other oxidants (e.g.  $H_2O_2$ , HOCl, chloramines and ONOO $^-$ ) preferentially oxidize exposed methionine residues.

The absence of efficient cellular detoxification mechanisms which remove these radicals can result in several human diseases (Storz, 2005). Oxidative stress and associated oxidative damage are mediators of vascular injury and inflammation in many cardiovascular diseases, including hypertension, hyperlipidemia, and diabetes. Increased generation of ROS has been demonstrated in experimental and human hypertension. Antioxidants and agents that interrupt NAD(P)H oxidase-driven  $*O_2^-$  production regress vascular remodeling, improve endothelial function, reduce inflammation, and decrease blood pressure in hypertensive models (Touyz and Schiffrin, 2004). ROS also induces miscoding and modifies DNA bases. DNA adducts in organs affect by persistent inflammatory processes and potential lead markers for assessing progression of inflammatory cancer-prone diseases (Bartsch and Nair, 2006).

## **2. Antioxidants**

To control oxidative processes, biological systems have been equipped with several antioxidant mechanisms. Antioxidant activity is obtained when the reaction between the ROS and the scavenger is faster than the reaction between the ROS and the target molecule. In an organism, many biomolecules present in tissue and in the intra- and extramolecular fluids can be targets of ROS-mediated damage. Antioxidant



enzymes such as SOD, catalase and peroxidase are concerned with the removal of  $O_2^{\bullet-}$  and  $H_2O_2$ . Metal ions can be sequestered to inhibit uncontrolled dismutation of  $O_2^{\bullet-}$ , the Fenton reaction. ROS can be scavenged in an aqueous environment by small molecules such as vitamin C, glutathione and uric acid. In a lipid environment, vitamin E scavenges ROS-derived radicals and protects the membranes. In spite of all this, the antioxidant system has failed; damage to endogenous molecules may be repaired.

Generally, as in all chemical reactions, the reaction rate of scavenging reaction is determined by the chemical and physical properties. The combination of these properties and the concentration of the scavenger and by the rate constant determine its final antioxidant activity. To be effective, the antioxidant itself and its relevant metabolites should become available to the tissue that is prone to oxidative stress. Within pharmacology, the absorption, distribution, metabolism and excretion of antioxidant are studied. For the evaluation of the ideal antioxidants, four aspects have been distinguished:

1. The ROS-scavenging capacity
2. The capacity to regenerate endogenous antioxidants
3. The role in repair systems
4. The metal-chelating capacity

Moreover, *in vivo* antioxidant activity can be determined by the measurement of: (1) the antioxidant levels, (2) the degree of damage (e.g., to lipids, proteins) and (3) a physiological function. Several things need to be considered when evaluating the value of an antioxidant: free radical quenching, ability to chelate metals, interactions with other antioxidants, bioavailability and cell concentration, any effects on gene expression and whether the molecule is located in the cell membrane or aqueous phase.

### **3. $\alpha$ -Lipoic acid (LA)**

#### **3.1 Biochemistry of LA**

LA or thioctic acid (chemical name: 1, 2-dithiolane-3-pentanoic acid) is present in all kinds of prokaryotic and eukaryotic cells. In human beings, it is a part of several 2-oxo acid dehydrogenases that take part in energy formation. Linked to lysine residues of the 2-oxo acid dehydrogenase multienzyme complexes (Morris et al., 1995; Fujiwara et al., 1996), LA acts as a cofactor. It binds with acyl groups and transfers them from one part of the enzyme complex to another. In this process, LA is reduced to dihydrolipoic acid (DHLA) inside the cell by an enzyme called dihydrolipoyl dehydrogenase (lipoDH) or glutathione reductase (GR) (Arner et al., 1996). LipoDH is located in the mitochondria of the cell, and utilizes NADH to provide the electrons for the reduction. Free LA is rapidly reduced inside the cell and its reduced form contributes greatly to its antioxidant capabilities (Biewenga et al., 1997). DHLA is subsequently reoxidized by lipoamide dehydrogenase under the formation of NADH. Overall, LA and DHLA act as a redox couple, carrying electrons from the substrate of the dehydrogenase to  $\text{NAD}^+$  and restoring the 2-oxo acid oxidation. The destruction of the cofactor function of LA involves in pathological processes. Also, oxidative stress near the dehydrogenase complex can lead to oxidative destruction (Correa and Stoppani, 1996), thereby adversely affecting the functioning of LA as a cofactor. LA is bound to proteins and, consequently, free LA has not been detected in human beings (Packer et al., 1995). However, after therapeutic application, free LA can be found in the circulation (Teichert and Preiss, 1995). It is likely that the therapeutic effects originate from free, unbound LA.

#### **3.2 Physical and chemical characteristics**

LA contains a five-membered ring, which contains two sulfur atoms and a carboxylic acid group (Figure 1). It is completely insoluble in water, but is soluble in some organic solvents such as methanol and ethyl ether. The reduction of LA to DHLA is done synthetically by  $\text{NaBH}_4$  (Arner et al., 1996). The physical and

chemical characteristics of both LA and DHLA are listed in Table 1. The high pKa for the thiol groups of DHLA indicate that the molecule is strong nucleophile, even more so than glutathione.

### 3.3 The bioavailability of LA

LA is found in vegetable such as potato, spinach and tomato. It is also synthesized in mammalian cells (Glantzounis et al., 2006). Food derived from tissue with a high metabolic activity has a high LA content (Herbert and Guest, 1975). Meat from metabolic organ such as pig heart has LA content of 1.1-1.6 mg/kg, whereas calf muscle contains only 0.07-0.15 mg/kg (Mattulat and Baltes, 1992). This indicates that most LA in the diet originates from the multienzyme complexes. Proteolytic enzymes do not effectively cleave the peptide bond between LA and lysine. Therefore, it has been suggested that, after digestion, LA is absorbed as lipoyllysine. In addition LA can be obtained by *de novo* biosynthesis from fatty acids and cysteine (Carreau, 1979). From food or biosynthesis, only minor amounts of free LA will enter the circulation. After oral application, free LA is obtained in the relatively high amounts. The therapeutic dose exceeds the dietary intake by far.

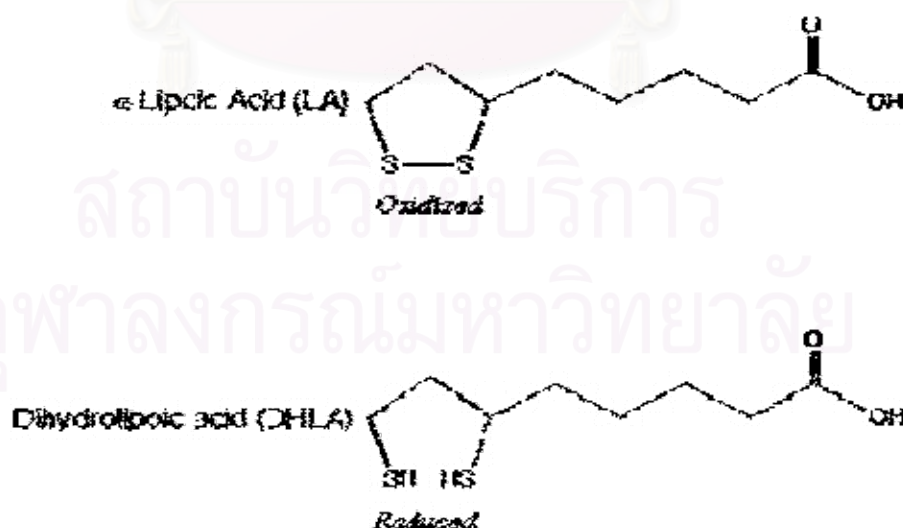


**Figure1** The structure of LA and its reduced form, DHLA (Packer et al., 1995)

**Table 1** Characteristics of LA and DHLA

	<b>LA</b>	<b>DHLA</b>
Molecular Weight (g/mol)	206.35	208.35
Melting Point (°C)	60-62	---
Boiling Point (°C)	---	180
pKa (COOH)	5.3	4.58
pKa (SH)	---	10.7
Chemical Appearance	Yellow crystals	Yellow liquid
$\lambda_{\max}$ – UV (nm)	333	---

### 3.4 Antioxidant properties

LA and DHLA can act as antioxidants against a variety of radicals, including  $\cdot\text{OH}$ ,  $\text{O}_2\cdot^-$ ,  $\text{LOO}\cdot$ ,  $\cdot\text{NO}$  and  $\text{HOCl}$  *in vitro* (Packer et al., 1995). Several tests have been performed to determine the antioxidant activity of LA and DHLA *in vivo*. Most *in vivo* test consist of animal model for a certain disease of which it is assumed that oxidative stress accompanies its etiology. For example, streptozotocin is used in animal models for diabetes. It induces high blood glucose levels, which subsequently induce oxidative stress (Dene et al., 2005). LA minimizes oxidant generation and macromolecular damage in skeletal muscle of aged rats. It also dose-dependently prevented the development of clinical signs in a rat model for multiple sclerosis and acute experimental allergic encephalomyelitis (EAE) that are caused from ROS (Schreibelt et al., 2006). The administration of LA and DHLA could provide protection from the harmful effects of free radicals inducing ischemia and reperfusion injury (Glantzounis et al., 2006). DHLA, but not LA, was able to inhibit the peroxidation of linoleic acid and of the non-HDL fraction catalyzed by rabbit reticulocyte 15-lipoxygenase (Lapenna et al., 2003). These data showed that both LA and DHLA not only chelate ROS directly, but they also reduce the pathology that is caused by ROS.

### 3.5 Regeneration of endogenous antioxidants

One of the most important properties of LA is its ability to regenerate vitamin C, glutathione (GSH) and indirectly vitamin E. Vitamin E is an antioxidant that resides in the lipid bilayer of cell membrane. Its purpose is to stop the chain reaction begun by lipid radicals. Vitamin C then reacts with the  $\alpha$ -tocopherol radical, thereby removing the radicals from the lipid bilayer and moving it into the cytosol where it can be dealt with by resident enzyme. Scavenging of ROS, especially radicals, is efficient only when it forms a relatively stable oxidation product that can be safely regenerated or degraded. GSH and vitamin C are endogenous molecules that take part in the regeneration of oxidized antioxidants. Through a cooperative set of reactions, the different antioxidants interact with each other. For example, after scavenging, the vitamin C radical is formed, leading to the following interplay of antioxidants. The vitamin E radical also can be regenerated by GSH (Rose and Bode, 1995). LA, after reduction to DHLA, is able to contribute to the nonenzymatic regeneration of GSH and vitamin C. Bast and Haenen (1988) studied the interplay between DHLA and GSH. They observed synergism in the protection against  $\text{Fe}^{2+}$ -vitamin C-induced lipid peroxidation. DHLA does not regenerate the chromanoxyl radical present in vitamin E directly. However, vitamin E can be regenerated by DHLA in a cascade of regenerating reactions.

### 3.6 Repair of oxidative damage

Methionine oxidation of some residues leads to inactivation of the protein. This is observed for several enzymes, hormone, chemotactic factors and plasma proteinase inhibitors. For these peptides, inactivation by methionine oxidation has been regarded as part of regulatory, physiologic process. A particular example of oxidative regulation is the regulation of the activity of proteinase inhibitors resulting in loss of protease inhibitory activity. Inactivation of protease inhibitors may alter the proteinase-antiproteinase balance in favor of the protein-degrading enzyme. Protein degradation facilitates phagocytosis of invading organisms but should be restricted to exogenous material. A poorly controlled proteinase-antiproteinase balance results in



degradation of endogenous tissue, and this forms the basis for pathological processes such as lung emphysema (Sigalov and Stern, 1998).

LA can improve the repair of oxidized methionine residue by increasing the amount of reduced thioredoxin (Biewenga et al., 1998). DHLA is derived from LipoDH-dependent reaction; the ultimate effect of LA is making NADH available as a source for reductive reactions instead of NADPH (Sigalov and Stern, 2002).

### 3.7 Metal chelation

Metal chelation is a property of a compound that can result either in antioxidant or in prooxidant activity. Antioxidant activity is obtained when a complex is formed in which the metal is shielded and all co-ordination sites for  $O_2$  are occupied. In addition, antioxidant activity is obtained when electron density is withdrawn from the metal chelator, so electrons cannot be transferred to  $O_2$ . Prooxidant activity is obtained when co-ordination sites for  $O_2$  are present and the metal is reduced. The ligand transfers electrons to the metal, and the electrons are subsequently transferred to  $O_2$ . The most important transition metal in oxidative stress is iron. Studying iron complexation ( $Fe^{2+}$  or  $Fe^{3+}$ ) by antioxidants in aqueous solutions at pH 7.4 is hampered by the formation of insoluble iron by hydroxides. Therefore, iron complexation in an aqueous environment is studied mostly by displacing a known iron chelator (Ou et al., 1995).

In polar but nonaqueous solvents, it was shown that LA forms complexes with  $Mn^{2+}$ ,  $Cu^{2+}$ ,  $Zn^{2+}$ ,  $Cd^{2+}$  and  $Pb^{2+}$  (Sigel et al., 1978). In addition, LA does not chelate  $Fe^{3+}$ . DHLA chelates  $Co^{2+}$ ,  $Ni^{2+}$ ,  $Cu^{2+}$ ,  $Zn^{2+}$ ,  $Pb^{2+}$ ,  $Hg^{2+}$  and  $Fe^{3+}$  resulting in complexes poorly soluble in water. Evidence has been produced that the DHLA complex with  $Fe^{3+}$  is more stable than that with  $Fe^{2+}$  (Sigel et al., 1978).

LA may provide antioxidant activity by chelation of iron. The complexation of metals by DHLA also may result in antioxidant activity. This was suggested for lipid peroxidation induced by  $Cd^{2+}$  (Muller and Menzel, 1990). However, DHLA is also an effective reducing agent for some transition metals, resulting in prooxidant activity. For example, DHLA can easily reduce  $Fe^{3+}$  to  $Fe^{2+}$ . This reduction increase the amount of  $Fe^{2+}$  and consequently promotes ( $Fe^{2+}$ / vitamin C)-induced lipid



peroxidation (Bast and Haenen, 1988). In general, DHLA has to compete with other chelating molecules for metals.

### 3.8 Prooxidant activity

Prooxidant activity is defined as the activity of an antioxidant in a situation where it produces more oxidative stress than antioxidant effect. The ability of a compound to donate an electron to an oxidant can make that compound an antioxidant. Under different conditions, however, exactly the same ability can turn that compound into a prooxidant. This can be demonstrated by thiols. Usually thiols are considered to be antioxidants. However thiols can also promote  $O_2^{\bullet-}$  formation by direct reaction with  $O_2$ . LA and DHLA are thiol containing compounds. They exhibit direct free radical scavenging properties and as a redox couple, with a low redox potential of -0.32 V, is a strong reductant (Cakatay, 2006). Several studies provided evidence that LA supplementation decreases oxidative stress and restores reduced levels of other antioxidants *in vivo*. However, there is also evidence indicating that LA and DHLA may exert prooxidant properties *in vitro* (Moini et al., 2002; Cakatay and Kayali, 2005; Coleman et al., 2006) and *in vivo* (Cakatay and Kayali, 2005; Cakatay et al., 2005; Konrad, 2005). LA through its prooxidant properties acutely stimulates the insulin-signaling cascade, thereby increasing glucose uptake in muscle and fat cells. On the other hand, LA appears to protect the insulin-signaling cascade from oxidative stress-induced insulin resistance through its reducing capacities. In addition, LA seems to inhibit hepatic gluconeogenesis by interfering with fatty acid oxidation, as well as to increase peripheral glucose utilization by activating pyruvate dehydrogenase resulting in increased glucose oxidation. These different properties render LA a potentially attractive therapeutic agent for the treatment of insulin resistance (Konrad, 2005). LA was recently shown to stimulate glucose uptake into 3T3-L1 adipocytes by increasing intracellular oxidant levels and/or facilitating insulin receptor autophosphorylation presumably by oxidation of critical thiol groups present in the insulin receptor beta-subunit (Moini et al., 2002). LA and DHLA can effectively induce apoptosis in human colon cancer cells by a prooxidant mechanism that is initiated by an increased uptake of oxidizable substrates into mitochondria

(Wenzel et al., 2005). DHLA also stimulated  $O_2^{\bullet-}$  production in rat liver mitochondria and submitochondrial particles (Moini et al., 2002). Remarkably, LA inhibits the prooxidant activity of DHLA.

#### **4. *Spinacea oleracea***

Spinach (*Spinacea oleracea*) is a flowering plant in the family Amaranthaceae, native to central and southwestern Asia. It is an annual plant (rarely biennial), which grows to a height of up to 30 cm. Spinach may survive over winter in temperate regions. Spinach is a rich source of iron. In reality, a 60 gram serving of boiled spinach contains around 1.9 mg of iron (slightly more when eaten raw). A good many green vegetables contain less than 1 mg of iron for an equivalent serving. Spinach also has high calcium content. It also is a rich source of Vitamin A, Vitamin C, Vitamin E and several vital antioxidants including LA. It is a source of folic acid, and this vitamin was first purified from spinach (Williams, 1993).

#### **5. Skin**

The skin is the largest and the most heterogeneous organ in a body. It composes of tissues that grow, differentiate and renew themselves constantly. The skin constructs of three major layers: epidermis, dermis and subcutaneous tissue (Touitou et al., 1994)

##### **5.1 The epidermis**

The multilayered structure of the epidermis varies in thickness, depending on cell size and the number of cell layer. The epidermis composes of four strata. It ascending from the proliferative layer of basal cells: the stratum germinativum, the stratum granulosum (the malpighian layer), the stratum lucidum (the granular layer) and stratum corneum (SC, the horney layer). The epidermis changed in an ordered fashion from metabolically active and dividing cells to dense, dead and keratinized protein. The SC is the superficial layer of the epidermis. This region is considered as a nonviable epidermis providing 10-15 layers of much flattened, keratinized dead cells,

stacking up in highly organized units of vertical columns. It is approximately 10-20 micron thick. Previous studies indicated that the SC is not uniformly homogeneous. SC continuously evolves from below to the skin surface, and the layers represent various stages of corneocyte and intercellular lipid maturation. Each SC cell contains mainly of keratin (~70%) and lipid (~20%).

## 5.2 The dermis

The dermis interfaces with the epidermis at the epidermal-dermal junction. It is ten to forty times thicker than the epidermis, depending on site of the body. Dermis makes up the bulk of the skin. The dermis is metabolically less active than the epidermis; it is a matrix of loose connective tissue composed of polysaccharides and protein (collagen and elastin) that embedded in a ground substance containing a variety of lipid, protein and carbohydrate. This matrix contained nerves, blood vessels, hair follicles, sebaceous and sweat glands. The function of the dermis is to nourish the epidermis and to anchor it to the subcutaneous tissue.

## 5.3 The subcutaneous tissue

Subcutaneous tissue serves as a receptacle for formation and storage of fat. The subcutaneous tissue a place for dynamic lipid metabolism; it supports nerve and blood vessels passing to the dermis. The subcutaneous fat spreads all over the body. Its thickness varied with the age, sex, endocrine and nutritional status of the individual. Consequently, the skin is an effective barrier to the penetration of substances including drugs. The skin is an important organ with respect to metabolism and immunology. Due to its heterogeneous structure and its dynamic nature, which could not be maintained in *in-vitro* conditions, only *in-vivo* studies could provide reliable data related to the permeation, metabolism and generally clearance of the drug within and from the skin.

## 6. Delivery system

Current interest in drug delivery technologies is exceedingly high. The transdermal route has the potential to be an extremely efficient site for the delivery system. The skin represents the largest and most easily accessible organ of the human body and provides the most convenient and patient-friendly interface for drug administration. In addition, the transdermal route offers sustained and controlled drug delivery. Despite the fact that the skin represents a suitable target for drug delivery, the functional properties that enable it to act as an excellent barrier also serve to limit the access of active ingredients into and across the epidermis. The keratinised epidermal cells, with their tight junction, form the SC (a membrane of effectively 10–20 $\mu$ m thickness), which forms the permeability barrier, the true barrier for transdermal delivery. The skin is extremely efficient at keeping out large molecular weight agents and therapeutic levels are never going to be realistically achieved by passive absorption.

Enhancement methods are based on two strategies: increasing skin permeability and/or providing a driving force acting on the drug. Based on these strategies, chemical methods (e.g., chemical enhancers, liposomes) or physical methods (phonophoresis, iontophoresis or electrophoresis) have been developed (Prausnitz 1997). Chemical enhancers modify the skin barrier and enhance drug transport across the skin. They promote the transport of both hydrophilic and lipophilic drugs. For better skin delivery technologies, the system should both preserve inherent activity as well as to enhance their benefits through novel formulation and delivery methods.

## 7. Polyrotaxanes (PRx)

Polyrotaxanes (PRx) is a novel nanotechnology for the delivery system. This system is well known as supramolecular assembly in which many cyclic compounds are threaded onto a linear polymeric chain capped with bulky end groups. Complexation of CDs threaded onto poly(ethylene glycol) (PEG) has been thoroughly studied as on the PRx. The average molecular weight of poly(ethylene

glycol) was between 400-10,000 g/mol. PRx containing CDs can be synthesized by first treading many CDs on polymer chain and then blocking the ends of polymer chain with bulky groups (Ooya et al., 2001). Drug conjugated with PRx might have different properties from free drug especially solubility, stability, and penetration (Watanabe et al., 2002).



**Figure 2** Polyrotaxanes structure (Yui and Ooya, 2004)

PRx can increase the solubility of drugs from the hydrophilic external part of PRx and also improves the absorption of active ingredient (Yui and Ooya, 2004). PRx can more or less disrupt the skin membrane and they can also act as real carriers of the active ingredients inside the skin. In this case they are true absorption enhancer. According to the literature, PRx is capable of including phospholipids especially phosphatidylcholine and sphingomyelin, so PRx may effect the permeability of drugs through the skin via the interaction with these components of the skin leading to reversible imbalance of bilayer and increase membrane fluidity (Ooya et al., 1998). The mechanisms of the PRx to enhance the permeability of drugs through the skin have been extensively discussed in relation to:

1. Changing the structure or dissolving skin lipids.
2. Altering the conformation or denaturing skin proteins.
3. Disruption of water structure in skin.
4. Increasing membrane fluidity.

Ooya and Yui (1999) reported that the interaction of PRx with SC was examined by means of a differential scanning calorimetry. The phase transition temperatures of treated and untreated were observed around 60 °C that are different



from other penetration enhancers such as azone and DMSO. The PRx interacted with lipid components in the SC and significantly decreased bound water content although ordered lipid bilayers were maintained (Ooya and Yui, 1999).

## **8. Deoxyribonucleic acid (DNA)**

Deoxyribonucleic acid (DNA) is a nucleic acid that contains the genetic instructions for the development and functioning of living organisms. All living things contain DNA genomes. The main role of DNA in the cell is the long-term storage of information. The genome is often compared to a set of blueprints, since it contains the instructions to construct other components of the cell, such as proteins and RNA molecules. The DNA segments that carry this genetic information are called genes, but other DNA sequences have structural purposes, or are involved in regulating the expression of genetic information. In eukaryotes such as animals and plants, DNA is stored inside the cell nucleus, while in prokaryotes such as bacteria, the DNA is in the cell's cytoplasm. Unlike enzymes, DNA does not participate directly in most of the biochemical reactions it controls; rather, various enzymes act on DNA and copy its information into either more DNA, in DNA replication, or transcribe and translate it into protein. In chromosomes, chromatin proteins such as histones compact and organize DNA, which helps control its interactions with other proteins in the nucleus.

DNA is a long polymer of simple units called nucleotides (Butler et al., 2001), which are held together by a backbone made of sugars and phosphate groups. This backbone carries four types of molecules called bases, and it is the sequence of these four bases that encodes information. The major function of DNA is to encode the sequence of amino acid residues in proteins, using the genetic code. In living organisms, DNA does not usually exist as a single molecule, but instead as a tightly-associated pair of molecules (Watson and Crick, 1974). These two long strands entwine like vines, in the shape of a double helix. The nucleotide repeats contain both the backbone of the molecule, which holds the chain together, and a base, which interacts with the other DNA strand in the helix. In general, a base linked to a sugar is called a nucleoside and a base linked to a sugar and one or more phosphate groups is called a nucleotide. If multiple nucleotides are linked together, as in DNA, this



polymer is referred to as a polynucleotide. The backbone of the DNA strand is made from alternating phosphate and sugar residues. The sugar in DNA is the pentose (five carbons) sugar 2-deoxyribose. The sugars are joined together by phosphate groups that form phosphodiester bonds between the third and fifth carbon atoms of adjacent sugar rings. These asymmetric bonds mean a strand of DNA has a direction. In a double helix the direction of the nucleotides in one strand is opposite to their direction in the other strand. The DNA double helix is stabilized by hydrogen bonds between the bases attached to the two strands. The four bases found in DNA are adenine (A), cytosine (C), guanine (G) and thymine (T). These bases are classified into two types; adenine and guanine are fused five- and six-membered heterocyclic compounds called purines, while cytosine and thymine are six-membered rings called pyrimidines. A fifth pyrimidine base, called uracil (U), usually replaces thymine in RNA and differs from thymine by lacking a methyl group on its ring. Uracil is normally only found in DNA as a breakdown product of cytosine, but a very rare exception to this rule is a bacterial virus called PBS1 that contains uracil in its DNA (Takahashi and Marmur, 1963).

DNA can be damaged by many different sorts of mutagens. These include oxidizing agents, alkylating agents and also high-energy electromagnetic radiation such as ultraviolet light and x-rays. The type of DNA damage produced depends on the type of mutagen. For example, UV light mostly damages DNA by producing thymine dimers, which are cross-links between adjacent pyrimidine bases in a DNA strand (Douki et al., 2003). On the other hand, oxidants such as free radicals or hydrogen peroxide produce multiple forms of damage, including base modifications, particularly of guanosine, as well as double-strand breaks (Cadet et al., 1999). It has been estimated that in each human cell, about 500 bases suffer oxidative damage per day (Shigenaga et al., 1989). Of these oxidative lesions, the most dangerous are double-strand breaks, as these lesions are difficult to repair and can produce point mutations, insertions and deletions from the DNA sequence, as well as chromosomal translocations (Valerie and Povirk, 2003).

## 9. Cancer

ROS within cells act as second messengers in intracellular signaling cascades which induce and maintain the oncogenic phenotype of cancer cells. ROS are tumorigenic by virtue of their ability to increase cell proliferation, survival, cellular migration, and also by inducing DNA damage leading to genetic lesions that initiate tumorigenicity and sustain subsequent tumor progression (Valko et al., 2007). However, it is also known that ROS can induce cellular senescence and cell death and can therefore function as anti-tumorigenic agents. The cumulative production of ROS through either endogenous or exogenous insults is termed oxidative stress and is common for many types of cancer cell that are linked with altered redox regulation of cellular signaling pathways. Oxidative stress induces a cellular redox imbalance which has been found to be present in various cancer cells compared with normal cells; the redox imbalance thus may be related to oncogenic stimulation. DNA mutation is a critical step in carcinogenesis and elevated levels of oxidative DNA lesions (8-OH-G) have been noted in various tumors, strongly implicating such damage in the etiology of cancer. It appears that the DNA damage is predominantly linked with the initiation process (Valko et al., 2006). Therefore, the mechanisms by which cells respond to ROS depends on the molecular background of cell and tissues, the location of ROS production and the concentration of individual ROS species. Carcinoma cells produce ROS at elevated rates *in vitro*, and *in vivo* many tumors appear persistent to oxidative stress (Storz, 2005).

## 10. Apoptosis

### 10.1 Definition

Cell death, a tightly controlled, finely orchestrated event, may be described either as apoptotic or nonapoptotic cell death, traditionally called 'necrosis'. Apoptosis is a process of cell suicide, the mechanisms of which are encoded in the chromosomes of all nucleated cells. Physiological cell death that removes unwanted cells plays an important role in the development, tissue homeostasis and defense

against viral infection and mutation. Apoptosis is regulated by complex molecular signaling systems. Tissue ischemia and reperfusion activate these molecular systems, which therefore represent a therapeutic target for novel treatment to preserve cellular integrity in critical organs such as the brain and heart (Zimmermann and Green, 2001).

Apoptotic cells undergo orderly, energy-dependent enzymatic breakdown into characteristic molecular fragments of deoxyribonucleic acid (DNA), lipids and other macromolecules, which are packaged into small vesicles that may be phagocytosed and reused. The cells involute and die with minimal harm to nearby cells. In contrast 'necrotic' cell death is characterized by inflammation and wide spread damage (Zeiss, 2003).

Apoptosis specially refers to an energy-dependent, asynchronous, genetically controlled process by which unnecessary or damaged single cells self-destruct when the apoptosis genes are activated (Kaufmann and Gores, 2000). Briefly, the cell shrinks and detaches from neighboring cells and the nucleus is broken down. The nuclear fragments and organelles condense and are ultimately packaged in membrane-bound vesicles, exocytosed and ingested by surrounding cells. Membrane integrity is preserved and dyes are only taken up late in the process (Kam and Ferch, 2000). The differences between apoptosis and necrotic cell deaths are summarized in Table 2 (Zeiss, 2003).

**Table 2** Differences between apoptosis and necrosis

<b>Apoptosis</b>	<b>Necrosis</b>
Physiological or pathological	Always pathological
Asynchronous process in single cells	Occurs synchronously in multiple cells
Genetically controlled	Caused by overwhelming noxious stimuli
Late loss of membrane integrity	Early loss of membrane integrity
Cell shrinkage	Generalized cell and nucleus swelling
Condensation of nuclear contents	Nuclear chromatin disintegration
No inflammatory reaction	Inflammatory reaction

## 10.2 Morphological features

There are three distinct phases of apoptosis. During the first phase, the cell detaches from its substratum and adjacent cells with a loss of microvilli and junctional complexes or desmosomes. The DNA is digested by specific endonuclease into fragments and ultimately packed into vesicles. The changes in DNA include strand breakage and condensation of nuclear chromatin. This chromatin appears as characteristic crescent-shaped 'caps' under light microscopes. The endoplasmic reticulum swells and exocytoses its contents. The cell becomes denser as the cytoplasm shrinks and involutes. In the second phase, the cell produces pseudopodia (budding) which contain organelles or nuclear fragments, and these break off into multiple membrane-bound vesicles. The remaining cell becomes a round, smooth membrane-bound remnant (apoptotic body). In the third phase, the cell membrane becomes permeable to dyes such as Trypan Blue. The apoptotic body and membrane-bound buds may then be phagocytosed by macrophages, epithelial cells, vascular endothelium or tumor cells. The entire process occurs may take only 15 min, and therefore may be undetectable on tissue sections (Mikadze and Mamatsashvili, 2006).

The techniques to identify and quantify apoptosis include staining with nuclear stains such as Hoechst 33258 that allow visualization of nuclear chromatin clumping. Modern video microscopy allows visualization of the temporal sequence of events that occur over 15-20 min to 24 h (Oancea et al., 2006).

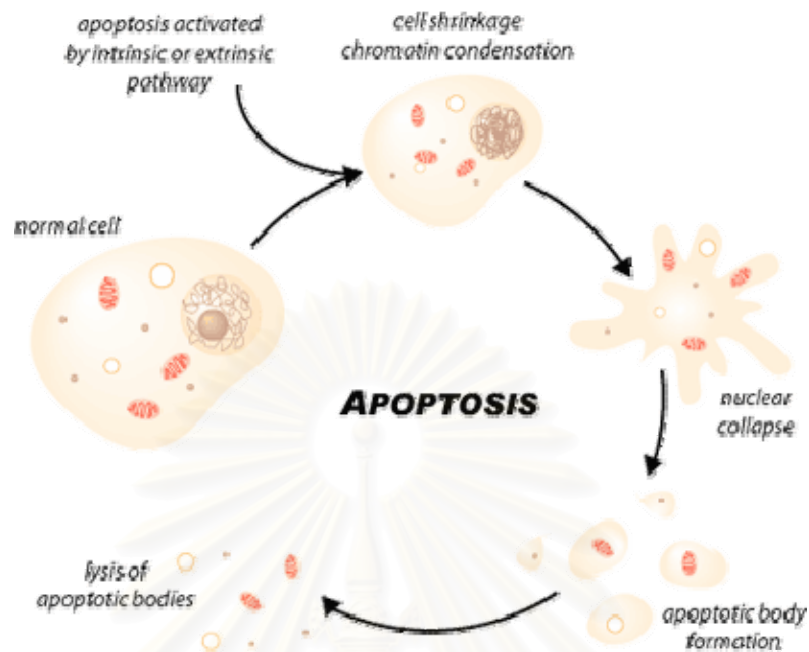


**Figure 3** Apoptosis process (Mikadze and Mamatsashvili, 2006)

### 10.3 Mechanisms of apoptosis pathway

#### 10.3.1 Mitochondrial pathway

The mitochondrion is not only the cell's powerhouse; it is also its arsenal. Mitochondria sequester a potent cocktail of proapoptotic proteins. DNA damage, ischemia and oxidative stress are all examples of apoptotic signals that lead to cell death through the mitochondria. This pathway is induced by the agents that cause direct cell membrane damage including heat, ultraviolet light and oxidizing agents (e. g.  $O_2^{\bullet-}$ ,  $H_2O_2$ ). Excessive production of reaction of ROS, such as  $O_2^{\bullet-}$ ,  $H_2O_2$  and  $OH^-$  damages lipid membranes, proteins nucleic acids and extracellular matrix glycosaminoglycans.

The mitochondrial pathway of apoptosis begins with the permeabilisation of the mitochondrial outer membrane. The mechanisms through which this occurs remain controversial, however, it is thought that permeabilisation



can be either permeability transition pore dependent or independent (Green and Kroemer, 2004). The opening of the permeability transition pore triggers the dissipation of the proton gradient created by electron transport, causing the uncoupling of oxidative phosphorylation. The opening of the permeability transition pore also causes water to enter the mitochondrial matrix, which results in swelling of the intermembranal space and rupturing of the outer membrane causing the release of apoptogenic proteins (Crompton, 1999). Released proteins include cytochrome c (Yang and Cortopassi, 1998), and apoptosis inducing factor (AIF) (Lorenzo et al., 1999; Susin et al., 1999). Cytochrome c in conjunction with apoptosis protease activating factor (APAF-1) and pro-caspase 9 form an 'apoptosome' (Susin et al., 1999; Zou et al., 1999). This complex promotes the activation of caspase 9, which in turn activates effector caspases that collectively orchestrate the execution of apoptosis.

Permeability transition pore independent mitochondrial membrane permeabilisation is regulated by Bcl-2 family members, which are characterised by Bcl-2 homology (BH) domains (Green and Kroemer, 2004). The Bcl-2 family can be subdivided into anti-apoptotic members such as Bcl-2 and Bcl-xL and pro-apoptotic species such as Bax and Bad. Pro-apoptotic members are grouped into two categories based on the expression of BH domains. Multi-domain proteins comprise BH domains 1-3 and include BH3 only proteins consists of Bad, Bik, Bid, Puma, Bim, Bmf and Noxa. The BH3 only proteins activate multi-domain pro-apoptotic species (Korsmeyer et al., 2000; Wei et al., 2000; Letai et al., 2002) and disrupt the function of anti-apoptotic Bcl-2 family members (Letai et al., 2002). It is thought that multi-domain Bcl-2 family members form channels in the outer mitochondrial membrane through which apoptogenic proteins of the intermembranal space are released (Korsmeyer et al., 2000; Nechushtan et al., 2001; Kuwana et al., 2002).

Bcl-2 family is intimately involved in the regulation of cytochrome c crossing the mitochondrial outer membrane. The addition of pro-apoptotic Bcl-2 family members to isolated mitochondria is sufficient to induce



cytochrome c release, whereas overexpression of Bcl-2 family member will prevent it. Interruption of the mitochondrial pathway, which can occur by several different mechanisms, can also enhance tumor cell accumulation. Overexpression of antiapoptotic Bcl-2 family members is widely observed in human cancer cells and is associated with a poor prognosis in several neoplasms. As indicated above, these antiapoptotic Bcl-2 family members appear to exert their effects by blocking cytochrome c release, can also be produced by decreased expression of proapoptotic Bcl-2 family members such as Bax.

### 10.3.2 Death receptor pathway

Death receptors are cell surface receptors belonging to the tumor necrosis factor (TNF) super family, which trigger apoptosis upon ligand binding. The best characterized death receptors are Fas (initially known as CD95 or APO-1) (Dhein et al., 1995; Dhein et al., 1995), TNF-related apoptosis-inducing ligand-R1 (TRAIL-R1) (Tartaglia et al., 1993; Pan et al., 1997), TRAIL-R2 (MacFarlane et al., 1997) and TRAMP (Bodmer et al., 1997).

Fas is a transmembrane glycoprotein death receptor that is activated by binding of Fas ligand (Fas-L) to cell membranes (Ashkenazi and Dixit 1998). Intracellular molecules known as Fas associated death domain (FADD) are produced. Fas receptors are found in epithelial tissues, tumors and haemopoietic tissues, and may be induced in other tissues that do not express them. The Fas pathway is important in controlling the immune response. Cytotoxic T lymphocytes expressing Fas ligands activate cells bearing Fas receptors and induce apoptosis. The TNF receptor system mediates different biochemical pathways. Cancer cells are susceptible to TRAIL-induced apoptosis. Following binding of TNF receptor, intercellular molecules called 'death domains' are produced. A TNF receptor associated death domain (TRADD) has been identified. TNF may suppress apoptosis by binding to the receptor, TNFR2, which activates a protein known as Nuclear Factor kB (NF-kB), classed as an inhibitor of apoptosis (IAP) that prevents the execution phase of apoptosis. It is a DNA binding protein that regulates many pro-

inflammatory genes for the production of cytokines and other pro-inflammatory molecules.

FADD also interacts with pro-caspase-8 to form a complex at the receptor called the death inducing signaling complex (DISC). Once assembled, DISC induces the activation of caspase-8, which in turn precipitates the activation of downstream effector caspases. The BH3 only protein Bid is cleaved by pro-caspase 8 and translocates to the mitochondria to activate the intrinsic pathway (Luo et al. 1998), thereby linking the two death pathways. In addition to death receptors the TNF superfamily comprises decoy receptors (DcR), which inhibit death signaling through the sequestration of ligand. Decoy receptors include DcR1, DcR2 and osteoprotegerin, which bind to TRAIL and DcR3, which binds Fas ligand (Ashkenazi and Dixit, 1999). Death receptor signaling is also regulated by cellular FLICE-like inhibitory protein (c-FLIP) an endogenous inhibitor that interacts with FADD to antagonize apoptosis (Irmeler et al., 1997).

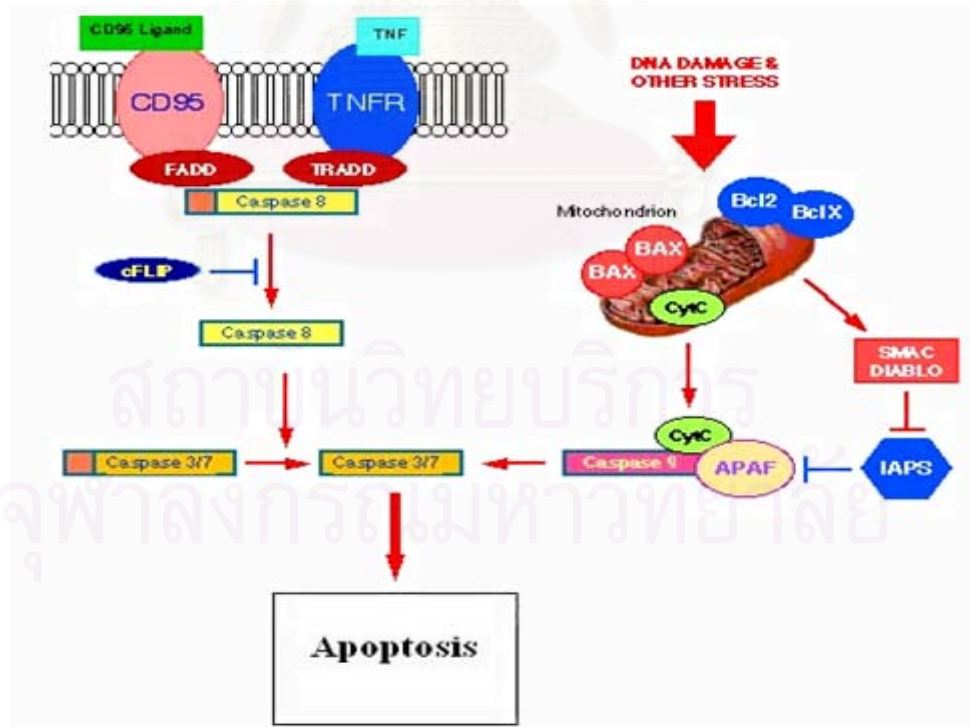


**Figure 4** Apoptosis pathway (Susin, Lorenzo et al. 1999; Zou, Li et al. 1999)

### 10.4 Clinical relevance of apoptosis

Apoptosis has a central role in the pathogenesis of human disease when the genes controlling the apoptotic process are suppressed, overexpressed or altered by mutation. Disordered apoptosis is implicated in a variety of human diseases (Table 3). Research into apoptosis has led to the possibility of new therapeutic approaches to some intractable human diseases (Kam and Ferch, 2000).

**Table 3** Human diseases associated with disordered apoptosis

<b>Apoptosis</b>	<b>Human disease</b>
<b>Increased apoptosis</b>	
Central nervous system	Degenerative diseases (Alzheimer's and Parkinson's disease) Cerebral ischaemia
Myocardium	Peri-infract border zones
Lymphocytes	Lymphocyte depletion in sepsis and HIV infection
Macrophages	Bacillary dysentery ( <i>shigella dysenteriae</i> )
<b>Decreased apoptosis</b>	
Epithelial tissues	Carcinogenesis
Blood vessels	Intimal hyperplasia
Lymphocytes	Autoimmune disorders
Haemopoietic system	Leukemia, lymphoma

### 11. The Bcl-2 family

One of the principle apoptotic regulators is the family of endogeneous Bcl-2 oncoproteins whose members have both pro- and anti-apoptotic activity. The Bcl-2 gene was first identified by Yoshida Tsujimoto in Carlo Croce's lab at the site of translocations characteristic of follicular lymphoma, the most common cancer of

blood cells in humans. Croce was systematically identifying the genes at the breakpoints of translocations in B-cell lymphomas, and naming them Bcl. Bcl-2 is located on chromosome 18. Bcl-2 is divided into three subfamilies:

1. Bcl-2 subfamily ( pro-survival): Bcl-2, Bcl-x<sub>L</sub>, Bcl-w, Mcl-1 and A1;
2. Bax subfamily (pro-apoptotic): Bax, Bak, and Bok;
3. BH3 subfamily (pro-apoptotic) Bad, Bid, Bik, Blk, Hrk, BNIP3 and BimL;

Bcl-2 transfected B-cell were shown to be resisted towards apoptosis. It is the fine control of these proteins which induces or prevents apoptosis in cells. For instance, Bcl-2 and Bcl-x<sub>L</sub> are the two most important anti-apoptotic proteins while Bax , Bad, Bak, Bid, Bik and Bcl-x<sub>S</sub> represent the principle pro-apoptotic ones (Petros et al., 2004). It is believed that the main mode of action of these proteins is through the formation of homo- and heterodimers which, once formed in particular combinations, may result in cellular life or death. For instance, the formation of Bax/Bax homodimer promotes cell death, the Bcl-2/Bcl-2 homodimer provides signals for cell survival and the Bax/Bcl-2 heterodimer protect cell from apoptosis. Bcl-2 protein is inserted post-translationally into intracellular membranes, primarily the outer mitochondrial membranes, the nuclear envelope and the cytosolic face of the endoplasmic reticulum. It is this insertion into membranes that gives this protein the ability to regulate apoptosis (Sharpe et al., 2004). More recent evidence suggests that the Bcl-2 family of protein controls the mitochondrial membrane potential and release of cytochrome c (Hacker and Weber, 2007). Although it is known that this release is mediated by polyprotein channel called the permeability transition pore, the exact mechanism still remains unclear. The control of release of cytochrome c across the mitochondrial membrane by Bcl-2 family is highly important in regulating apoptosis since cytochrome c is one of the major factors necessary for activation of caspase cascade. In fact, it is hypothesized that cytochrome c together with the Apaf –1 cofactor directly activates this cascade through caspase-9 (Alexandre et al., 2006; Malet et al., 2006).

Activation of mitochondrial pathway is likewise tightly regulated. Antiapoptotic Bcl-2 family members inhibit cytochrome c release, possibly by modulating the ability of proapoptotic family members such as Bas and Bak to facilitate opening of the voltage-dependent anion channel in the outer mitochondrial

membrane. Conversely, a subset of the pro-apoptotic Bcl-2 family members (the so-called “BH3” only” family members) appears to facilitate apoptosis by binding to and neutralizing the antiapoptotic family members. The associations between these various apoptotic regulators are not static, but instead reflect phosphorylation-associated changes in affinity of various Bcl-2 family members for each other and for other polypeptides.

It is possible that the Bcl-2 family members control homeostasis of the mitochondria. Apoptosis signals alter mitochondrial physiology (for example, ion exchange or oxidative phosphorylation) such as the organelle swells, resulting in the physical rupture of the outer membrane and release of intermembrane proteins into the cytosol. The need to form a channel large enough for cytochrome c to pass through is thereby neatly bypassed as proteins can be assumed to simply diffuse through the tears in the lipid bilayer.

Mitochondrial homeostasis could be influenced directly by the Bcl-2 family members or indirectly, through modulation of other mitochondrial proteins. The VDAC protein again is prominent candidate for such regulation, as it is a subunit of the mitochondrial permeability transition pore (PTP), a large channel whose opening results in rapid loss of membrane potential and organellar swelling. Opening of the PTP quickly leads to cytochrome c release and apoptotic cell death, and pharmacological inhibitors of the PTP can act as potent inhibitors of cytochrome c release, and hence prevent apoptosis. However, cytochrome c exit can also occur in the absence of membrane potential loss, suggest that the PTP cannot be the sole target of the Bcl-2 family proteins (Alexandre et al., 2006; Malet et al., 2006).

## 12. Cisplatin

Cisplatin or cis-diamminedichloroplatinum(II) is a potent antitumor drug. It has been approved as anti-cancer drug in the USA in 1979. The clinical application of cisplatin has increased enormously. It has become the leading and most widely used anticancer drug (30000 patients are cured each year in the USA). The drug is also registered widely in many other countries. Complete remissions are obtained for testicular cancers in more than 85% of all treated patients, whereas high efficacy in



the treatment of ovarian and bladder cancer and considerable activity in osteogenic sarcoma, head and neck cancer, endometrial and cervical cancer as well as non—small cell lung cancer have been reported (Reedijk and Lohman, 1985; Osman et al., 2000) Cisplatin-based combination chemotherapy regimens are currently used as front-line therapy in the treatment of testicular cancer, ovarian germ cell tumors, epithelial ovarian cancer, head and neck cancer, advanced cervical cancer, bladder cancer, mesothelioma, endometrial cancer, non-small cell lung cancer, malignant melanoma, carcinoids, penile cancer, adrenocortical carcinoma and carcinoma of unknown primary. Cisplatin-based chemotherapy is used with radiation therapy in the treatment of esophageal cancer, localized cervical cancer and head and neck cancer (Curran, 2002). It is used as consolidation therapy for many types of solid tumors that have failed standard treatment regimens.

The therapeutic effects of cisplatin are significantly improved by dose escalation. However, high-dose therapy with cisplatin is limited by its cumulative ototoxicity, hepatotoxicity, nephrotoxicity and neurotoxicity (Vickers et al., 2004; Koc et al., 2005; McDonald et al., 2005; Sastry and Kellie, 2005). All of these toxicity occur after the formation of DNA-platinum adducts (Vickers et al., 2004; McDonald et al., 2005). Experimental evidence indicates that the cytotoxicity of cisplatin is mediated by platinum-DNA mono adducts and intra- and interstrand diadducts (Hah et al., 2006) or the formation of cisplatin metabolites. The acute nephrotoxicity observed is consistent with the concentration-dependent binding of platinum to sulfhydryl groups in the renal tubules (Borch and Pleasants, 1979). Platinum (II) compound has high affinity to sulfur (Borch and Pleasants, 1979) and the platinum anticancer drugs kinetically prefer sulfur over nitrogen donors (Deubel, 2004). Low molecular weight sulfur-containing compounds, sodium thiosulfate, *N*-acetylcysteine (NAC) and glutathione ethyl ester, have shown to rescue cell death from alkylating agent (Muldoon et al., 2001). A large number of sulfur-containing compounds such as procainamide, diethyldithiocarbamate, *N*-methyl-D-glucaminedithio carbamate, methimazole, sulfathiazole and amifostine have been shown to reduce the nephrotoxicity of cisplatin without inhibiting its antitumor effect (Borch and Pleasants, 1979; Jones et al., 1992; Yee et al., 1994; Korst et al., 1998; Osman et al., 2000).

## **13. Electrospray ionization mass spectrometry (ESI-MS)**

### **13.1 History of ESI-MS**

The number of papers presented at the American Society for Mass Spectrometry (ASMS) perhaps best exemplifies the popularity of an ionization technique in the mass spectrometry community. A comparison of the major sample ionization techniques for mass spectrometry shows that electron impact ionization (EI) has had a commanding lead over other ionization techniques over the years. However, since the late 1980's there has been a steady increase in the number of scientific investigations using electrospray ionization (ESI) and a parallel decline in those using EI. Since 1994 ESI has been the most widely used ionization technique (Smith, Snyder et al. 1995). The first reported of the coupling of an ESI source to a mass spectrometer was in 1979 ESI. It has proven to be the ionization source of choice for LC/MS interfacing due to its versatility and applicability to a large number of compounds. The ESI source was first available commercially interfaced to a mass spectrometer in 1989 and has gained immensely in popularity recently. Electrospray ionization has the capability of preserving weak bonds and interactions that may exist in solution. Electrospray mass spectra do not show fragmentation that are characteristic of "hard" ionization methods such as electron impact (EI) where sufficient energy is imparted into the analyte molecules during ionization to cause excessive fragmentation of the analyte. ESI provides a "soft" ionization method, and interfacing with a mass spectrometer provides an instrument capable of studying large and fragile polar molecules such as oligonucleotides and peptides that play important roles in biological systems.

### **13.2 Mechanism of formation of ions**

There are many processes that occur sequentially during the formation of charged ions from liquid solution of the analyte. Charging of the liquid is the first essential step in ESI. This is achieved by flowing the liquid containing the analyte

into a small capillary to which a high voltage is applied. As the charged liquid emerges from the capillary, a droplet forms at the tip. These droplets are then pushed into the gas phase using a bath gas. Assisted by the nebulizing gas and/or heat, the droplets evaporate and form smaller droplets.

### 13.2 Study of noncovalent complexes by ESI-MS

In recent years, mass spectrometry has gained in importance as a technique in the study of noncovalent associations of biomolecules such as proteins and DNA. The gentle nature of ESI has facilitated the production of intact ions of noncovalently associated structures in the gas phase. Generation of multiply charged species by ESI makes the  $m/z$  of large molecules within the mass range of quadrupole and ion trap instruments. Using gentler interface conditions than normally used, ESI-MS has been applied to the study of numerous noncovalent complexes. The studies involving the noncovalently bound heme group in myoglobin (Katta and Chait, 1991), protein-nucleic acid complexes (Veenstra, 1999) and DNA quadruplex structures (Goodlett et al., 1993) were some of the early works in this field.

## CHAPTER III

### METHERIALS AND METHODS

#### MATERIALS

1.  $\alpha$ -Lipoic acid, LA (Sigma Chemical Inc., St. Louis, MO)
2. Dihydrolipoic acid, DHLA (Sigma Chemical Inc., St. Louis, MO)
3. *N*-acetyl cysteine, NAC (Sigma Chemical Inc., St. Louis, MO)
4. Rotenone, ROT (Sigma Chemical Inc., St. Louis, MO)
5. Diphenylene iodonium, DPI (Sigma Chemical Inc., St. Louis, MO)
6. Sodium formate, NaF (Sigma Chemical Inc., St. Louis, MO)
7. Lactacystin, LAC (Sigma Chemical Inc., St. Louis, MO)
8.  $\alpha$ -Cyclodextrin, CD (Sigma Chemical Inc., St. Louis, MO)
9. Cisplatin (Sigma Chemical Inc., St. Louis, MO)
10. Mn(III)tetrakis (4-benzoic acid) porphyrin, MnTBAP (Calbiochem, La Jolla, CA)
11. Catalase (Boehringer Mannheim, Indianapolis, IN).
12. Dichlorofluorescein diacetate, DCF-DA (Molecular Probes, Eugene, OR)
13. Dihydroethidium bromide, DHE (Molecular Probes, Eugene, OR)
14. Hoechst 33342 (Molecular Probes, Eugene, OR)
15. Caspase-8 / FLICE fluorometric substrate, IETD-AMC (Alexis Biochemicals, San Diego, CA)
16. Caspase-9/Mch6 fluorometric substrate, LEHD-AMC (Alexis Biochemicals, San Diego, CA)
17. Caspase-8 inhibitor, z-IETD-fmk (Alexis Biochemicals, San Diego, CA)
18. Caspase-9 inhibitor, z-LEHD-fmk (Alexis Biochemicals, San Diego, CA)

19. Pan-caspase inhibitor, z-VAD-fmk (Alexis Biochemicals, San Diego, CA)
20. Lipofectamine ( Invitrogen, Carlsbad, CA).
21. Monoclonal antibody against Bcl-2 (Santa Cruz Biotechnology, Santa Cruz, CA)
22. Peroxidase-conjugated secondary antibodies (Sigma Chemical Inc., St. Louis, MO).
23. Monoclonal  $\beta$ -actin antibody (Sigma Chemical Inc., St. Louis, MO).
24. Dickerson dodecamer (Integrated DNA Technology , Coralville, IA)
25. DNA sequence 5'-C-C-G-C-G-C-G-C-G-C-C-3' (Integrated DNA Technology , Coralville, IA)
26. DNA sequence 5'-G-G-C-G-C-G-C-G-C-G-G-3' (Integrated DNA Technology ( Coralville, IA).
27. Acetone, analytical grade (Labscan)
28. Ethyl acetate, analytical grade (Labscan)
29. Methanol, HPLC grade (Labscan)
30. Ethanol, HPLC grade (Labscan)
31. Hexane, HPLC HPLC grade (Labscan)
32. Ammonium hydroxide, 28% Ammonia in water (Sigma-Aldrich, St. Louis, MO)
33. Formic acid, LC-MS grade (Sigma-Aldrich , St. Louis, MO)
34. RPMI-1640 medium (Invitrogen, Carlsbad, CA)
35. Fetal bovine serum (Invitrogen, Carlsbad, CA)
36. L-glutamine (Invitrogen, Carlsbad, CA)
37. Penicillin/ streptomycin. (Invitrogen, Carlsbad, CA)
38. Bullet kit CC-3130 ( Cambrex Corp.)
39. EDTA (Invitrogen, Carlsbad, CA)
40. Commercial protease inhibitor mixture (Roche Molecular Biochemicals)



41. Nitrocellulose membrane (Pierce)
42. SRB solution (Sigma-Aldrich , St. Louis, MO)
43. Poly (ethylene glycol) (Suntechno Chemical Co., Tokyo, Japan)
44.  $\alpha$ -Cyclodextrin (Bio-Research Corporation of Yokohama, Yokohama, Japan)
45. Z-L-Phe (Wako Pure Chemical Co.Ltd., Osaka, Japan)
46. Z-L-Arg (Wako Pure Chemical Co.Ltd., Osaka, Japan)
47. *N,N'*-dicyclohexylcarbodiimide (Wako Pure Chemical Co.Ltd., Osaka, Japan)
48. *N*-hydroxysuccinimide (Wako Pure Chemical Co.Ltd., Osaka, Japan)
49. Dimethyl sulfoxide (Nakalai Tesque, Inc., Kyoto, Japan)

## **PLANT MATERIALS**

Sample of fresh spinach was obtained from a local grocery store.

## **MEMBRANES**

Human skin was donated by Phayathai 2 hospital, Bangkok, Thailand.

## **CELLS AND PLASMIDS**

1. Human lung epithelial cell line NCI-H460 (the American Type Culture Collection, Rockville, MD)
2. Normal human dermal fibroblasts CC-2511 (Cambrex Corp., East Rutherford, NJ)
3. The Bcl-2, GPx, and SOD plasmids were provided by Dr. Christian Stehlik (West Virginia University Cancer Center, Morgantown, WV)

## EQUIPMENTS

1. Rotary evaporator (Buchi, USA)
2. High performance liquid chromatography system (Shimadzu, Japan)
  - Liquid chromatography : LC-10ADvp
  - UV-VIS detector : SPD-10Avp
  - System controller : SCL-10Avp
3. Modified Franz diffusion cell
4. Ultracentrifugation (Beckman, USA)
5. Hot air oven (Binder)
6. Ultrasonic bath (Handelman, Han et al.)
7. Vortex mixer (Vortex-genic)
8. Modified column chromatography
9. RF-531PC spectrofluorometer (Shimadzu, Japan)
10. Fluorescence microscopy (Carl Zeiss Axiovert, Göttingen, Germany)
11. Bicinchoninic acid assay kit (Pierce Biotechnology, Rockford, IL)
12. Chemiluminescence (Supersignal<sup>®</sup> West Pico, Pierce)
13. Imaging densitometry using analyst/PC densitometry software (Bio-Rad, Richmond, CA)
14. Centricon<sup>™</sup> YM-3 centrifugal filtration device (Millipore Corporation, Bedford, MA)
15. Finnigan LCQ<sup>™</sup> Deca mass spectrometer (Thermo Electron Corporation, Waltham, MA)
16. The high throughput liquid chromatography (Varian, Inc., Palo Alto, CA)
17. Helix DNA column (Varian, Inc., Palo Alto, CA)
18. Microplate photometer (Titertex Multiskan MC, Flow Laboratories Ltd., Irvine, Scotland)
19. NMR (Varian 300 MHz FT-NMR Gemini 750, Palo Alto, USA)
20. HPLC column C18 : 4.6 ×150mm (Intersil ODS )
21. 0.45- $\mu$ m Minisart SRP 25 filter (Bie & Berntsen, Rodovre, Denmark)
22. UV/VIS Spectrometer V-550 (JASCO, Japan)

## METHODS

### 1. Extraction of $\alpha$ -LA from *Spinacea oleracea*

Fresh *Spinacea oleracea* leaves (1kg.) was dried under 45 °C 10 h until the weight was constant (100g). After that dry spinach was glided and homogenized. After washed twice with 500 mL of light petroleum (b.p. 30–60 °C) to remove a large portion of the carotenoids and waxes, leaves 30 g were extracted with 3 times of 250 mL of TRIS-HCl buffer (50 mM, pH 8.1), D-manitol (0.33 M), EDTA (2.5 mM), magnesium chloride (2 mM), dithiothreitol (3 mM) and sodium ascorbate (2.5 mM). The combined extracts were filtered and centrifuged at 1500 g for 10 min to isolate the chloroplast fraction. The supernatant was centrifuged at 8200 g for 10 min to recover a mitochondrial preparation. The mitochondrial pellet obtained from the precipitate was denatured with boiling 80 % ethanol and centrifuged, and the pellet was extracted three times with 15 mL water to eliminate water soluble substances. Another part was extracted three times with 15 mL ethanol (Edenharder et al., 2001; Lester et al., 2004). The ethanol fraction was evaporated and separated by column chromatography using silica gel as the stationary phase and chloroform-ethanol-water (65:25:4) as the mobile phase.

### 2. DHLA synthesis

LA (6.00 g) was dissolved in 117 mL of 0.25 N sodium bicarbonate ( $\text{NaHCO}_3$ ), and then a total of 1.2 g of sodium borohydride ( $\text{NaBH}_4$ ) was added portionwise. The mixture was well stirred and kept below 5°C. After 30 min 100 mL of toluene was added and the colorless reaction mixture was acidified to pH 1 with ice-cold 5 N HCl. The content of toluene layer was distilled under reduced pressure then characterized using ESI-MS.

### 3. HPLC assay

#### 3.1 Determination of LA

A reverse-phase HPLC assay was developed and validated for the determination of LA. Sample was separated on an Intersil ODS C18 column (4.6 ×150mm, 5 µm particle size) and elute with methanol, water and acetic acid (60: 39.96: 0.04). The mobile phase solution was filtered through 0.45 µm nylon membrane and degassed before use. The injection volume was 10µL, and the elution was isocratic with flow rate 1.0 mL/min. The detection was carried out at 330 nm. The total chromatographic analysis time per sample was 20 min with the retention time of LA elute at 9.758 min.

#### 3.2 Assay validation

Accuracy was performed by triplicated injections of working standard solution and sample solution. The theoretical concentration, the measured concentration and % recovery of LA were determined. Peak area was used to calculate the measured concentration. The method linearity was obtained by plotting the measured concentration versus the theoretical concentration, and the least squares regression equation was calculated. The intra-day precisions were performed by duplicated injections of six replicated sample solutions, and the % CV of peak area of LA was determined. The LOD and LOQ were calculated from the results of analysis of sample solution for validation by plotting the concentration against peak area. The equation for LOD is  $3.3(SD/S)$  where, SD is the residual standard deviation of regression line and S is the slope. The equation for LOQ is  $10 (SD/S)$  where, SD is the residual standard deviation of the regression line and S in the slope.

## 4. LA – PRx complex and cholesterol modified-LA –PRx complex synthesis

### 4.1 Polyrotaxane synthesis

#### 4.1.1 Amino-terminated PEG preparation

PRx was synthesized using  $\alpha$ -CDs, PEG ( $M_n = 1000$  and  $2000$ ) and Z-L-Phe. Amino-terminated PEG was prepared by the following two steps: activation of PEG by chloride substitution of terminal hydroxyl groups in PEG and amination of the activated PEG. PEG 0.02 mole was dissolved in chloroform 50 mL. Then it was slowly added in the bottle containing adipoyl chloride (140 mL) dissolved in chloroform (140 mL). The reaction was done at  $60\text{ }^\circ\text{C}$  under nitrogen condition to eliminate acid chloride. After completely adding PEG, the mixture was stirred for 12-16 h and maintained the temperature at  $60\text{ }^\circ\text{C}$ . Then the solution was poured in the excess amount of ether and stirred to obtain the activated PEG as white powder. The precipitate was washed with ether for 5 times after that it was filtered out and dried under vacuum over night. The activated PEG (18.32g; 7.99 mmol) was dissolved in dichloromethane 100 mL. The mixture was slowly added to ethelene diamine (26.68 mL; 199.75mmol) 5 times of the end group of PEG-Cl that was dissolved in dichloromethane (150 mL). After completely added of activated PEG, the mixture was stirred for 2 h at room temperature under nitrogen condition. Then it was poured in the excess amount of ether to obtain the precipitate as white powder. The precipitate was washed 3 times in ether and dried under vacuum overnight.

#### 4.1.2 Pseudopolyroxtaxane synthesis

Amino-terminated PEG (17.10 g, 7.308 mmol) which was dissolved in water (120 mL) was added to a saturated aqueous solution of  $\alpha$ -CDs (266.38 g, 274.05 mmol) at room temperature and ultrasonically agitated for 2 h, followed by stirred for 24 h. The white precipitate was dried under vacuum freeze dry 3 days then glided.



### 4.1.3 End-capping

The end-capping reaction of the inclusion complex was carried out by using alpha-Benzylloxycarbonyl-L-phenylalanine (Z-L-Phe-OH ; 167.74 g, 560.40 mmol), N-Hydroxybenzotriazole (HOBt ; 113.58g, 840.60 mmol), Benzotriazole-1-yl-oxy-tris-(dimethylamino)-phosphonium hexafluorophosphate (BOP reagent ; 371.78g, 840.60 mmol) in 150 mL of dimethylformamide (DMF), followed by the addition of the inclusion complex (149.30g, 5.604 mmol) and N-ethyl-diisopropylethylamine (DIEA; 840.60 mmol, 143.91 mL). After stirring for 24 h, the solution was poured into excess acetone to obtain as a crude product. After dried under vacuum 2 days, crude product was washed with DMF and water to remove impurities. Then *N,N'*-dicyclohexylcarbodiimide (DCC) was added to the solution and stirred for 20 h at 5°C. After removing *N,N'*-dicyclohexylurea (DCUrea) by filtration, the filtrate was evaporated to obtain a crude product. The crude product was recrystallized from ether and washed in the excess amount of ether. The resulting precipitate was collected by centrifugation and dried in vacuum at room temperature to obtain PRx as a white powder.

### 4.2 PRx -cholesterol conjugation

Cholesterol chloroformate (0.201g, 0.04 mmol) and PRx (0.5g, 0.02 mmol) were dissolved in the mixture of DMSO (10 mL) and DMF (10 mL) then heated up to 60 °C and stirred until dissolved well. After that triethanolamine (62.1 µL, 0.04 mmol) was added and stirred at 60 °C for 3 h under nitrogen atmosphere. The solution was poured in the excess amount of ether to obtain the white precipitate. The crude product was recrystallized from petroleum ether and washed in the excess amount of petroleum ether. The resulting precipitate was collected by centrifugation and dried in vacuum at room temperature to obtain cholesterol modified PRx as a white powder.

### 4.3 LA-PRx complex and cholesterol-modified LA-PRx complex synthesis

PRx (0.5g, 0.02mmol) or cholesterol modified PRx (0.5g) was dissolved in DMSO (4mL) after that LA (0.4g, 1.9mmol) was added and stirred until dissolved in the dark room. DCC (0.8g, 3.8 mmol) was dissolved in DMSO and dichloromethane then added in PRx / cholesterol-modified PRx containing LA. Each preparation was stirred in the dark room for 24 h. After removing DC urea by filtration, the filtrate was evaporated to obtain a crude product. The crude product of PRx was recrystallized from ether and the crude product of cholesterol modified PRx was recrystallized from petroleum ether. The resulting precipitates were collected by centrifugation and dried in vacuum at room temperature to obtain LA-PRx complex and cholesterol-modified LA-PRx as a white powder.

## 5. Characterization

### 5.1 Mass spectrometry

All mass spectra were performed using a Finnigan LCQ™ Deca mass spectrometer equipped with a commercial ESI source. For ESI-MS experiments, nitrogen was used as sheath gas (100psi) at a flow rate of 30 arbitrary units. An electrospray voltage was set at 5.2 kV and a capillary temperature was set at 150 °C. Ions were sampled into the mass spectrometer with an ion injection time set at 200 ms. Three microscans were summed per scan. Samples of LA or DHLA were infused into the source region at a rate of 5  $\mu$ L/min. The oligonucleotide-platinum adducts were also studied in negative mode, but cisplatin adducts were studied in positive mode. The ESI interface and mass spectrometer parameters were optimized to obtain maximum sensitivity. MS/MS and MS<sup>n</sup> experiments were performed using isolation with of 4 Th. The relative collision energy was control between 5-25% of maximum, depending on the precursor ion and the MS<sup>n</sup> stage.

## 5.2 NMR Spectroscopy

The chemical structure of polyrotaxanes (PRx), modified cholesterol PRx and the content of the  $\alpha$ -CDs were characterized using the 300 MHz  $^1\text{H}$ -NMR spectroscopy. PRx 15 mg was dissolved in DMSO 700  $\mu\text{L}$  and then measured NMR spectrum.

## 5.3 UV Spectrometry

The complex of LA-PRx and cholesterol modified LA-PRx was characterized using UV spectrometry. The amount of each preparation 10 mg was dissolved in 2mole/L NaOH 1 mL and measures the absorbance at 208.

# 6. Penetration study

## 6.1 Skin preparation

The human skin specimens came from male and female patients of age 25-45 years who underwent abdominal plastic surgery. Immediately after removal, the skin specimens were wrapped in saline-moistened gauze and transported on ice. The skin was stored at  $-70\text{ }^\circ\text{C}$  until use. Before use, the skin was thawed for 1 h at room temperature and subcutaneous fat was removed with scapel. The epidermal membrane was separated from dermis by immersing the skin for 1 min in water at  $60\text{ }^\circ\text{C}$ . The epidermal membrane was then peeled off by forceps. SC was isolated from epidermal membrane by incubation in 1% solution of trypsin in PBS (pH 8.0) for 4 h at  $37\text{ }^\circ\text{C}$  then peeling off by forceps. SC was rinsed 3 - 5 times with deionized water to remove remaining epidermal cells. The skin samples were used immediately.

## 6.2 Penetration study

Modified Franz diffusion cell was used to study the permeation. They consisted of donor and receptor compartments. The donor compartment was secured to the receptor compartment using a clamp. SC was mounted on the receptor compartment with the SC side facing upward into the donor compartment. The donor compartment was filled with the formulation. The top of the diffusion cell was covered with paraffin film. The dorsal region of the skin was faced to the donor chamber and LA in the different preparation (2 mg of LA/mL, 2.0 mL) was applied on this region. The diameter of the Franz cell was 1.6 cm corresponding to an effectively permeable area of 2.01 cm<sup>2</sup>. The receptor chambers contained 10 mL of 0.1%  $\gamma$ -CD in PBS was used as the receptor fluid. The temperature of receptor fluid was maintained at 37  $\pm$ 1°C to produce a skin surface temperature of 32  $\pm$  1°C with continuously stirring by a magnetic bar. LA in 50 % ethanol in water (2.0 mg/mL, 2.0mL) was used as control. Two milliliters of receptor fluid was collected every h for 24 h. After the receptor medium was withdrawn, an equal volume of fresh receptor solution was immediately replaced. The collected solutions were analyzed by HPLC. The standard LA solution for HPLC analysis was prepared at 2  $\mu$ g/mL. The cumulative amount of LA and the flux of LA from PRx and cholesterol modified PRx in the receptor compartment were calculated in  $\mu$ g and  $\mu$ g/h/cm<sup>2</sup>, respectively.

## 7. Cytotoxicity assay

### 7.1 Normal human dermal fibroblasts culture.

Normal human dermal fibroblasts (NHDF) were cultured using an FGM Bullet kit CC-3130 containing 500 mL of fibroblast basal medium supplemented with huma fibroblast growth factor-2 (hFGF-2), insulin, fetal bovine serum (FBS), and gentamycin/amphotericin-B. Cells cultures were maintained in a humidified atmosphere of 5% CO<sub>2</sub> at 37°C. Cells were passaged at preconfluent densities by the use of a solution containing 0.05% trypsin and 0.5 mM EDTA.

## 7.2 Cytotoxicity assay of LA, LA-PRx complex and cholesterol modified LA-PRx complex

The effect of cell growth was determined by quantitation of cell mass of the surviving monolayer colorimetrically after staining with basic dye methylene blue. Cells were seeded at  $10^4$  cells/well in 96-well microtiter plate and incubated for 24 h to confluence. After that cells in each well were treated with each treatment then incubated at 37 °C and 5% CO<sub>2</sub> for 24 h. After 24 h treatment, cells in each well were washed twice with 200 µL of PBS. Cells were then fixed by adding 100 µL of 10% formalin in PBS to each well for 30 min and followed by adding methylene blue in 0.01 M –borate buffer (pH8.5) to each well. After 30 min, excess dye was removed by five wash with borate buffer. Bound methylene blue was extract with 100 µL of 1:1 (v/v) ethanol and 0.1 M HCl. The plates were then gently shaken and quantitated at the absorbance 650 nm by microplate photometer.

## 8. The effect of LA, LA-PRx complex and cholesterol modified LA-PRx complex on cell growth

NHDF was cultured followed the procedure on 7.1. Cell proliferation was evaluated by the quantitative sulphorhodamine B (SRB) colorimetric assay where the amount of dye bound to cells after staining gives a measure of cell growth. Cells were seeded on 96-well plates at a concentration of 10,000 cells per well and incubated at 37 °C in 5% CO<sub>2</sub> incubator. Twenty –four h later, cells were treated with different concentrations of LA, LA -PRx complex and cholesterol modified LA- PRx complex, and exposed for 48 h. At the end of the incubation, cells were fixed with 50% trichloroacetic acid (1 h at 4 °C), washed with distilled water, air dried, and stained for 30 min at room temperature with 50 µL of 0.4% w/v SRB solution in 1% acetic acid. Unbound SRB was then removed and cells were quickly rinsed four times with 1% acetic acid. After air-drying, protein- bound SRB was solubilized in 150 µL 10 mM Tris buffer for 5 min on gyratory shaker. The pink SRB was quantified by measuring the optical density at 540 nm. The percentage growths were calculated using the



following formula, if T is greater than or equal to  $T_0$ , percentage growth =  $100[(T-T_0)/(C-T_0)]$  and if T is less than  $T_0$ , percentage growth =  $100 [(T-T_0/T_0)]$ .

Where T is optical density of test, C is the optical density of control, and  $T_0$  is the optical density at time zero. From the percentage growths, a dose response curve was generated and  $IC_{50}$  values were interpolated from the growth curves.

## **9. The effect of LA, DHLA, LA-PRx complex, cholesterol modified LA-PRx complex on DNA-Damage**

### 9.1 Effect of cisplatin (PT) on double strand DNA (dsDNA)

#### 9.1.1 DNA preparation

Each DNA was washed four times with 1 M ammonium acetate at pH 7.4 using a Centricon® YM-3 centrifugal filtration device to replace sodium counterions with ammonium. The DNA concentrations in the stock solutions were diluted 1-10 times and determined by UV measurements at 260 nm by a Beckman DU® 640 spectrophotometer using the Oligo Quant module. The recovered oligonucleotide was annealed by heating the solution to 95 °C and cooling gradually over 3 h to room temperature. To ascertain the presence of DNA duplexes thermal denaturation experiments were performed using a heated circulating water bath with the Beckman DU® 640 spectrophotometer.

#### 9.1.2 DNA-platinum adduct preparation

The stock solution of cisplatin (PT; 0.33 mM initial concentration) was prepared in deionized water. Cisplatin in the different molar ratios (1-10 times of DNA) were incubated with self-complementary double strand DNA (Dickerson dodecamer) at 37 °C. The formation of adducts was studied at 0.5, 1.0, 2.0, 3.0, 4.0 and 24 h after incubation. The adducts were studied using ESI-MS and dHPLC at 260 nm.

### 9.1.3 Double strand DNA analysis using dHPLC

The high throughput denaturing high performance liquid chromatography (dHPLC)/autosample system was used to detect dsDNA. The standard double strand DNA(dsDNA) and adducts were done by injecting (5 $\mu$ L) samples into a Helix DNA column, 3.0 x 75 mmID. Samples were eluted with a mobile phase of solvent A [100 mM triethylammonium acetate (TEAA), pH 7.0, 0.1 mM ethylenediamine tetraacetic acid (EDTA)] and solvent B (100 mM TEAA, pH 7.0, 0.1mM EDTA and 25% acetonitrile) at oven temperature 50 °C and UV detection at 260 nm. Separation was achieved by gradient elution conditions with flow rate of 0.3 mL/min at the first 6 min and flow rate of 0.5 mL/min at the last 5 min.

## 9.2 The effect of LA and DHLA on DNA protection

9.2.1 Effect of LA and DHLA on the formation of DNA-platinum adducts determined by dHPLC

LA or DHLA (10-40 times of PT) were dissolved in NH<sub>4</sub>OH and added into the solution that contained cisplatin (PT) and self-complementary double strand DNA (Dickerson dodecamer) then incubated at 37 °C for 0.5, 1.0, 2.0, 3.0, 4.0 and 24 h. The adducts were studied using dHPLC.

9.2.2 Effect of LA and DHLA on the formation of DNA-platinum adducts determined by ESI-MS

LA or DHLA in equal molar of cisplatin (PT) was immediately added to the system containing dsDNA (Dickerson dodecamer ; 1:10 mole). The mixture was incubated at 37 °C for 24 h. The dsDNA-platinum adducts were studied using ESI-MS in negative mode. Acetic acid (AA) also was added in the same molar ratio of LA and DHLA to study the protection effect of dsDNA.

### 9.2.3 DNA-platinum adduct of non self-complementary dsDNA (heteroduplex undecamer)

The same procedures as 9.1.1-9.2.2 were conducted using non self-complementary dsDNA (heteroduplex undecamer) and single strand DNA (ssDNA) instead of self-complementary dsDNA. ESI-MS in negative mode and dHPLC were used in this study.

### 9.2.4 The effect of LA, DHLA, antioxidants and chelating agent on DNA protection

Each 100  $\mu\text{M}$  of self-complementary double strand DNA (Dickerson dodecamer) or non self-complementary double strand DNA (heteroduplex undecamer) was incubated with cisplatin (100 $\mu\text{M}$ ) and LA, DHLA, NAC, GSH or EDTA (100  $\mu\text{M}$ ) at 37 °C for 4 h. The amount of each dsDNA was studied using dHPLC.

### 9.2.5 The effect of LA, DHLA, sulfur containing antioxidants and chelating agent on DNA recovery

Each 100  $\mu\text{M}$  of self-complementary double strand DNA (Dickerson dodecamer) or non self-complementary double strand DNA (heteroduplex undecamer) was incubated with cisplatin (100 $\mu\text{M}$ ) at 37 °C for 4, 12 and 24 h. The amount of each dsDNA was studied by dHPLC to ensure that dsDNA was damaged at 4h. After that LA, DHLA NAC, GSH or EDTA (100  $\mu\text{M}$ ) was added in those damage DNA then incubated at 37 °C for 4 h. The amount of each dsDNA was studied again using dHPLC.

9.3 The effect of LA, LA-PRx complex and cholesterol modified LA-PRx complex on DNA protection

LA, LA-PRx complex or cholesterol modified LA-PRx complex (100  $\mu\text{M}$ ) was added into the solution that contained cisplatin and self-complementary double strand DNA (Dickerson dodecamer) then incubated at 37 °C for 0.5, 1.0, 2.0, 3.0,4.0 and 24 h and analyzed for the percentage of dsDNA by dHPLC.

## **10. Apoptosis assay of human epithelial lung cancer H-460 cells**

10.1 The effect of cisplatin induced apoptosis in human epithelial lung cancer H-460 cells

### 10.1.1 Human epithelial lung cancer H-460 cell culture

Human epithelial lung cancer H-460 cells were cultured in RPMI-1640 medium. The medium supplemented with 5% fetal bovine serum (FBS) and 2 mM L-glutamine, and 100 units/ml penicillin/ streptomycin. Cells cultures were maintained in a humidified atmosphere of 5% CO<sub>2</sub> at 37°C. Cells were passaged at preconfluent densities by the use of a solution containing 0.05% trypsin and 0.5 mM EDTA.

### 10.1.2 Apoptosis study

The completely confluent cultured H-460 cells were treated with various concentration of cisplatin (0-500  $\mu\text{M}$ ) for a 12 h time period. The incidence of apoptotic cells were determined by Hoechst 33342 nuclear staining in cultured H460 cells. The apoptotic cells exhibited shrunken nuclei, chromatin condensation, and nuclear fragmentation. Apoptosis was determined by incubating the H-460 cells with 10  $\mu\text{g}/\text{mL}$  Hoechst 33342 for 30 min at 37°C and scoring the percentage of cells having intensely condensed chromatin and/or fragmented nuclei by fluorescence microscopy using a Pixera software (n = 300).

## 10.2 The effect of LA and DHLA on cisplatin induced apoptosis in H-460 cells

The completely confluence cultured H-460 cells were pre-treated with LA or DHLA (0-500  $\mu\text{M}$ ) for 0.5 h. After that H-460 cells were treated with 250  $\mu\text{M}$  cisplatin for 12 h. The incidence of apoptotic cells were determined by Hoechst 33342 nuclear staining in cultured H460 cells. The apoptotic cells exhibited shrunken nuclei, chromatin condensation, and nuclear fragmentation. Apoptosis was determined by incubating the H-460 cells with 10  $\mu\text{g/mL}$  Hoechst 33342 for 30 min at 37°C and scoring the percentage of cells having intensely condensed chromatin and/or fragmented nuclei by fluorescence microscopy using a Pixera software (n = 300).

## 10.3 LA and DHLA induced apoptosis in H460 Cells

The H-460 cells were treated with various concentrations of LA or DHLA (0-100  $\mu\text{M}$ ) for 24 h, and apoptosis was determined by Hoechst 33342 nuclear staining fragmentation. The apoptotic cells exhibited shrunken nuclei, DNA fragmentation, and intense nuclear fluorescence.

## 10.4 Effect of antioxidants on LA- and DHLA-induced apoptosis

H460-cells were pre-treated for 1 h with NAC (100 $\mu\text{M}$ ), catalase (1000 U/mL), MnTBAP (100 $\mu\text{M}$ ), sodium formate (10mM) and then treated with LA or DHLA (100  $\mu\text{M}$ ) for 24 h. Apoptosis was determined by Hoechst 33342 nuclear straining fragmentation. The apoptotic cells exhibited shrunken nuclei, DNA fragmentation, and intense nuclear fluorescence.



## 11. LA and DHLA induce caspase activation

Caspase activity was determined by fluorometric assay using the enzyme substrate Ile-Glu-Thr-Asp (7-amino-4-trifluoromethyl coumarin) (IETD-AMC) for caspase-8 and N-acetyl-Leu-Glu-His-Asp-AFC (7-amino-4-trifluoromethyl coumarin) (LEHD-AMC) for caspase 9, which are specifically cleaved by the respective enzymes at the Asp residue to release the fluorescent leaving group, amino-4-methyl coumarin (AMC). H460 cells were pre-treated with caspase-9 inhibitor z-LEHD-FMK (10 $\mu$ M) or pan-caspase inhibitor z-VAD-FMK (10  $\mu$ M) for 1 h. Then 100  $\mu$ M of LA or DHLA was added and incubated for 6 h. Cell extracts were performed by incubating the cells in lysis buffer containing 20 mM Tris-HCl (pH 7.5), 1% Triton X-100, 150 mM sodium chloride, 10% glycerol, 1 mM sodium orthovanadate, 50 mM sodium fluoride, 100 mM phenylmethylsulfonyl fluoride, and a commercial protease inhibitor mixture for 30 min on ice. After insoluble debris was pelleted by centrifugation at 14,000g for 15 min at 4°C, the supernatants were collected and assayed for protein content using a bicinchoninic acid assay kit. Cell extracts containing 50  $\mu$ g protein were incubated with 100 mM 4-(2-hydroxyethyl)-1-piperazine ethanesulfonic acid (HEPES) containing 10% sucrose, 10 mM dithiothreitol, 0.1% 3-[(3-chloroamidopropyl)-1] propane sulfonate, and 50  $\mu$ M caspase substrate in a total reaction volume of 0.25 mL. The reaction mixture was incubated for 2 h at 37°C. At the end of incubation, the liberated fluorescent group AMC was determined fluorometrically at the excitation and emission wavelengths of 380 nm and 460 nm, respectively.

## 12. LA and DHLA induced ROS generation

### 12.1 ROS generation assay

The subconfluent (90%) monolayers of H460 cells were treated with varying doses of LA or DHLA (0–100  $\mu$ M) 1 h. Intracellular hydroperoxide and superoxide anion production were determined by flow cytometry using dichlorofluorescein diacetate (DCF-DA) and dihydroethidium bromide (DHE) as

fluorescent probes. H-460 cells ( $1 \times 10^6$ /mL) were incubated with the probes (10  $\mu$ M) for 30 min at 37°C, after that they were washed, resuspended in phosphate buffered saline (PBS), and analyzed for fluorescence intensity using FACS Caliber at the excitation and emission wavelengths of 488 nm and 538 nm respectively for DCF fluorescence measurements, and at 488 nm and 610 nm for DHE measurements. The median fluorescence intensity was quantitated by CellQuest software analysis of the recorded histograms.

### 12.2 The effect of antioxidants on LA- and DHLA-induced ROS

H460 cells were treated with NAC (100  $\mu$ M), catalase (1000U/mL), MnTBAP (100  $\mu$ M), or sodium formate (10 mM) for 1 h. The cells were then treated with LA or DHLA (100  $\mu$ M) for 1 h and analyzed by flow cytometric analysis of ROS using DCF and DHE as fluorescence probe. The median fluorescence intensity was quantitated by CellQuest software analysis of the recorded histograms.

## 13. Responsibility of mitochondrial ROS on LA-induced apoptosis

To determine the cellular source of ROS induced by LA, H-460 cells were treated with LA in the presence or absence of diphenylene iodonium (DPI), a specific inhibitor of NADPH oxidase (Freeman and Crapo, 1982), or rotenone, a mitochondrial electron transport chain interrupter (Chen et al., 2003), and their effects on apoptosis and ROS generation were examined. H-460 cells were pre-treated with diphenylene iodonium (DPI) or rotenone (ROT) 1  $\mu$ M for 1 h. After that cells were treated with LA (100  $\mu$ M) for another 1 h, and analyzed by flow cytometric analysis of ROS using DCF and DHE as fluorescence probe. The median fluorescence intensity was quantitated by CellQuest software analysis of the recorded histograms.

## **14. The effect of antioxidant and Bcl-2 overexpression on LA-Induced apoptosis and ROS generation**

### 14.1 Effect of ROS on LA induced apoptosis using GPx and SOD overexpression cells

Authenticity of all plasmid constructs was verified by DNA sequencing. Stable transfectants of Bcl-2, glutathione peroxidase (GPx), and superoxide dismutase (SOD) were generated by culturing H-460 cells in a 6-well plate until they reached 80% confluence. One microgram of cytomegalovirus-neo vector and 15 µg of Lipofectamine reagent with 2 µg of Bcl-2, GPx, SOD, or control pcDNA3 plasmid were used to transfect the cells in the absence of serum. After 10 h, the medium was replaced with culture medium containing 5% FBS. Approximately 36 h after the beginning of the transfection, the cells were digested with 0.03% trypsin and the cell suspensions were plated onto 75-mL culture flasks and cultured for 24-28 d with G418 selection (400 µg/mL). Stable transfectants were identified by Western blot analysis and were cultured in G418-free RPMI medium for at least two passages before each experiment.

H-460 cells were either left untreated or pretreated with NAC (100 µM), catalase (1000U/mL), or MnTBAP (100 µM) for 1 h, followed by LA treatment (100 µM) for 9 h. The transfected cells, GPx-, SOD-, or mock-transfected cells, were treated with LA (100 µM) for 9 h. Cell lysates were then prepared and analyzed for Bcl-2 expression by Western blotting.

### 14.2 Effect LA on Bcl-2 level

Transfected cells were prepared according to 14.1 then they were treated with proteasome inhibitor, lactacystin, (LAC ; 10µM) for 1 h. Then with varying doses of LA (0–100 µM) was added. The degradation of Bcl-2 protein was studied at various times (0-9 h) using Western blotting assay.

### 14.3 Western blotting assay

H-460 cell extracts were performed by incubating the cells in lysis buffer containing 20 mM Tris-HCl (pH 7.5), 1% Triton X-100, 150 mM sodium chloride, 10% glycerol, 1 mM sodium orthovanadate, 50 mM sodium fluoride, 100 mM phenylmethylsulfonyl fluoride, and a commercial protease inhibitor mixture for 30 min on ice. After insoluble debris was pelleted by centrifugation at 14,000g for 15 min at 4°C, the supernatants were collected and assayed for protein content using a bicinchoninic acid assay kit. Equal amount of proteins per sample (20 µg) were resolved on a 10% sodium dodecyl sulfate-polyacrylamide gel electrophoresis (SDS-PAGE) and transferred onto 0.45-µm nitrocellulose membrane. The transferred membranes were blocked for 1 h in 5% non-fat dry milk in TBST (25 mM Tris-HCl pH 7.4, 125 mM NaCl, 0.05% Tween-20) and incubated with appropriate primary antibodies at 4°C overnight. Membranes were washed three times with TBST for 10 min, incubated with peroxidase-labeled isotype-specific secondary antibodies for 1 h at room temperature. The immune complexes were detected by chemiluminescence and quantified by imaging densitometry using analyst/PC densitometry software. Mean densitometry data from independent experiments were normalized relative to result in cells in the control. The data were presented as the mean  $\pm$  S.D. and analyzed by the Student's *t* test.

## CHAPTER IV

### RESULTS AND DICCUSSION

#### 1. Extraction of LA from *Spinacea oleracea*

The crude extract of *Spinacea oleracea* was separated and purified . The fraction that contained LA was corrected. The total yield of LA from this extraction is 1g from *Spinacea oleracea* 68 kg. The yield of LA from this experiment was very low because there is a few amount of free form of LA in leaving cells. Most of LA in plants and animals covalently bound with protein (Kang et al., 2007) in form of lipoate-protein ligase in mitochodria (Morris et al., 1994; Taylor et al., 2004). So the simple solvent extraction might not be appropriate for extraction the active ingredient that tightly bound with protein. The extraction method might need to develop for the further study.

#### 2. DHLA synthesis

The total yield of DHLA that was synthesized from LA was 91%. The synthesis of DHLA was followed the method of Gunsalus et al (1956). Yield of DHLA was very high and constant for each synthesis.

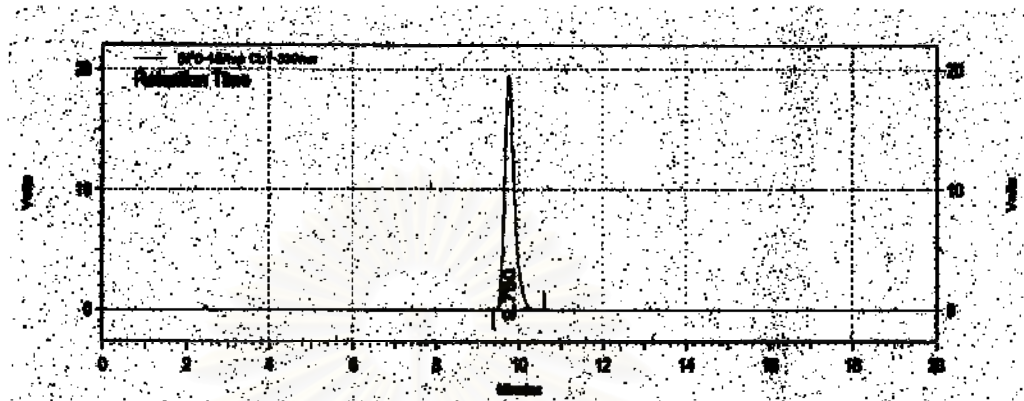
#### 3. HPLC assay

##### 3.1 Determination of LA

The fractions of crude extract from *Spinacea oleracea* were collected. Each fraction was analyzed by HPLC using LA from sigma as a standard (Figure 5A). The fraction containing LA was measured at 330 nm. The retention time was 9.758 (Figure 5B).



A



B

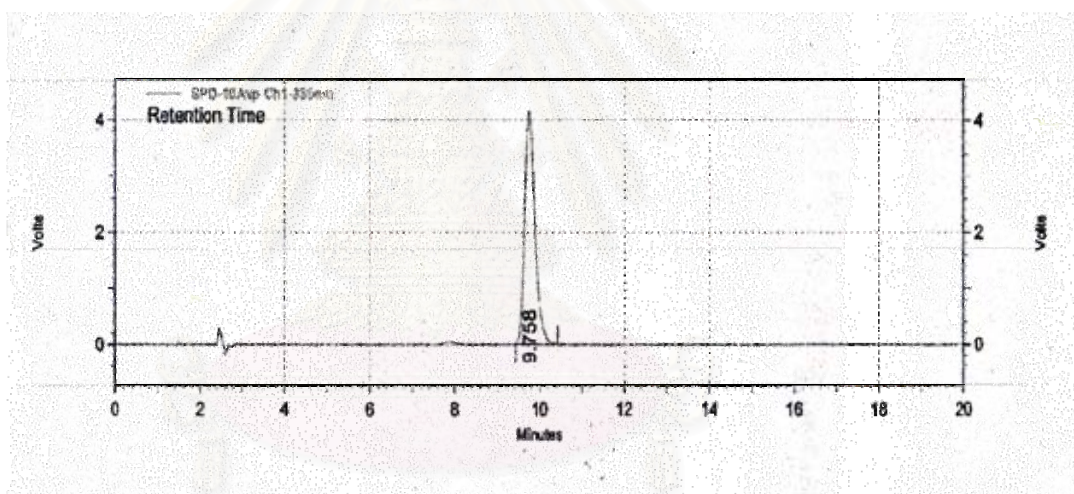


**Figure 5** The chromatogram of standard LA from Sigma (A) and LA from *Spinacea oleracea* (B)

### 3.2 Assay validation

The % recovery of the concentration of LA in the sample solutions for validation are shown in Table 4. The accuracy of triplicated determination across six concentrations gave the mean % recoveries of 97.86-99.47(See details in Tables 9, Appendix B). The intraday precision of assay for quantification gave coefficient of

variation (%CV) 0.47-0.97(See details in Tables 9, Appendix B). The precision of six determinations of LA 2 µg/mL provided mean %recoveries and %CVs of 99.36 (0.43), (Table 5). The obtained %recoveries (between 98.97-99.77) and %CVs (<1).This result indicated satisfactory accuracy and precision. The linearity curves were constructed by plotting the theoretical concentration and the measured concentrations. The curves were linear, ranging from 0.53-3.01 µg/mL. The regression analysis parameters of the calibration curves are shown in Figure 4 and summarized in Table 6 (See details in Table 11). The high coefficients of determination ( $r^2= 0.9999$ ) indicated high degree of correlations. The LOD was 0.28 µg/mL (See details in Table 12, Appendix B). The LOQ was 0.87 µg/mL (See details in Table 12, Appendix B). The validation results demonstrated good accuracy, precision, linearity, range and specificity of the method.

**Table 4** Accuracy (%recovery) and intra-day precision (%CV) of assay for quantification of LA ( $n = 3$ ) (See details in Tables 9, Appendix B)

Theoretical Conc. (µg/mL)	Measured Conc. (µg/mL)	Recovery (%)	SD	CV (%)
0.53	0.5272	99.47	0.0039	0.7465
1.0032	0.9817	97.86	0.0080	0.8102
1.5206	1.5089	99.23	0.0073	0.4843
2.0104	1.9922	99.09	0.0093	0.4672
2.5507	2.5059	98.24	0.0243	0.9685
3.0103	2.9682	98.60	0.0194	0.6522

**Table 5** Precision (%CV) of assay for quantification of LA ( $n = 6$ ) (See details in Tables 10, Appendix B)

Theoretical Conc. ( $\mu\text{g/mL}$ )	Measured Conc. ( $\mu\text{g/mL}$ )	Average Measure Conc. ( $\mu\text{g/mL}$ )	Recovery (%)	Average (Range)	CV (%)	SD
2.0104	2.0004	1.9975	99.50	99.36	0.4289	0.0086
2.0104	1.9821		98.59	(98.97-99.77)		
2.0104	1.9942		99.19			
2.0104	2.0058		99.77			
2.0104	1.9983		99.40			
2.0104	2.0039		99.66			

**Table 6** Linear regression analysis parameters for quantification of LA (See details in Tables 11 and Figures 24, Appendix B)

Theoretical Conc ( $\mu\text{g/mL}$ )	Measured Conc ( $\mu\text{g/mL}$ )	Intra-day		
		slope	y-intercept	$r^2$
0.5300	0.5272	0.9844	0.0041	0.99992266
1.0032	0.9817			
1.5206	1.5089			
2.0104	1.9922			
2.5507	2.5059			
3.0103	2.9682			

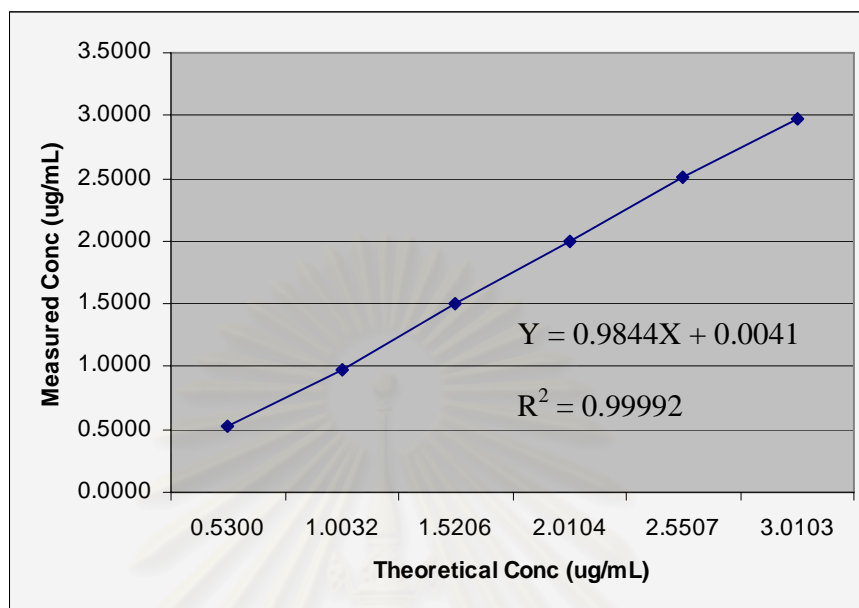


**Figure 6** The calibration curve of LA

#### 4. LA – PRx complex and cholesterol modified-LA –PRx complex synthesis

##### 4.1 PRx synthesis

Polyethylene glycol (PEG)  $M_n = 1000$  or PEG  $M_n = 2000$  was prepared in the form of amino-terminated PEG to obtain the white precipitate powder. Then they were reacted with  $\alpha$ - cyclodextrins (CDs). The reaction is shown in Figure 5. According to the result, PEG  $M_n 1000$  could not form white precipitate hydrolysable PRx. PEG  $M_n 2000$  could form hydrolysable PRx with 5 CDs. The molecular weight of this PRx is 7762.66.

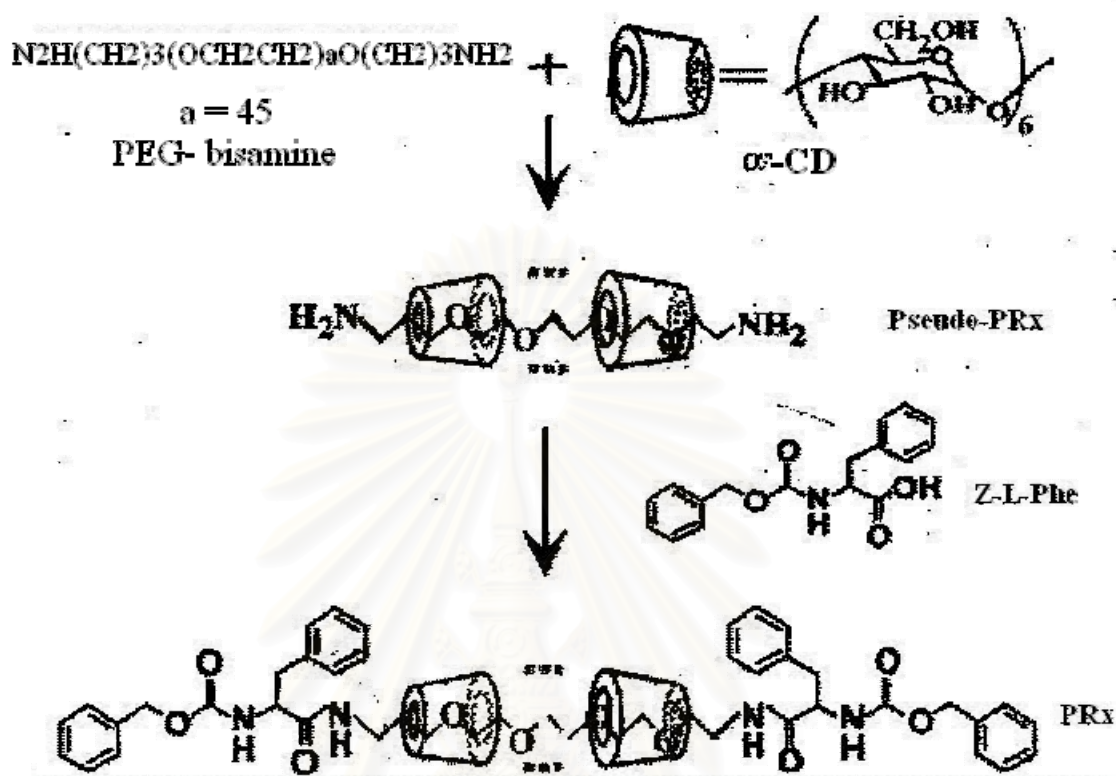


Figure 7 The synthetic procedure of PRx

#### 4.2 Cholesterol modified PRx synthesis

The modification of cholesterols to PRx was prepared by introducing cholesterol to PRx. The cholesterol was conjugated with PRx using ester bond. The calculation from NMR spectrum of cholesterol modified PRx showed that cholesterol 1 mole was introduced to PRx 1 mole (Figure 15B). The reaction is shown in Figure 6 and 7. The molecular weight of cholesterol modified PRx is 8251.6420.



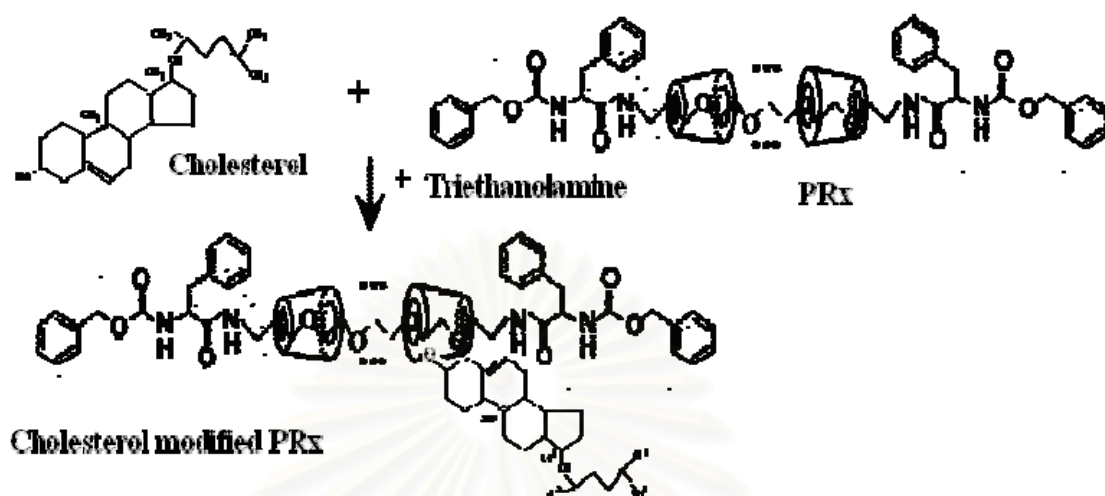


Figure 8 The synthetic procedure of cholesterol modified PRx

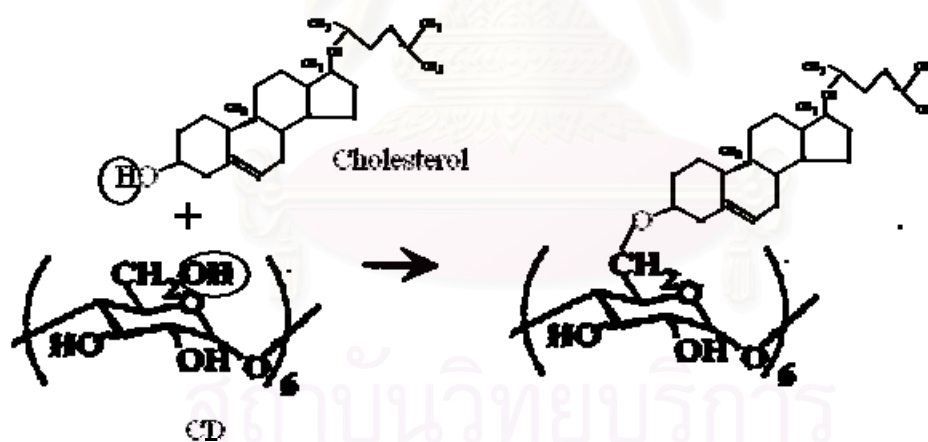
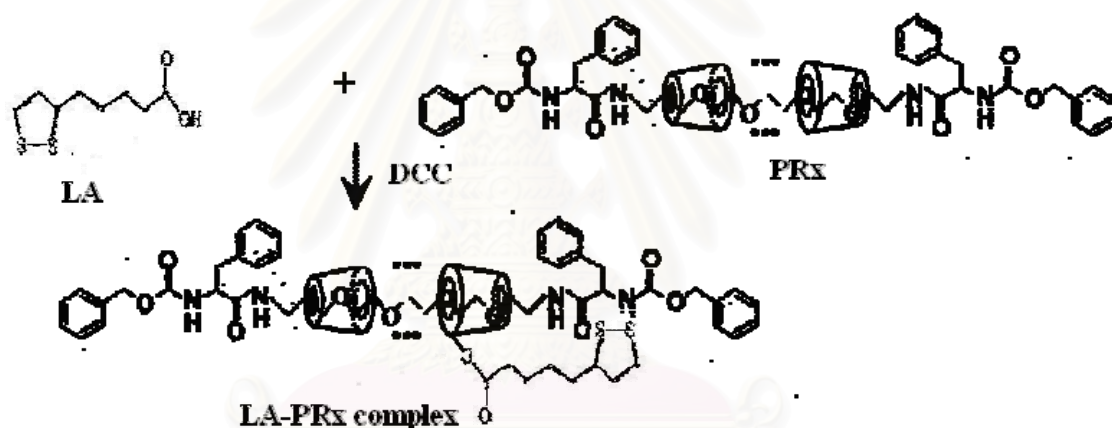


Figure 9 The reaction between  $\alpha$ -CD in PRx and cholesterol

#### 4.3 LA-PRx complex and cholesterol-modified LA-PRx complex synthesis

After the synthesis of PRx or cholesterol modified PRx, the excess amount of LA was introduced to these systems. The white powder of LA-PRx complex and cholesterol modified LA-PRx complex were obtained. The reactions are shown in Figure 8 -10. The calculation of the UV absorbance result showed that 4 moles of LA reacted with 1 mole of  $\alpha$ -CD in LA-PRx complex, and 3 moles of LA reacted with 1 mole of  $\alpha$ -CD in cholesterol-modified LA-PRx complex.



**Figure 10** The synthetic procedure of LA-PRx complex

สถาบันวิทยบริการ  
จุฬาลงกรณ์มหาวิทยาลัย

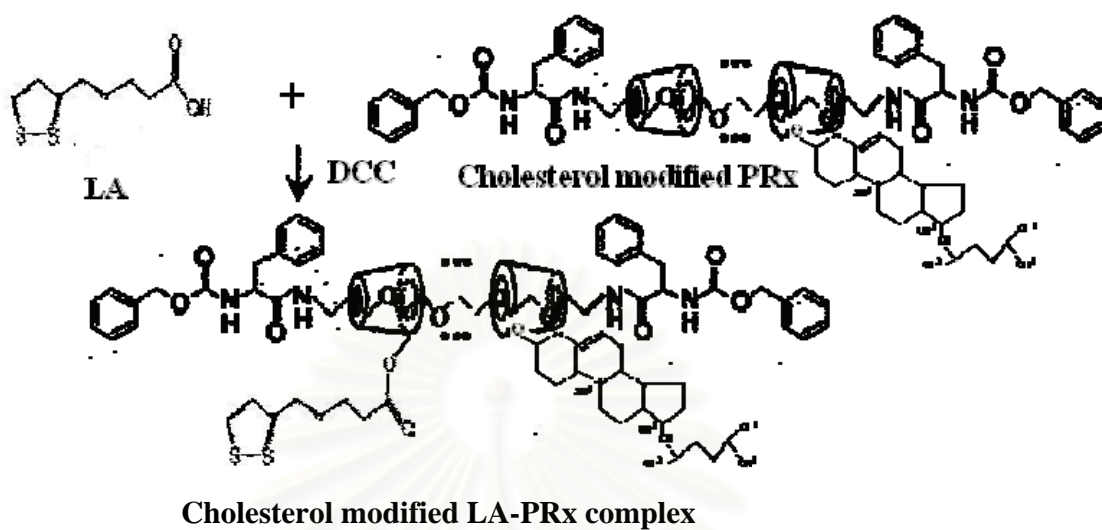


**Figure 11** The synthetic procedure of cholesterol modified LA-PRx complex

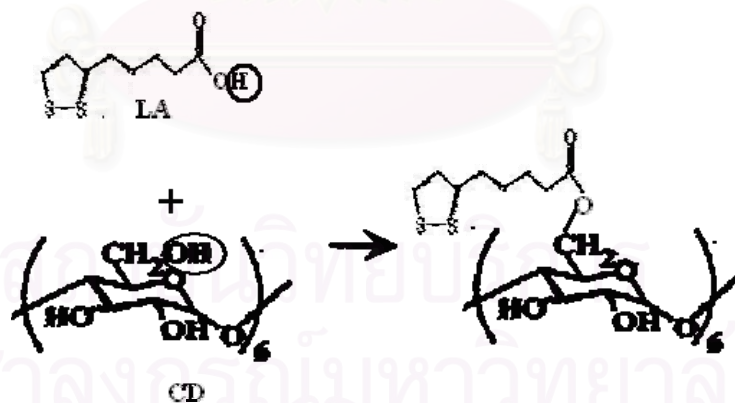


**Figure 12** The reaction between  $\alpha$ -CD in PRx and LA

## 5. Characterization

### 5.1 Mass spectrometry

#### 5.1.1 MS spectrum of LA

The extraction from *Spinacea oleracea* was characterized using LC-MS. The fraction that contained LA showed the m/z 205 ion in negative mode (Figure13).

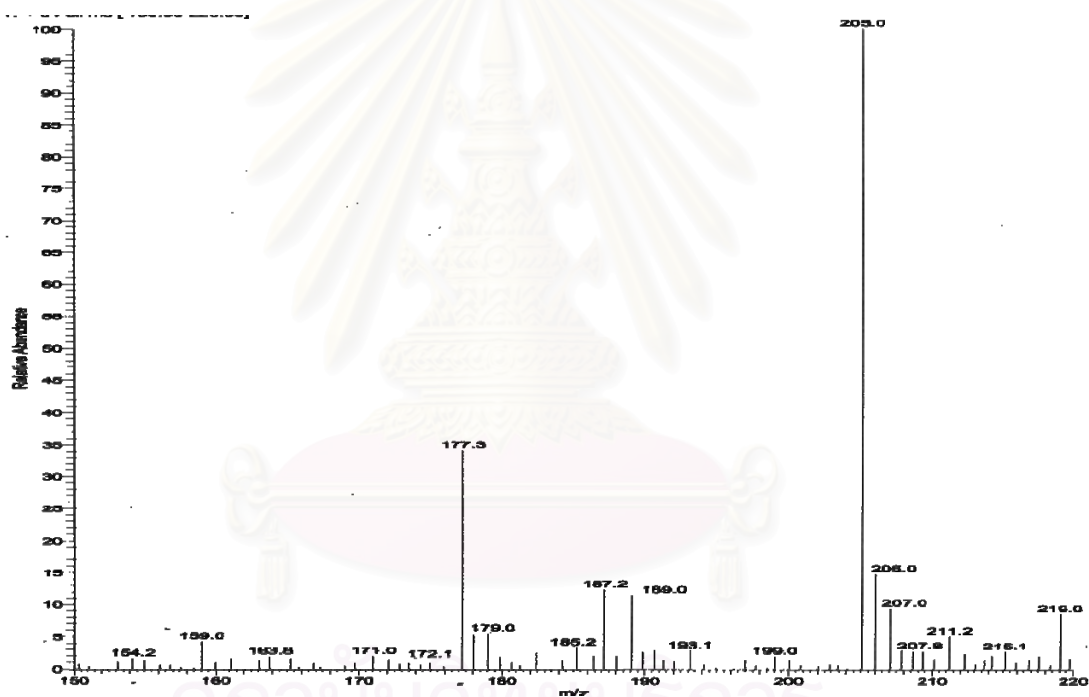
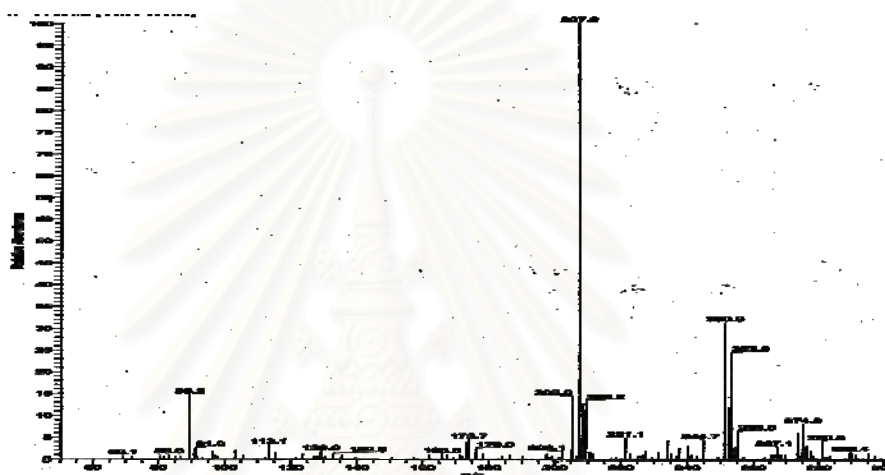


Figure 13 The mass spectrum of LA showed m/z 205 ion in negative mode.

### 5.1.2 MS spectrum of DHLA

DHLA was synthesized and characterized using ESI-MS in negative mode. The data showed DHLA fragment at  $m/z$  207 ion (Figure 14).



**Figure 14** The mass spectrum of DHLA showed  $m/z$  207 ion in negative mode.

### 5.2 NMR Spectrum of PRx and cholesterol modified PRx

The chemical structure of PRx was characterized using the 300 MHz  $^1\text{H}$ -NMR(DMSO- $d_6$ ,ppm):7.36-7.10 (m,10H x 2, aromatic protons of Z-L-Phe), 5.16 [d, 5H x 5, O(2)H of  $\alpha$ -CDs], 5.50 [m, 6H x 5, O(3)H of  $\alpha$ -CD], 4.40[t,6H x 5, O(6)H of  $\alpha$ -CD], 4.08 [m,1H x 5, C(5)H of Z-L-Phe]. 3.74-3.25[m,30H x 5, C(3)H, C(5)H, C(6)H, C(4)H, and C(2)H of  $\alpha$ -CD], 3.51(s,4H x 45, CH<sub>2</sub> of PEG), 3.12 [q, 2H x 15, C(2)H of Z-L-Phe], 3.05[m, 2H x 4, CH<sub>2</sub> of L-Phe]. The structure of cholesterol modified PRx showed one more NMR peak at 1.00-1.10 (m, 62H aromatic proton of cholesterol).



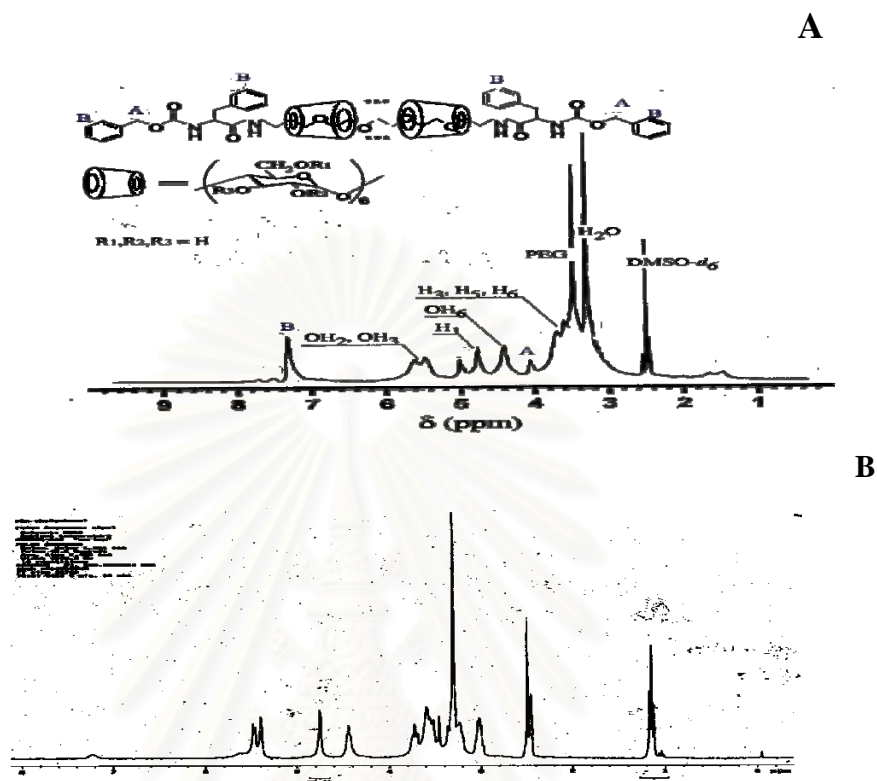


**Figure 15**  $^1\text{H-NMR}$  spectrum of PRx and cholesterol modified PRx in DMSO- $d_6$

### 5.3 The characterization of LA using UV Spectrometry

The standard curves were constructed by plotting the concentration of LA and the absorbance at 208 nm. The curves were linear, ranging from 0.007-0.140 mg/mL. The regression analysis parameters of the calibration curve are shown in Figure 14 (See details in Table 13, Appendix B). The high coefficients of determination ( $r^2 = 0.9994$ ) indicated high degree of correlations. The amount of LA in LA-PRx complex and cholesterol modified LA-PRx complex were measured and calculated. According to the absorbance (See details in Table 14, Appendix B), 1 mole of PRx contained LA 19 moles. According the theory, the maximum of LA could form complex with PRx or cholesterol modified PRx is 30 moles (1  $\alpha$ -CD contains 6 OH groups and 1 PRx/cholesterol modified PRx contains of 5  $\alpha$ -CDs). Therefore in this synthesis LA

formed complex with OH group of PRx 63.33 % or the amount of LA introduced to RRx was 4 moles per  $\alpha$ -CD 1 mole. The calculation of cholesterol modified LA-PRx showed that cholesterol modified PRx 1 mole contained LA 15 moles. According the theory that mention earlier, the amount of LA formed complex with OH group of cholesterol modified PRx was 3 moles per  $\alpha$ -CD 1 mole or 50% of total active OH groups.

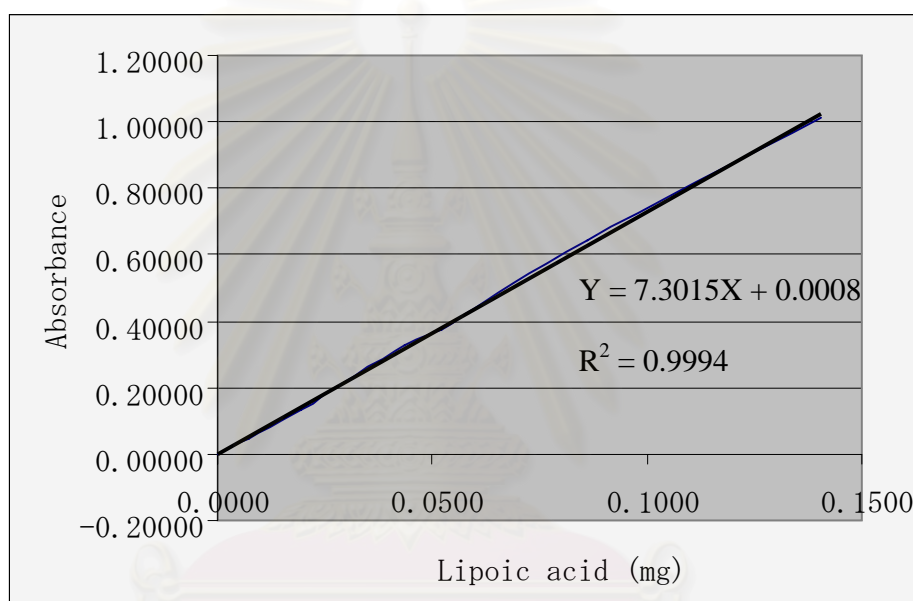


**Figure 16** The calibration curve of LA in PRx

## 6. Penetration study

LA-PRx complex and cholesterol modified LA-PRx complex were examined in term of penetration enhancer. The permeation study was performed in 4 replications. The receptor fluid was collected at 1, 2, 3, 4, 5, 6, 12 and 24 h. The cumulative amount of LA in the receptor compartment was investigated (See details in Table 15-16, Appendix B). The permeations of LA –PRx complex and cholesterol modified LA-PRx complex were compared with LA solution (See details in Table 17-20, Appendix B). The permeation results are shown in Figure 17 which demonstrated the cumulative amounts of LA in the receptor compartment (See details in Table 16, 18 and 20, Appendix B). Fluxes of total

LA passing through the skin were shown in Figure 16 (See details in Table 16, 18 and 20, Appendix B). The permeations of LA of 3 formulations were different. LA from LA solution could not be detected in the receptor compartment until 1 h (See details in Table 15-16, Appendix B). LA from LA-PRx complex also could not be detected in the receptor until 2 h (See details in Table 17-18, Appendix B). Interestingly, cholesterol modified LA-PRx complex could be detected since 0.5 h (See details in Table 19-20, Appendix B). The total amount 26.06, 44.02 and 44.09  $\mu\text{g}$  of LA was detected in the receptor fluid at 24 h from LA solution, LA-PRx complex and cholesterol modified LA-PRx complex respectively. (See details in Table 17-20, Appendix B). The highest flux of total LA from solution was  $0.13 \mu\text{g}/\text{h}/\text{cm}^2$  at 1h. Data is shown in Figure 18 (See details in Table 16, Appendix B). The highest flux of total LA from LA-PRx complex was  $0.24 \mu\text{g}/\text{h}/\text{cm}^2$  at 3 h and the highest flux of total LA from cholesterol modified PRx was  $0.31$  at 3 h. Data are shown in Figure 18 (See details in Table 18 and 20, Appendix B). The penetration of each formulation was also compared in the term of rate constant (k). The rate of penetration of LA from LA solution was constant. Differently, LA-PRx complex showed lag time for the penetration of LA through the skin. When cholesterol was added to LA-PRx complex, cholesterol enhanced the penetration of LA through the skin with short lag time of 0.5 h. Data are shown in Figure 17 (See details in Table 16, 18 and 20, Appendix B). Therefore, it could be concluded that the cholesterol modified LA-PRx complex enhanced the permeation of LA through the SC compared with the LA solution, but LA-PRx complex sustained the release of LA through the skin. However, since the total amount of LA loaded onto the skin was approximately  $1000 \mu\text{g}$ , the %permeation was calculated to be only 2.6% for the LA solution and 4.4% for the PRx formulation. It might be due to the hydrophobicity of LA, causing in the high entrapment of LA in lipid barrier of human SC.

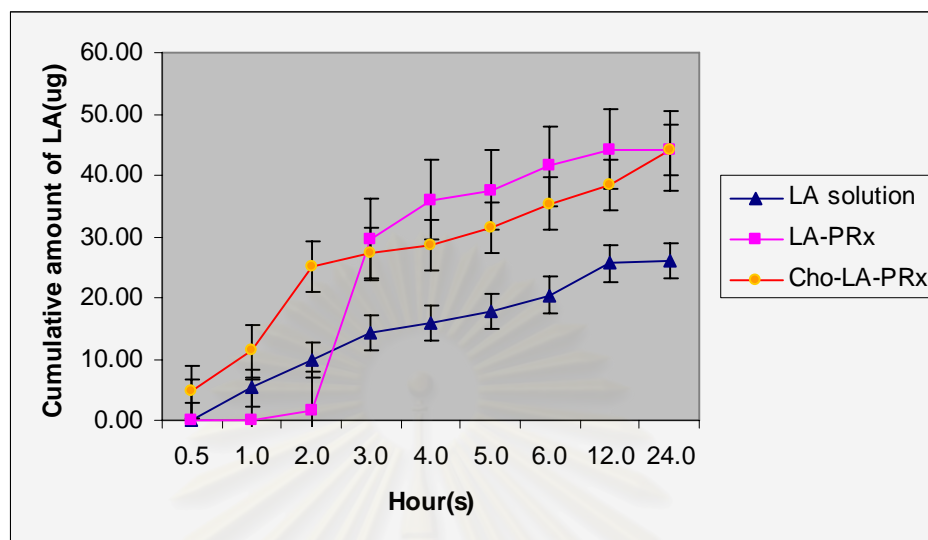


**Figure 17** The cumulative amount of LA from LA solution, LA-PRx complex and cholesterol modified LA-PRx complex.

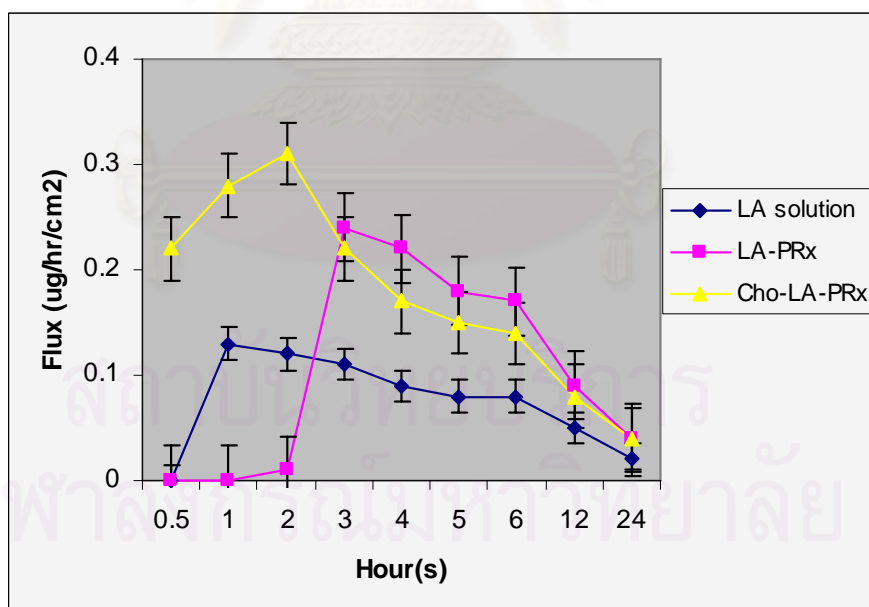


**Figure 18** Fluxes of LA through human SC from LA solution and LA-PRx complex and cholesterol modified LA-PRx complex

## 7. Cytotoxicity assay

The cytotoxicity of LA, LA-PRx complex and cholesterol modified LA-PRx complex was studied by varied the amount of test compound from 0-1000  $\mu\text{M}$ . The results showed that LA was not toxic to human skin fibroblast cells. The percentage of cell viability did not significantly decrease when compared with untreated control at  $\alpha = 0.05$  (See details in Tables 21, Appendix B). The delivery systems, LA-PRx complex and cholesterol modified LA-PRx complex were also not toxic to normal human skin fibroblast cells. The data are shown in Figure 19.

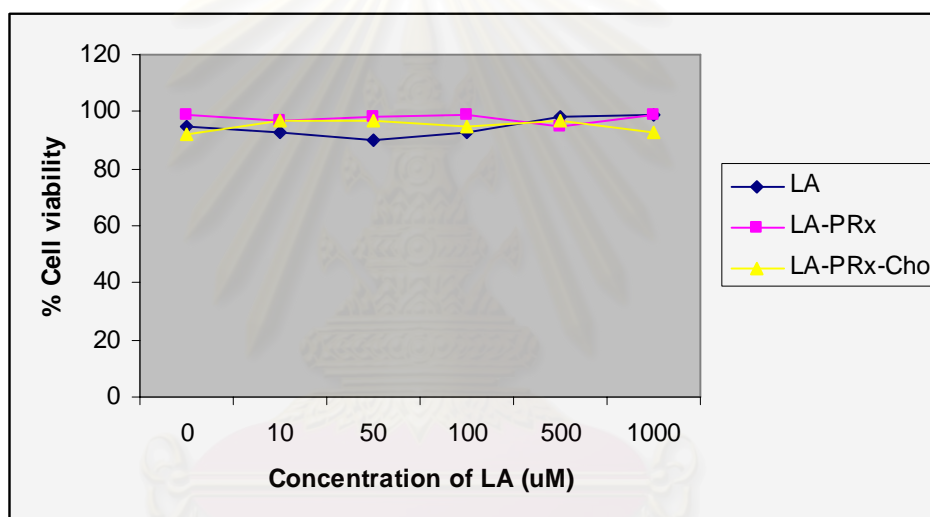


**Figure 19** Cell viability of human skin fibroblast after treatment with LA, LA-PRx complex and cholesterol modified LA-PRx complex ( $n=3$ )

## 8. The effect of LA, LA-PRx and cholesterol modified -LA-PRx on cell growth

LA, LA-PRx or cholesterol modified LA-PRx (0-1000  $\mu\text{M}$ ) was incubated with skin fibroblast cells. The growth rate of fibroblast cells were reduced to 59% when the concentrations of LA were increased up to 100  $\mu\text{M}$ . They could not inhibit cell growth to 50%. This study could not calculate  $\text{IC}_{50}$  of LA even the concentration of LA increased up to 1000  $\mu\text{M}$  (data are shown in Figure 18; Table 22, Appendix B). For LA-PRx complex and cholesterol modified LA-PRx complex, data are shown as same as LA. Both

formulations could not inhibit cell growth to 50%. Then we can not calculate  $IC_{50}$  even the concentrations of LA were increased up to 1000  $\mu$ M. Data are shown in Figure 20 (See details in Table 22 Appendix B). According to the result, LA and its delivery systems seemed to stimulate the growth of human skin fibroblast (Data are shown in Figure 20).

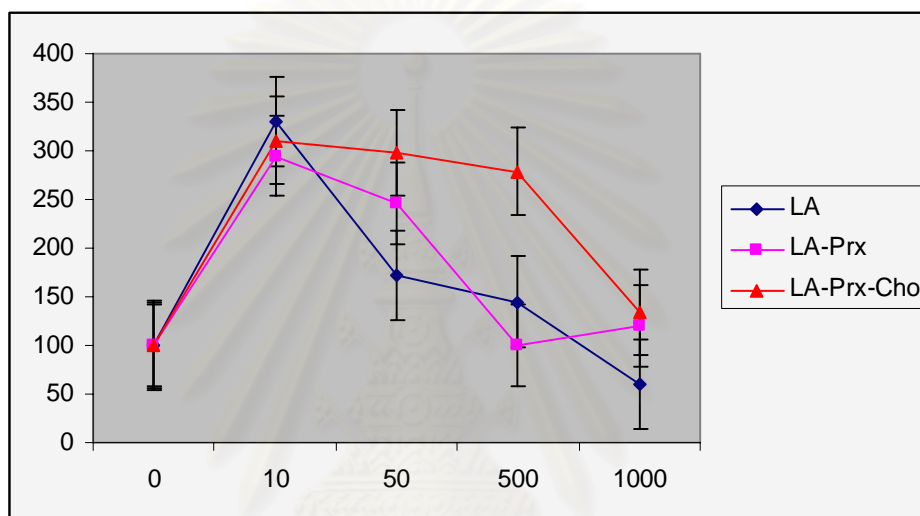


**Figure 20** Cell growth assay of skin fibroblast after incubated with LA, LA-PRx or cholesterol modified LA-PRx ( $n=3$ )

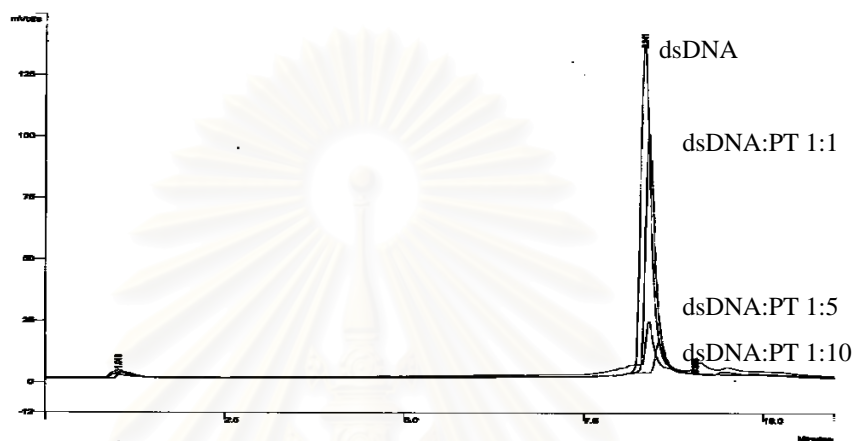
## 9. The effect of LA, DHLA, LA-PRx complex, cholesterol modified LA-PRx complex on DNA-Damage

### 9.1 Effect of cisplatin on self complementary double strand DNA (Dickerson dodecamer)

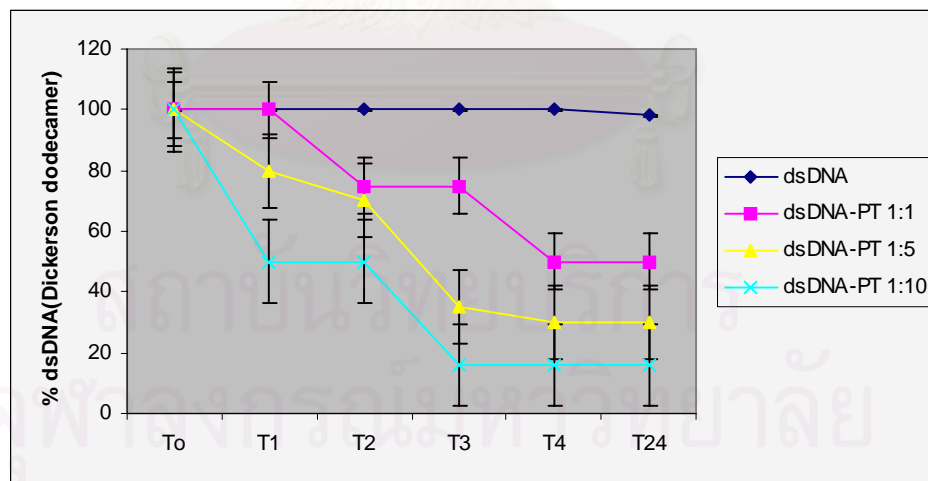
Cisplatin (PT) (1-10 times of dsDNA) was incubated at 37°C. The samples were analyzed by dHPLC at 0, 1,2,3,4 and 24 h. The peak of double strand DNA (dsDNA) was seen at 260 nm and came out at 8.3 min. The area under the curve of dsDNA at 260 nm is shown in Figure 21. After the incubation with cisplatin, the amount



of dsDNA (Dickerson dodecamer) was reduced and reached the steady state at 4 h. The percent reduction of dsDNA alone and incubation with to cisplatin (PT) in different molar ratios (1:1, 1:5 and 1:10) are shown in Figure 22 and Figure 23.

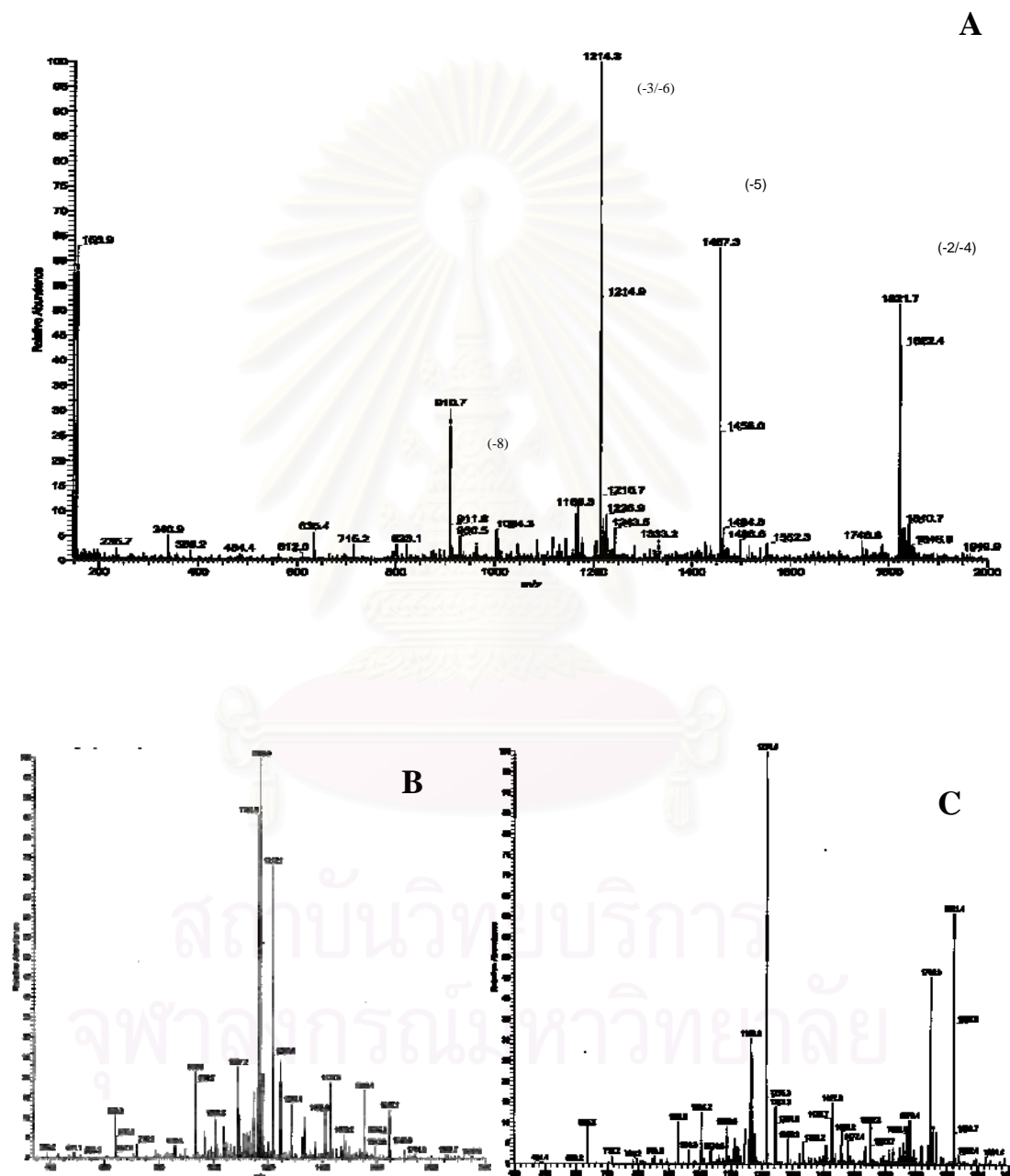


**Figure 21** Peak of dsDNA alone or dsDNA incubated with different molar ratios of cisplatin (PT) (1:1, 1:5 and 1:10) at 37 °C for 24 h.



**Figure 22** The percent of dsDNA (Dickerson dodecamer) reduction alone and dsDNA to PT in the different molar ratios (1:1, 1:5 and 1:10) after the incubation at 37°C for 1, 2, 3, 4 and 24 h.

Mass spectra of the self-complementary dsDNA (Dickerson dodecamer) sequence 5'-CGC GAA TTC GCG-3' showing the presence of -2 (1822), and -3 (1214), -4 (1822), -5 (1457), -6 (1214) and -8 (911) charges for parent structure (Figure 23A).



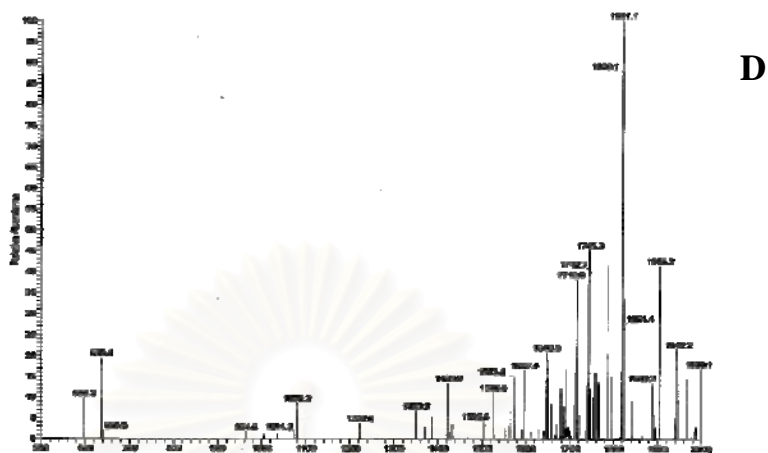


**Figure 23** The mass spectra of dsDNA (Dickerson dodecamer). The ions were found at  $m/z$  910.7, 1214.3, 1457.3 and 1821.7 for charge -8, -3/-6, -5, and -2/-4 in the order (A). Ms/ms spectra of DD for -3 or -6 ( $m/z$  1214, B), -5 ( $m/z$  1475, C) and -2 or -4 ( $m/z$  1822, D) charges were recorded at collision energy (CE) of 6%

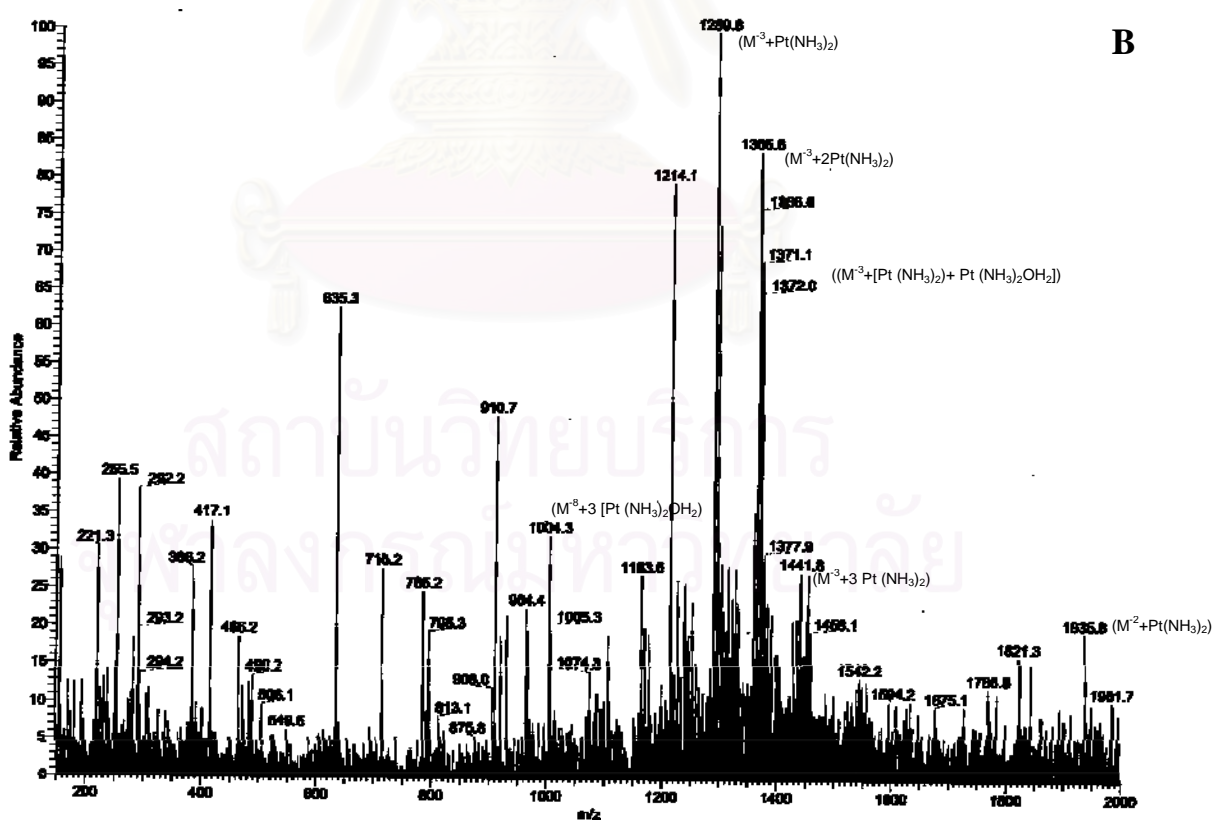
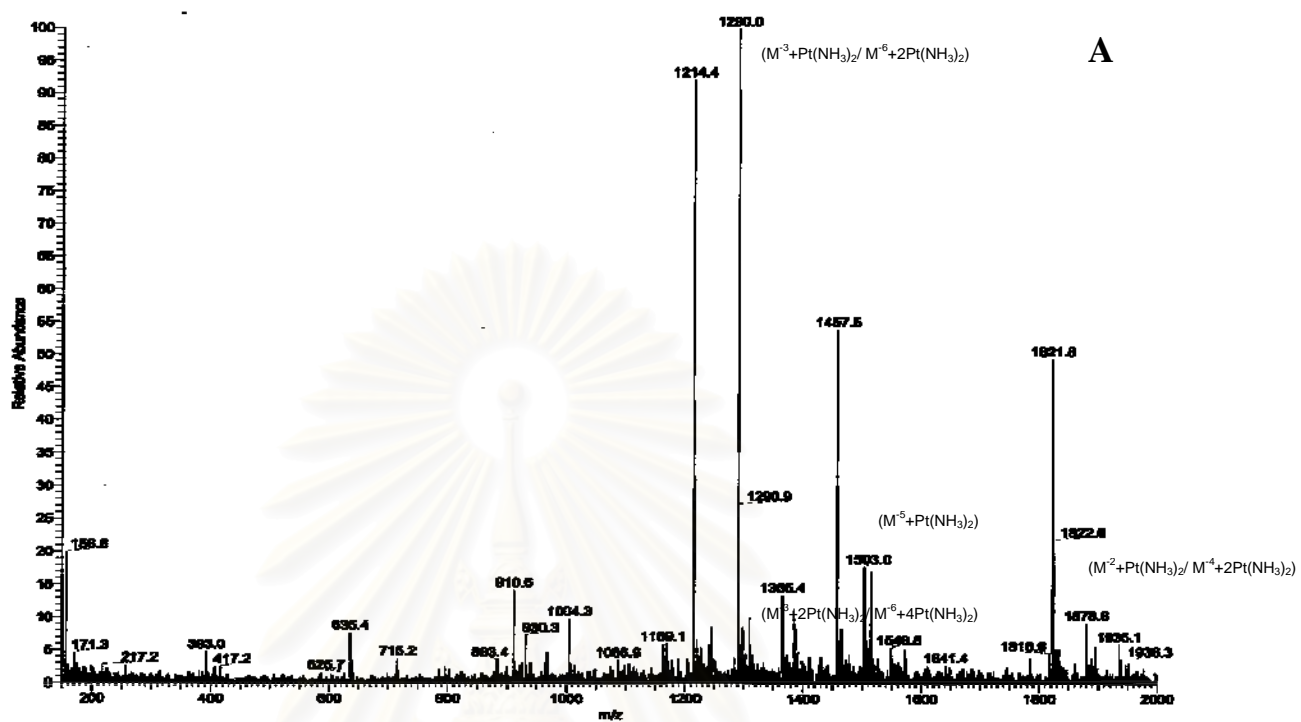
Figure 23B shows the mass spectra of dsDNA, Dickerson dodecamer, recorded at identical collision energy (CE) of 6%. The selected precursor ion  $m/z$  1214 for -3 or -6 charges. The main decomposition pathway of dsDNA, Dickerson dodecamer, involves the loss of adenine producing the ion of  $m/z$  1169.9. The  $m/z$  1164 product ion is formed by loss of guanine. The decomposition of  $m/z$  1457 ion at collision energy (CE) of 6% produced  $m/z$  1163.9, 1214.4, 1745.9 and 1821 ion (Figure 23C). The  $m/z$  1214.4 and 1821.4 product ions showed that dsDNA became single strand DNA (ssDNA). The  $m/z$  1745.9 ion was formed by loss of 2 guanine from -4 charges ion. The  $m/z$  1163.9 ion was formed by loss of 1 guanine from -3 charges ion. The decomposition of  $m/z$  1822 ion also involved the loss of 2 guanine and formed the  $m/z$  1745.3 ion.

After adding cisplatin (PT), the DNA-platinum adducts were observed in the full scan mass spectra. The DNA-platinum adducts,  $[M^{-3} + Pt(NH_3)_2]$  or  $[M^{-6} + 2Pt(NH_3)_2]$  ions were observed at  $m/z$  1290, the  $[M^{-5} + Pt(NH_3)_2]$  ion showed at the  $m/z$  1503, the  $[M^{-3} + 4Pt(NH_3)_2]$  ion showed at the  $m/z$  1515. The  $[M^{-5} + 2Pt(NH_3)_2]$  ion showed at the

m/z 1548, the  $[M^{-5} + 3(\text{Pt}(\text{NH}_3)_2)]$  ion showed at the m/z 1591, the  $(M^{-4} + \text{Pt}(\text{NH}_3)_2)$  ion showed at the m/z 1879, the  $[M^{-2} + \text{Pt}(\text{NH}_3)_2]$  ion showed at the m/z 1894 and the  $[M^{-4} + 2(\text{Pt}(\text{NH}_3)_2)]$  or  $[M^{-2} + \text{Pt}(\text{NH}_3)_2]$  ion showed at the m/z 1935. Theoretical number of the m/z ion for each charge is shown in Table 7.

**Table 7** Theoretical m/z of DNA-platinum adducts for each charge

Adduct Species	Average Molecular Weight (M/z)					
	-2	-3	-4	-5	-6	-8
Parent Mass	<b>1822</b>	<b>1214</b>	<b>1822</b>	<b>1457</b>	<b>1214</b>	<b>911</b>
Pt(NH <sub>3</sub> ) <sub>2</sub>	1936	1290	1879	1503	1252	940
2Pt(NH <sub>3</sub> ) <sub>2</sub>	2051	1366	1936	1548	1290	968
3Pt(NH <sub>3</sub> ) <sub>2</sub>	2166	1443	1994	1594	1328	997
4Pt(NH <sub>3</sub> ) <sub>2</sub>	2280	1519	2051	1640	1365	1026
Pt(NH <sub>3</sub> ) <sub>2</sub> OH <sub>2</sub>	1945	1296	1884	1506	1257	942
2Pt(NH <sub>3</sub> ) <sub>2</sub> OH <sub>2</sub>	2069	1379	1946	1556	1296	973
3Pt(NH <sub>3</sub> ) <sub>2</sub> OH <sub>2</sub>	2193	1461	2007	1605	1338	1004
4Pt(NH <sub>3</sub> ) <sub>2</sub> OH <sub>2</sub>	2316	1543	2069	1655	1379	1035
Pt(NH <sub>3</sub> ) <sub>2</sub> +Pt(NH <sub>3</sub> ) <sub>2</sub> OH <sub>2</sub>	2060	1373	1941	1552	1293	971
Pt(NH <sub>3</sub> ) <sub>2</sub> +2Pt(NH <sub>3</sub> ) <sub>2</sub> OH <sub>2</sub>	2184	1455	2003	1602	1335	1001
2Pt(NH <sub>3</sub> ) <sub>2</sub> +Pt(NH <sub>3</sub> ) <sub>2</sub> OH <sub>2</sub>	2175	1449	1998	1598	1332	999
Pt(NH <sub>3</sub> ) <sub>2</sub> +3Pt(NH <sub>3</sub> ) <sub>2</sub> OH <sub>2</sub>	2307	1537	2065	1651	1376	1032
2Pt(NH <sub>3</sub> ) <sub>2</sub> +2Pt(NH <sub>3</sub> ) <sub>2</sub> OH <sub>2</sub>	2298	1531	2060	1647	1373	1030
3Pt(NH <sub>3</sub> ) <sub>2</sub> +Pt(NH <sub>3</sub> ) <sub>2</sub> OH <sub>2</sub>	2289	1525	2055	1644	1370	1028



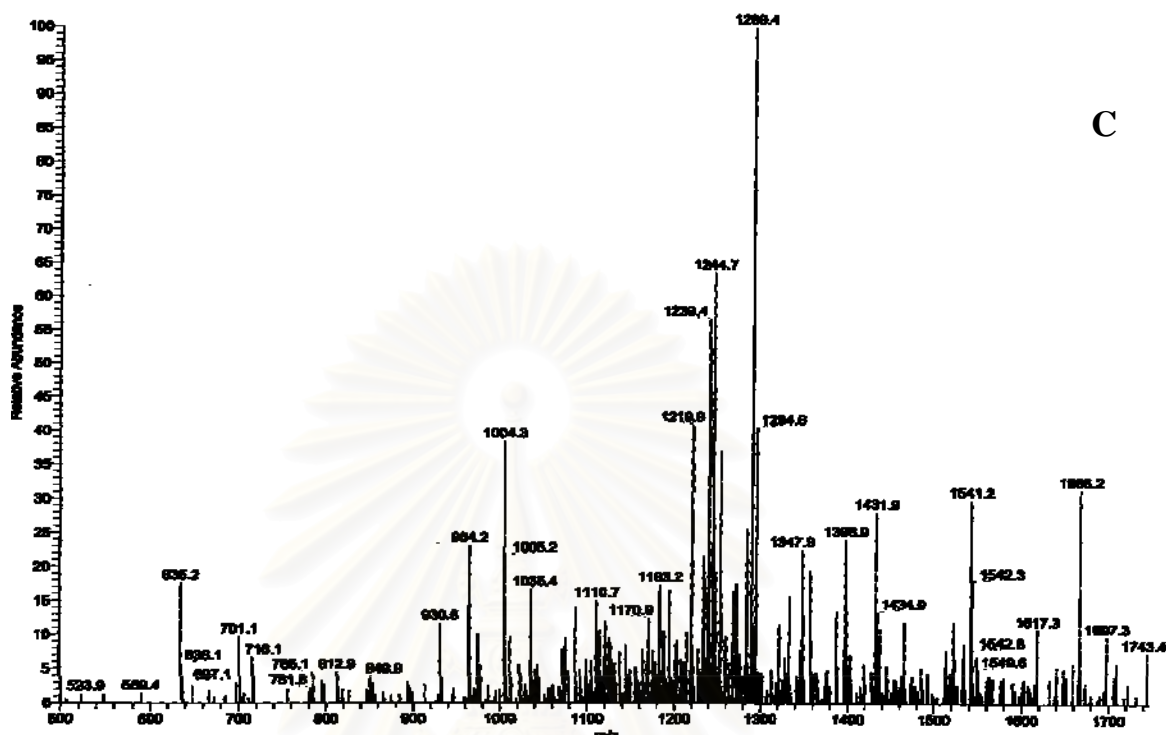


**Figure 24** MS spectra of dsDNA-platinum adducts (A) and ssDNA-Platinum adducts (B) at 24 h. DNA-platinum adducts were found at  $m/z$  1290,1365.4,1503,1548.8,1936.3 and the  $ms/ms$  spectra of the  $m/z$  1290 ion recorded at a CE 6% (C).

To study whether the adduct formation was the formation between cisplatin(Pt) and dsDNA or ssDNA, and the temperature using in MS condition make the DNA become single strand or not, ssDNA was used in this experiment. MS spectra of ssDNA showed the similar adducts as dsDNA but the intensity of each adduct was different (Figure 24B). The  $m/z$  of ssDNA-adducts are showed as following ;1004 ( $M^{-8}+3$  [Pt ( $NH_3)_2OH_2$ ]),1290 ( $M^{-3}+Pt$  ( $NH_3)_2$ ), 1366 ( $M^{-3}+2Pt$  ( $NH_3)_2$ ),1372 ( $(M^{-3}+[Pt$  ( $NH_3)_2)+ Pt$  ( $NH_3)_2OH_2$ )), 1379 ( $M^{-3}+ 2Pt$  ( $NH_3)_2OH_2$ ) and1442 ( $M^{-3}+3 Pt$  ( $NH_3)_2$ ). The decomposition of the  $m/z$  1290 ion also involved the loss of guanine ( $m/z$  1239.4) and adinine ( $m/z$  1244.7).



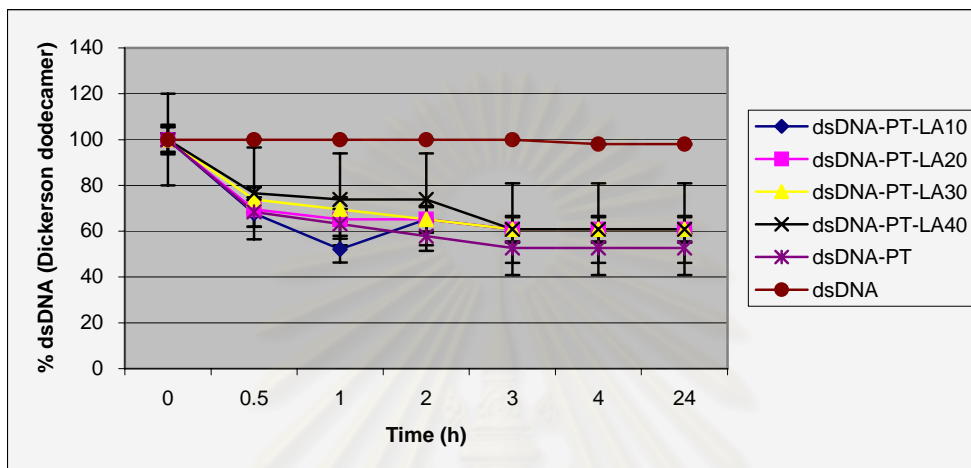
Once cisplatin (PT) goes inside the cell the chloride ions dissociate from the platinum due to the low intracellular chloride concentrations. They are displaced to allow the formation of aquated species, which represent the reactive forms of the compound. Cellular nucleophilic groups containing oxygen, nitrogen or sulfur atoms with unpaired electrons can bind to positively charge of platinum. These groups are present in many amino acid side chains as well as the purine bases of DNA or RNA nucleophiles in DNA, RNA and proteins (Cohen and Lippard, 2001). Binding of metal ions to the phosphate groups in nucleotides is quite common, especially for class A metal ions such as Mg(II), Ca(II), but also binding of Zn(II), Cu(II) and Ni(II) has been observed. In case of Pt(II) - a class B metal -, however, only binding to the nitrogen atoms of the nucleobases has to be considered, although Pt—phosphate interactions do occur in certain cases. The role of phosphate under physiological conditions could be only secondary for coordination. It appears to be a stabilizing, by involving in a hydrogen bond with a NH ligand at platinum (Reedijk, 1987). The primary target of cisplatin is genomic DNA, specially the N7 position of guanine bases. This point of attack first generations monofunctional adducts, which subsequently closes by coordination to the N7 position of adjacent purine to afford an intrastrand cross-link (Baik et al., 2003). The major adduct (65%) is clearly the intrastrand 1,2-d(GGX) cross-link, with minor incidences of 1,2(AGX) , 1,3d(GXG) and interstand crosslinks for cisplatin. Differently, the distribution of Pt-DNA adducts formed with carboplatin ( cisplatin analogous) appears to be 30% 1,2-d(GG),16% 1,2-d(AG) 36% 1,3-d(GXG), and only 3-4% interstand cross-link (Teuben et al., 1999).

## **9.2 The effect of LA and DHLA on DNA protection**

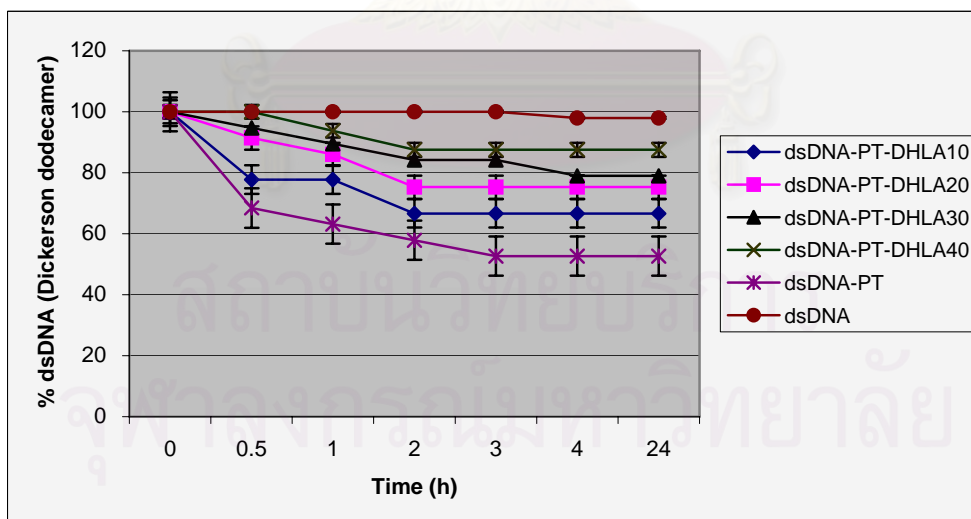
### **9.2.1 Effect of LA and DHLA on the formation of DNA-platinum adducts**

Figure 25 showed that the formation of DNA-platinum adducts reduced the percentage of dsDNA. LA increased the dsDNA by inhibiting the DNA-platinum adduct formation. The increased in LA concentration did not show the different inhibition. While the reduced form of LA, DHLA, reduced DNA-platinum adduct

formation in dose dependent manner as shown in Figure 26. The efficacy to protect the DNA damage was increased when the amount of DHLA increased.



**Figure 25** The percent of dsDNA in the system contained LA, dsDNA and cisplatin (PT) after incubation at 37 °C for 24 h ( $n=3$ )

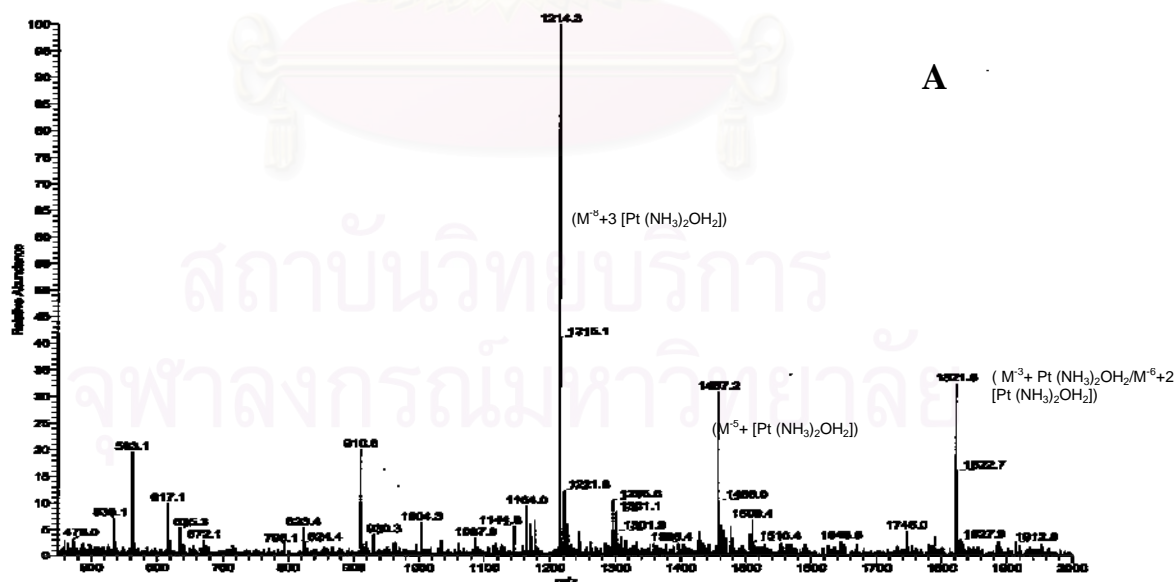


**Figure 26** The percent of dsDNA in the system containing DHLA, dsDNA and cisplatin (PT) after incubation 24 h ( $n=3$ )

### 9.2.2 LA and DHLA protected dsDNA from cisplatin (PT)

The adducts were found in the small amount after the adding of LA or DHLA when compare with the system without LA or DHLA. In the system containing LA, dsDNA and cisplatin (PT), the  $m/z$  ions of adducts were found at 1004.3 ( $M^{\delta}+3$  [Pt (NH<sub>3</sub>)<sub>2</sub>OH<sub>2</sub>]), 1295.6 ( $M^{-3}+Pt(NH_3)_2OH_2$  or  $M^{-6}+2$  [Pt (NH<sub>3</sub>)<sub>2</sub>OH<sub>2</sub>]), 1509.4 ( $M^{-5}+ [Pt (NH_3)_2OH_2]$ ) (Figure 27A) and in the system containing DHLA, dsDNA and cisplatin(PT), the  $m/z$  ions of adducts were found at 1290 ( $M^{-3}+ Pt(NH_3)_2$  or  $M^{-6}+ 2[Pt(NH_3)_2]$ ) and 1296.2 ( $M^{-3}+ Pt (NH_3)_2OH_2$  or  $M^{-6}+2 [Pt (NH_3)_2OH_2]$ ) (Figure 27B).

Acetic acid (AA) and cisplatin(PT) in the same molar ratio of 1:1 was added in the system containing dsDNA to study whether the efficacy to protect DNA damage of LA and DHLA come from carboxylic group of these compounds or not. AA had some effect to inhibit DNA-platinum adducts formation, but not as much as LA and DHLA. The adducts were found at  $m/z$  1004 ( $M^{\delta}+3$  [Pt (NH<sub>3</sub>)<sub>2</sub>OH<sub>2</sub>]), 1290 ( $M^{-3}+ Pt(NH_3)_2$  or  $M^{-6}+ 2[Pt(NH_3)_2]$ ), 1366 ( $M^{-3}+2Pt (NH_3)_2$ ) and 1935 ( $M^{-5}+ [Pt (NH_3)_2OH_2]$ ) (Figure 27C).



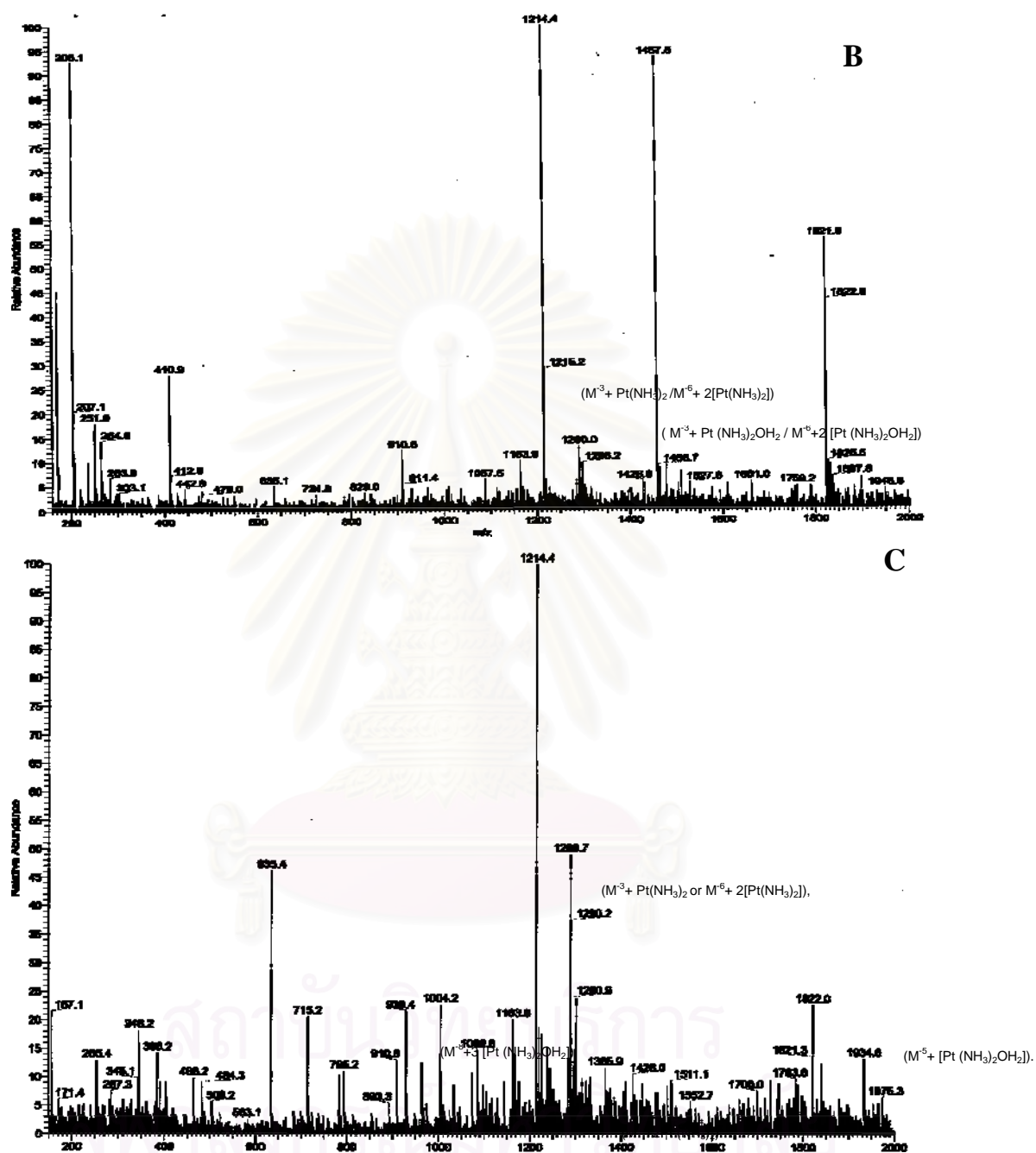


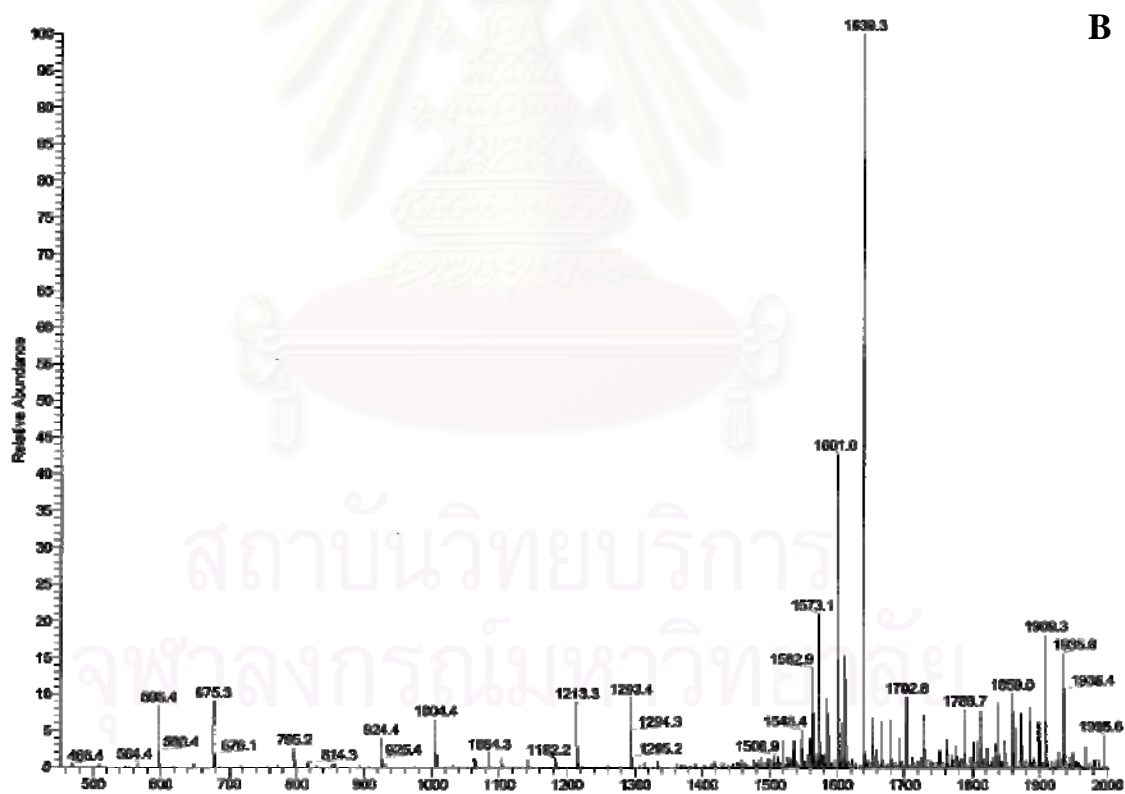
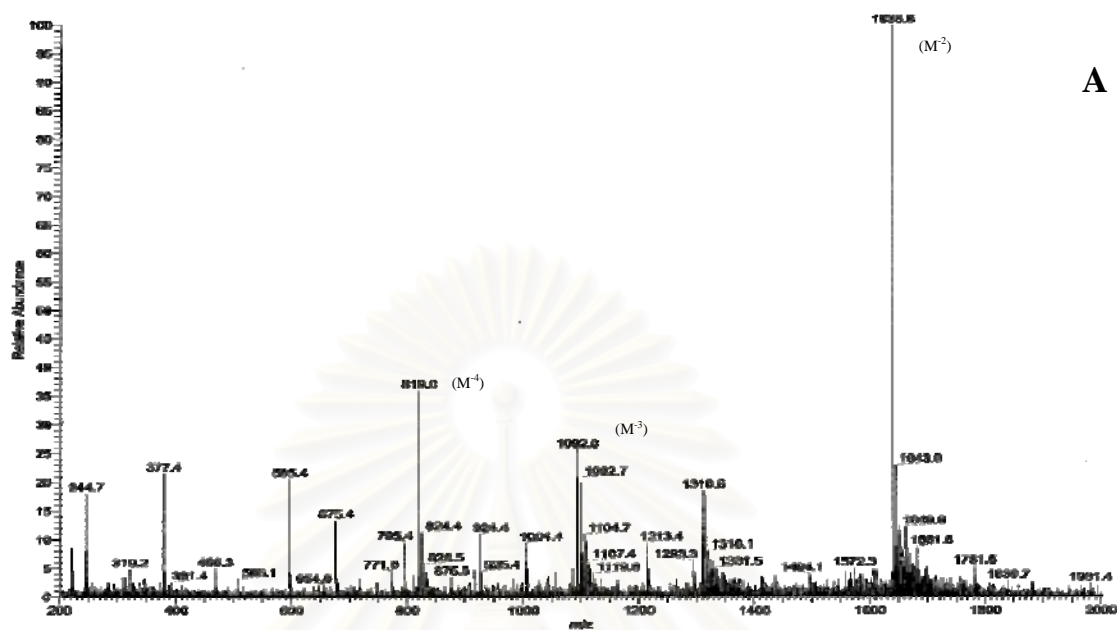
Figure 27 Mass spectra of dsDNA (Dickerson dodecamer) and adducts of system containing dsDNA, PT and LA (A), DHLA (B) or acetic acid (C) after incubated at 37 °C for 24 h.

### 9.2.3 DNA-platinum adduct of non-self complementary DNA heteroduplex undecamer

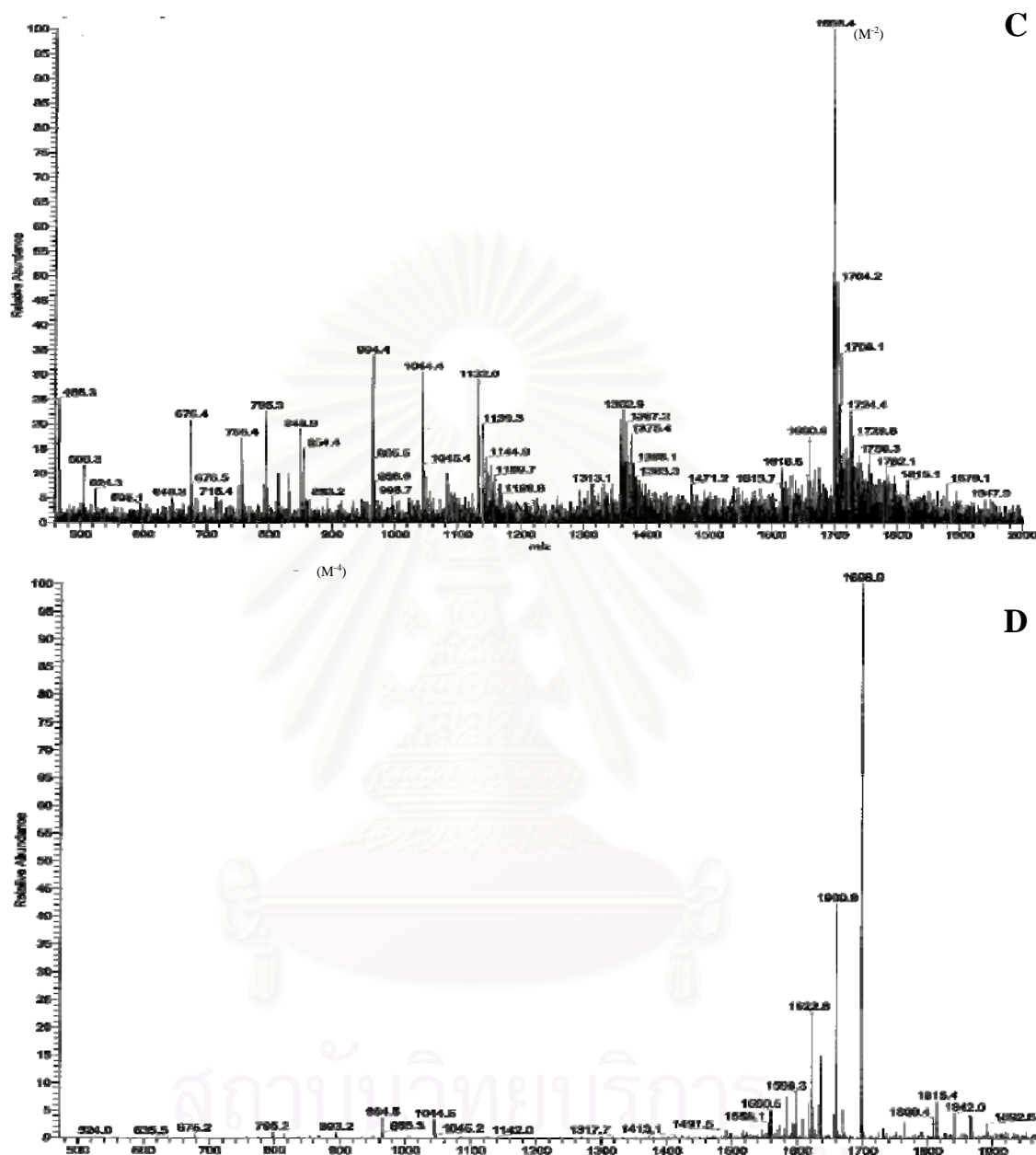
To study whether adduct was single strand or double strand including the different formation of adducts between 1,2 (GGX) and 1,3(GXG), another sequence undecamer DNA was used in this experiment. The undecamer DNA composed of ssDNA, 5' -CCG CGC GCG CC-3', which has molecular weight 3279 and 5' -GGC GCG CGC GG-3' which has molecular weight 3399. The molecular weight of duplex undecamer DNA is 6678. After desalting and annealing, ssDNA and duplex undecamer were study by ESI-MS in negative mode. According the theory, the m/z ions in mass spectra were shown in the Table 8.

**Table 8** The theoretical m/z ion of ssDNA and duplex undecamer DNA at different charge

Charge	SS 3279	SS3399	Heteroduplex
-2	1639.5	1699.5	
-3	1093	1133	
-4	819.7	847.7	1669.5
-5	655.8	679.5	1335.6
-6	546.5	566.5	1113
-7			954
-8			834.7
-9			742



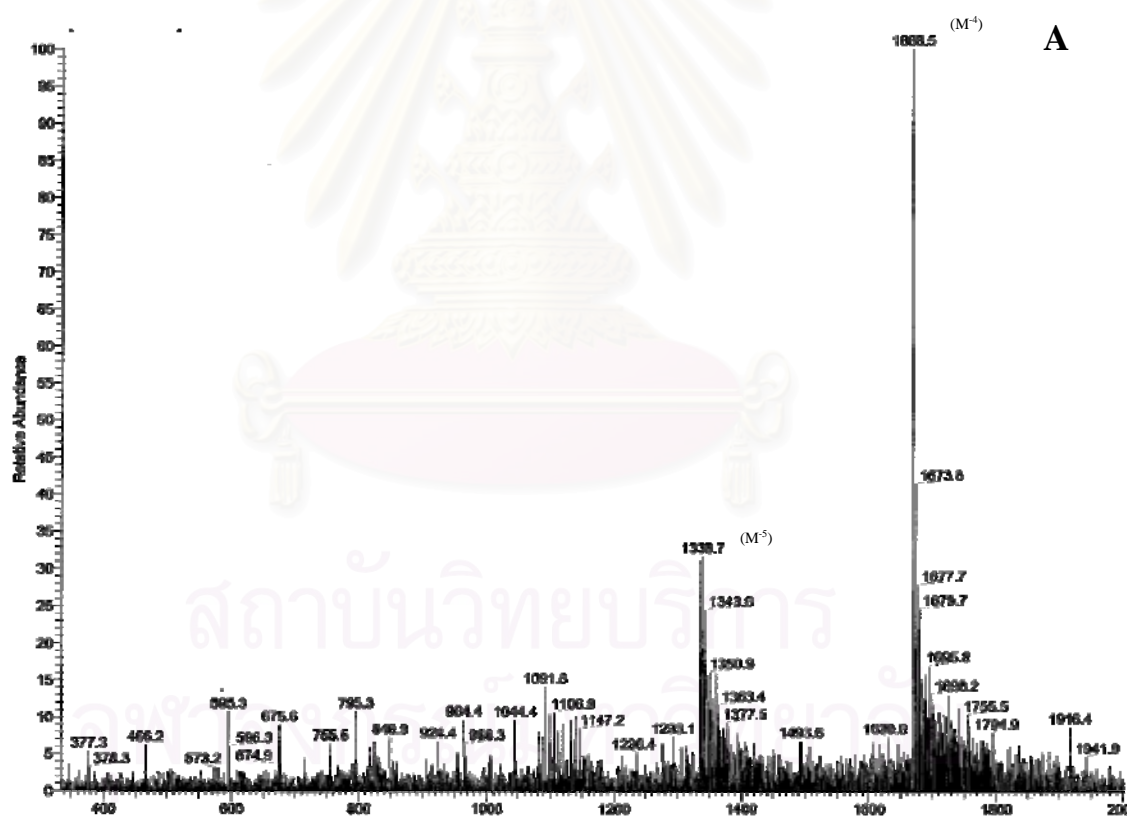


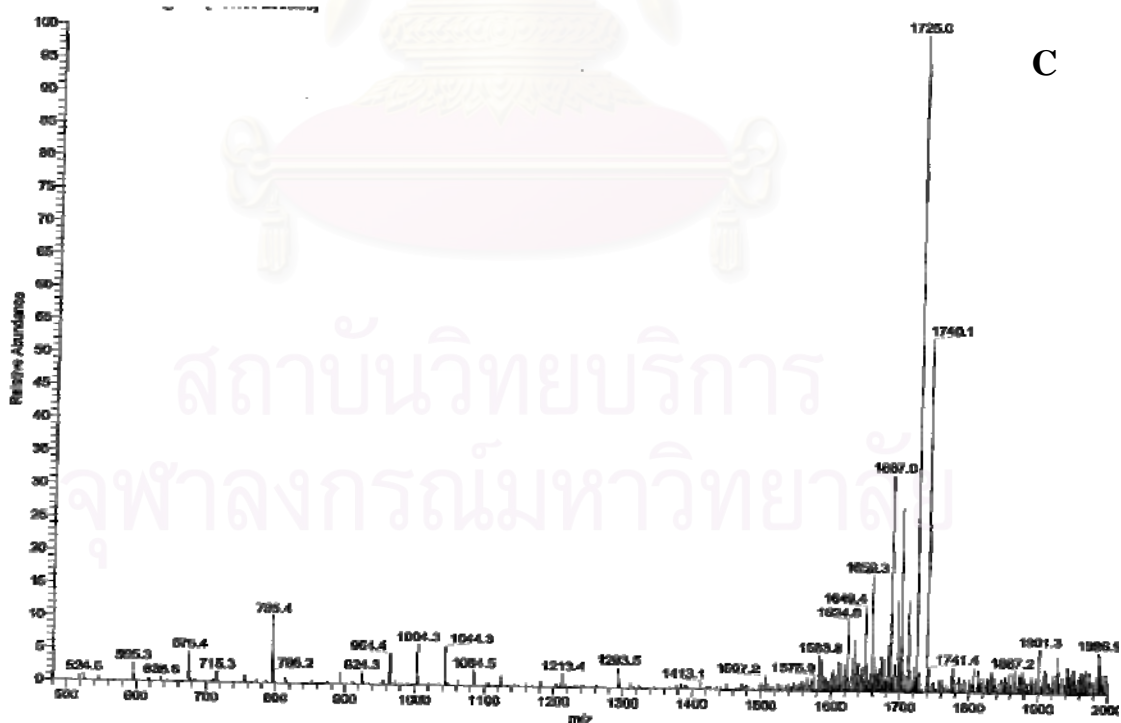
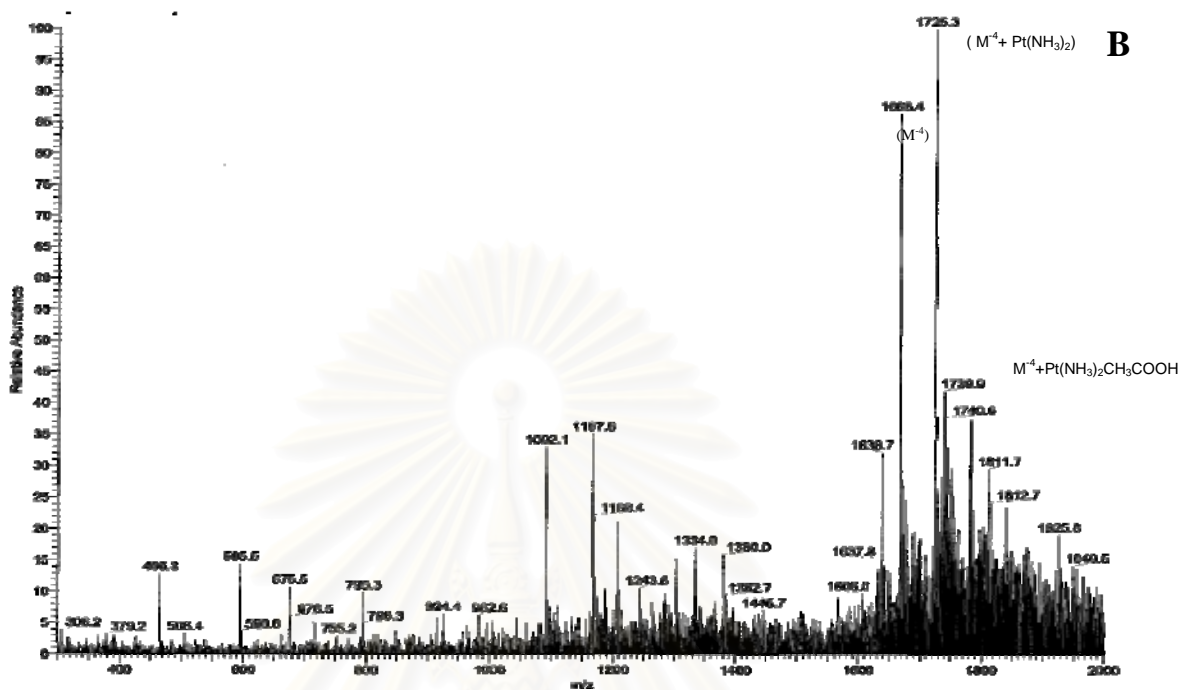


**Figure 28** The full scan mass spectra of ssDNA MW 3279 (ss3279) showed the m/z 1638.8, 1092 and 819 ion for  $-2$ ,  $-3$  and  $-4$  charges (A). The ms/ms spectra of m/z 1639.3 ion recorded at 7% CE (B) The full scan mass spectra of ssDNA MW 3399 (ss3399) showed m/z 1698.4 1132 and 848.9 ion for  $-2$ ,  $-3$  and  $-4$  charges (C) and the ms/ms spectra of 1698.4 recorded at 7% CE (D).

The mass spectra of ssDNA, 5' -CCG CGC GCG CC-3', which has molecular weight 3279 (ss3279), was seen at the m/z 1638.8, 1092 and 819 ion for -2,-3 and -4 charges. The decomposition pathway of ss3279 also involved in the loss of guanine (m/z 1573) and adenine (m/z 1563). For the mass spectra of ssDNA, 5' -GGC GCG CGC GG-3' which has molecular weight 3399 (ss3399), the m/z 1698.4 1132 and 848.9 ion was recorded for -2,-3 and -4 charges and the breakdown of ss3399 involved in the loss of guanine (m/z 1623).

For the duplex undecamer DNA, the molecular weight of this duplex DNA is 6678. The mass spectrum was recorded at 1338.7 and 1668.5 for -4 and -5 ion.





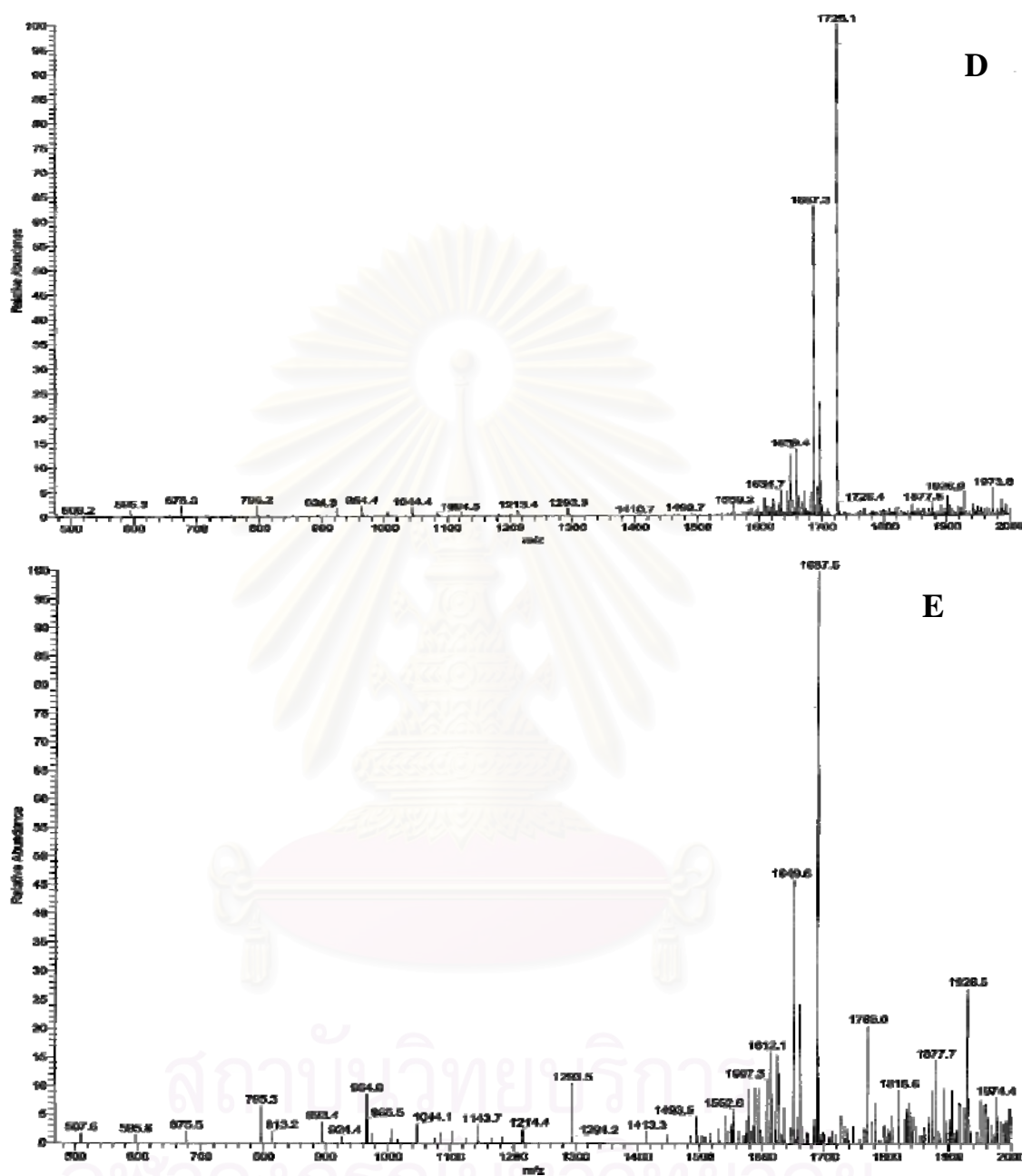


**Figure 29** Mass spectra of duplex undecamer DNA MW 6678 recorded at  $m/z$  1668.5 and 1336.7 for  $-4$  and  $-5$  ion (A). After adding PT, the DNA-platinum adduct's ion was recorded (B). The  $ms/ms$  spectra of 1740 (C) and 1725 ion (D) recorded at CE 7%. After giving the 7% CE to the  $m/z$  1687.5 ion the  $msn$  spectra was recorded (E).

The adducts of undecamer DNA showed the DNA with  $\text{Pt}(\text{NH}_3)_2\text{CH}_3\text{COOH}$  and the DNA with  $\text{Pt}(\text{NH}_3)_2$  at the  $m/z$  1740 and 1725 ion ( $M^4 + \text{Pt}(\text{NH}_3)_2$ ). The main decomposition pathway of  $m/z$  1740 ion involves the loss of  $[\text{CH}_3\text{COOH}]^-$  ion ( $m/z$  1725 ; Figure 29C) and the decomposition pathway of  $m/z$  1725 ion involves the loss of 1 guanine at  $m/z$  1687.3 ion (Figure 29D) after giving 7% CE and after giving another 7% CE, it loss another guanine at the  $m/z$  1649.6 ion (Figure 29E). After forming Platinum-DNA adducts, the MS of undecamer DNA showed that the adducts had still been dsDNA. According to the time to reach the steady state of adduct of Dickerson dodecamer DNA and undecamer DNA, the mechanism to form adducts of PT with 1,2-d(GG) and 1,3-d(GXG) seems to be different. The data from undecamer DNA and Dickerson dodecamer DNA showed that the formation of intrastrand 1,2-d(GG) occurred very quickly and reach steady state within 1 hr and it form only one adduct species. Differently, the formation of 1,3-d(GXG) took around 4 h to reach steady state and it form many types of platinum-adducts. However, which types of platinum adducts that cause the toxicity still have not known.

After LA or DHLA and cisplatin (PT) in the molar ratio of 1:1 were added into the system containing undecamer DNA. The mass spectra showed the adducts in Figure 28. Both LA and DHLA completely prevented the formation of DNA-platinum adduct DNA-  $\text{Pt}(\text{NH}_3)_2\text{CH}_3\text{COOH}$  at the  $m/z$  1740 ion. They also nearly completely inhibited the formation of DNA-  $\text{Pt}(\text{NH}_3)_2$  at the  $m/z$  1725 ion in undecamer DNA.

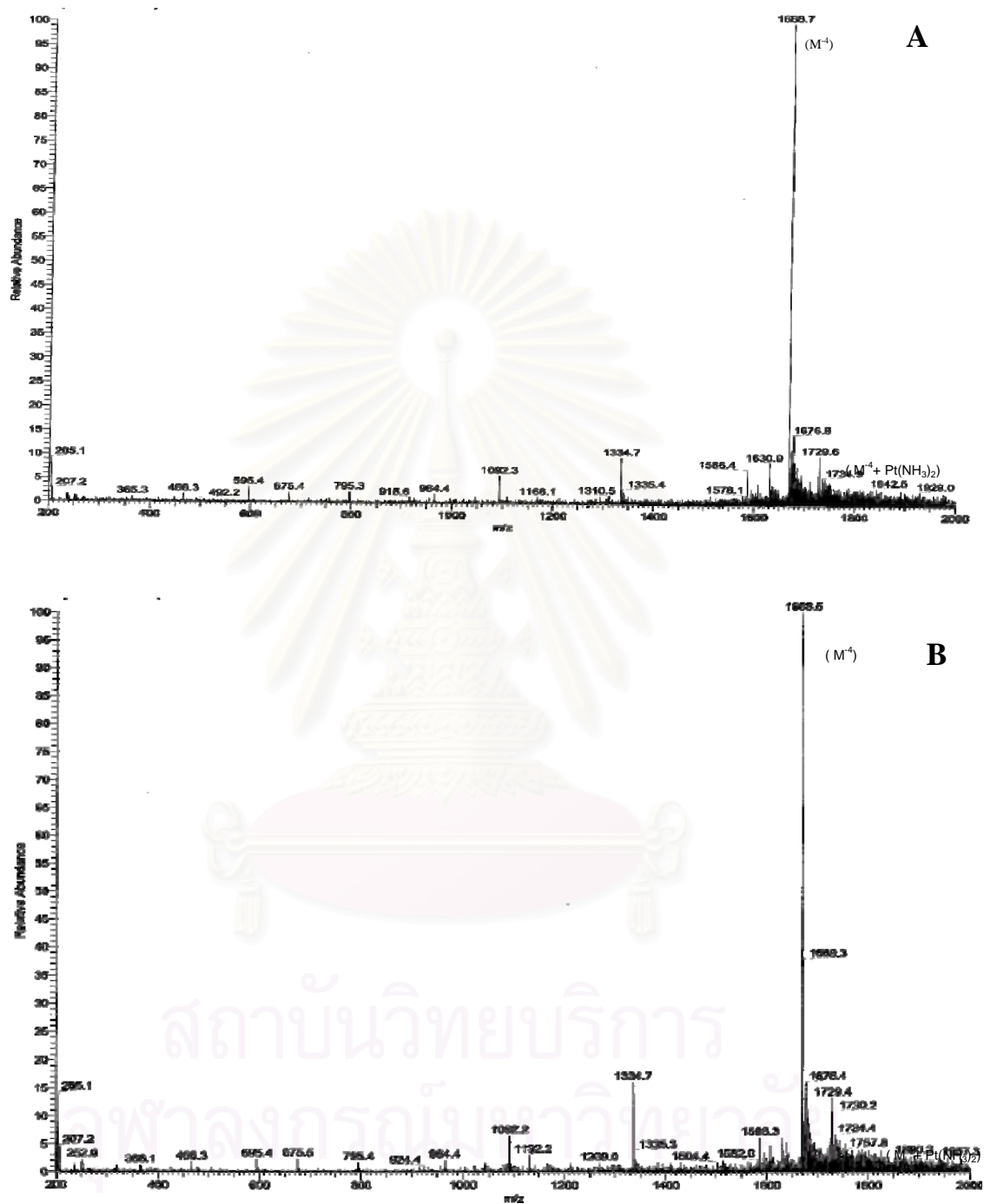


**Figure 30** Full scan mass spectra of undecamer DNA showed the DNA-adduct formation protection efficacy of LA (A) and DHLA (B)



The effect of cisplatin (PT) on undecamer DNA also was studied using dHPLC. Cisplatin (PT) was added to undecamer DNA in the molar ratio of 1:1 and incubated at 37° C. The sample was studied for 24 h. The result showed that the cisplatin (PT) reduced the amount of undecamer DNA very fast in the first 1 h. After the addition of LA or DHLA, both LA and DHLA prevented the reduction of undecamer DNA. The data are shown in Figure 31. The efficacy of LA and DHLA to protect DNA increased when the concentration of LA and DHLA increased. The results of dHPLC together with ESI-MS, might explain that cisplatin (PT) formed the adduct with dsDNA and changed it to be ssDNA so the amount of dsDNA detected by dHPLC was reduced. After adding LA or DHLA, the formation of adducts was reduced (according to ESI-MS result; Figure 30), therefore dHPLC results showed the high amount of dsDNA.



สถาบันวิทยบริการ  
จุฬาลงกรณ์มหาวิทยาลัย

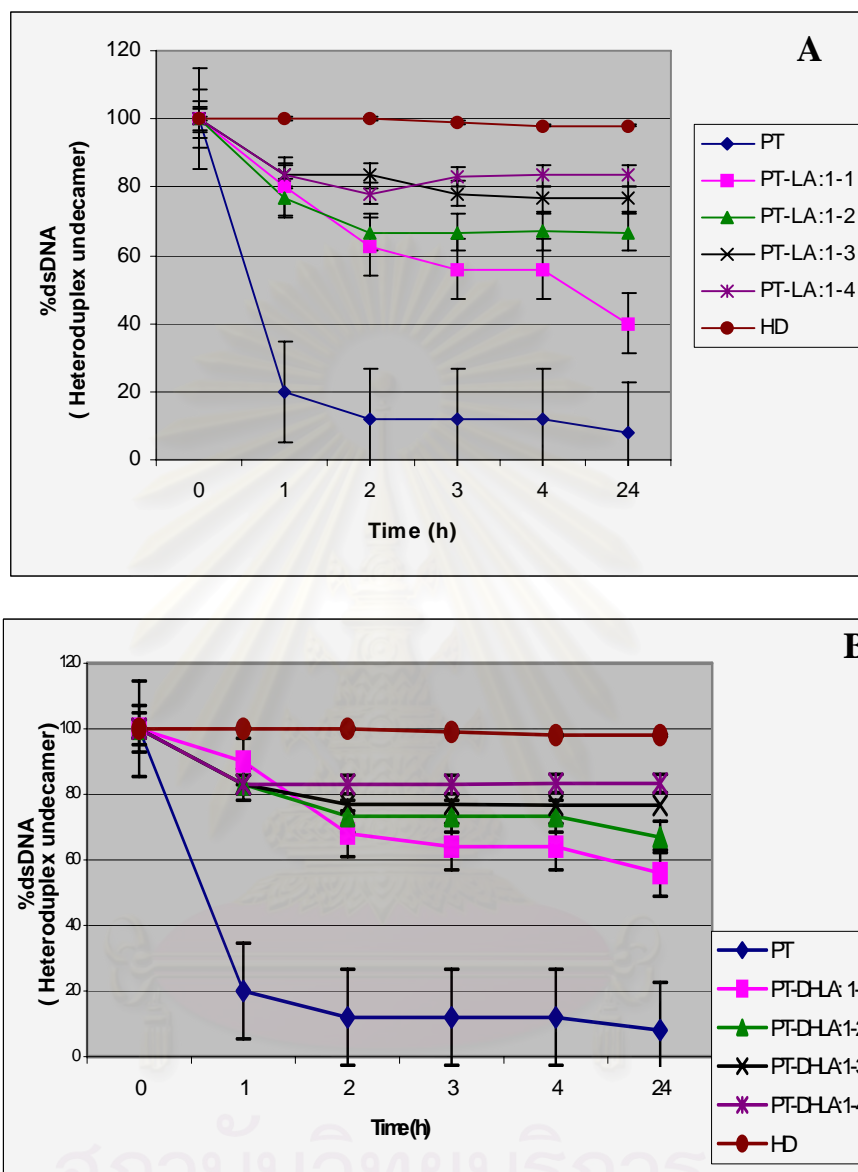


**Figure 31** Cisplatin(PT) reduced the amount of dsDNA heteroduplex undecamer (HD) when studying by dHPLC. After adding of LA (A) or DHLA (B), both of them prevent the reduction of undecamer DNA by cisplatin (PT) in dose dependent manner.

To predict the mechanism of LA and DHLA on protection of the DNA damage from cisplatin (PT), LA or DHLA was incubated with cisplatin at 37 °C. After that it was studied using ESI-MS. ESI-MS analysis of LA or DHLA and cisplatin (PT) showed that LA and DHLA form complex with PT by platinum from cisplatin(PT) inserted in between 2-sulfur group and from the stable heterocyclic ring. The structures of adducts were predicted according to the m/z from mass spectra as in the following (Figure 32). The adduct of platinum-LA was found at m/z 436 ion and the ammonium adduct of platinum-LA adduct was found at 453 ion. The degradation of platinum-LA adduct involved in the loss of NH<sub>3</sub>.

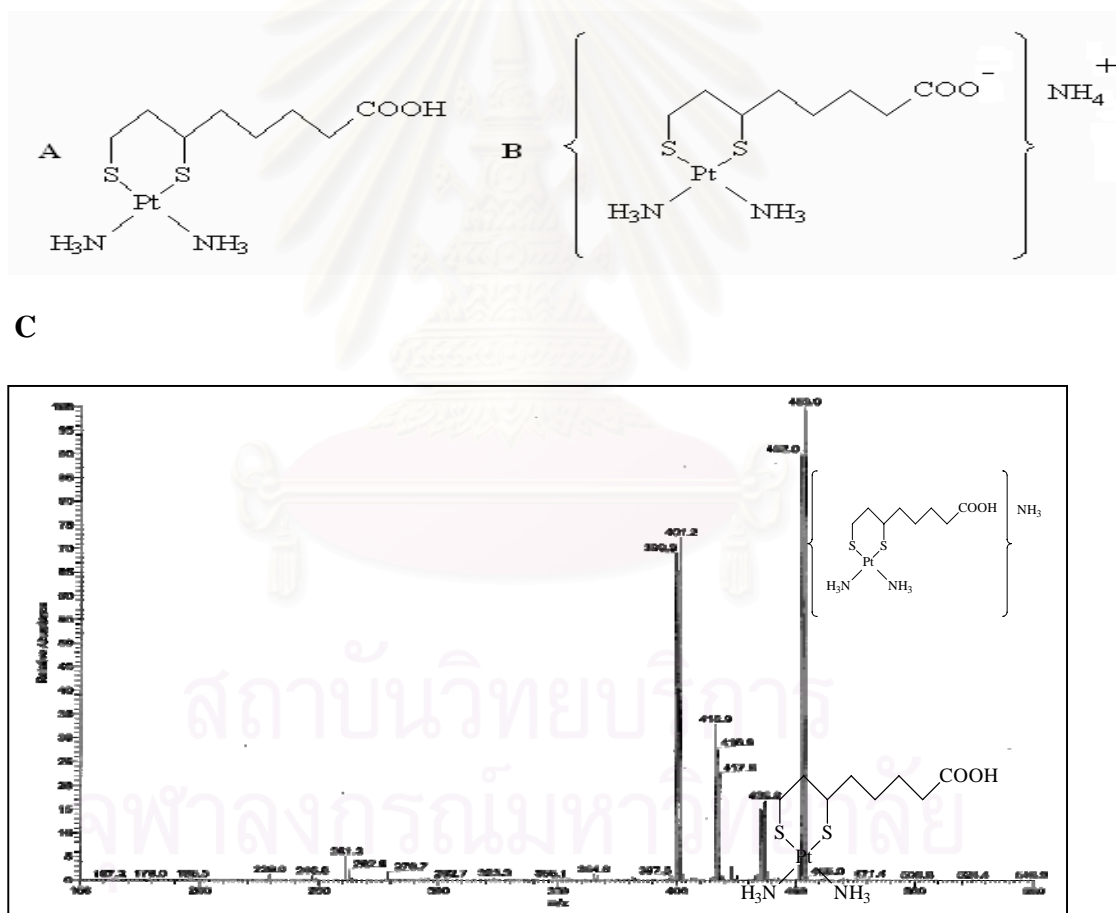


**Figure 32** The structure of LA-platinum adduct (A) and the ammonium adduct of platinum-LA (B). The ms/ms spectra of LA-cisplatin adduct at CE 15% was recorded (C).

#### 9.2.4 The effect of LA, DHLA, antioxidants and chelating agent on DNA protection

To compare the efficacy of LA and DHLA with other sulfur-containing antioxidants, glutathione and *N*-acetylcysteine (NAC) were used. Both types of dsDNA, self-complementary DNA (Dickerson dodecamer) and non self-complementary DNA, (heteroduplex undecamer) were used in the investigation. As mention earlier, heteroduplex undecamer DNA composes of two adjacent guanine (5'-GGC GCG CGC GG-3' and 5' CCG CGC GCG CC-3'). Another DNA, Dickerson dodecamer, does not have adjacent guanine but it contains 1,3 d- (GXG) (d(5'-CGCGAATTCGCG-3')), The formation of DNA-platinum adducts was different (data are shown in Figure 24B and 29B), therefore the efficacy of LA, DHLA and other antioxidants to protection of DNA damage might be different for each type of DNA. In this experiment EDTA, strong chelating agent, was also used to rule out whether the protection mechanism of LA and DHLA come from the chelating or not. The result from dHPLC showed that LA and DHLA can prevent the damage of DNA as good as glutathione and NAC. Interestingly, EDTA slightly protected DNA from cisplatin (PT) (Figure 33). Therefore the mechanisms of LA and DHLA for the protection of the DNA damage were not only from the chelating ability, but might also from the antioxidant ability. The results of both types of DNA were similar, as a result LA, DHLA and antioxidants could protect both guanine in the adjacent position and 1,3 d- (GXG) position.

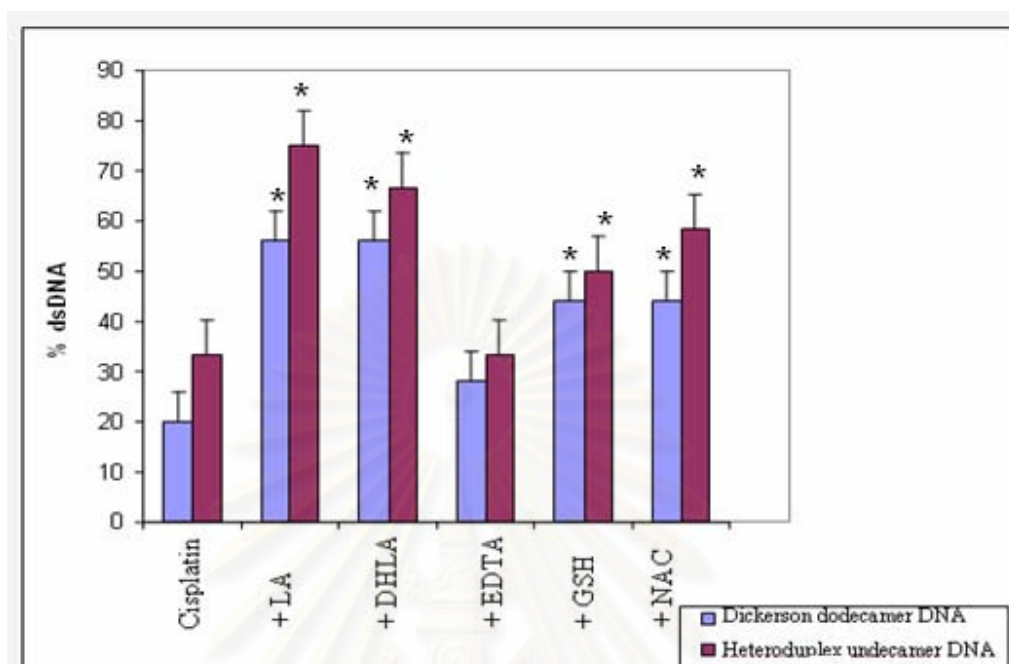


**Figure 33** The protection effect of different sulfur-containing compound and chelating agent to DNA in the system containing cisplatin ( $n=3$ , \*,  $p<0.05$  compare with treated control)

### 9.2.5 The effect of LA, DHLA, antioxidants and chelating agent on DNA recovery

Double strand DNAs were incubated with cisplatin in different periods (4-24 h). After 4 h samples were determined using ESI-MS to confirm whether platinum-adducts were formed. LA, DHLA, GSH, NAC or EDTA was added 4,12 and 24 h after cisplatin (PT) incubation to study the recovery efficacy. The result showed that LA and DHLA could recover both types of DNA, self-complementary DNA (Dickerson dodecamer) and non self-complementary DNA (heteroduplex undecamer) if they were added within 4 h of cisplatin (PT) incubation (Figure 34). But they did not have any effect if they were added at 12 and 24 h. GSH and NAC also showed the same results as LA and DHLA. In contrast, chelating agent, EDTA, could not recover DNA even within

4 h. The results showed the similar effect as the protection effect. Thus, LA, DHLA and antioxidants could recover both guanine in the adjacent position and 1,3 d- (GXG) position.

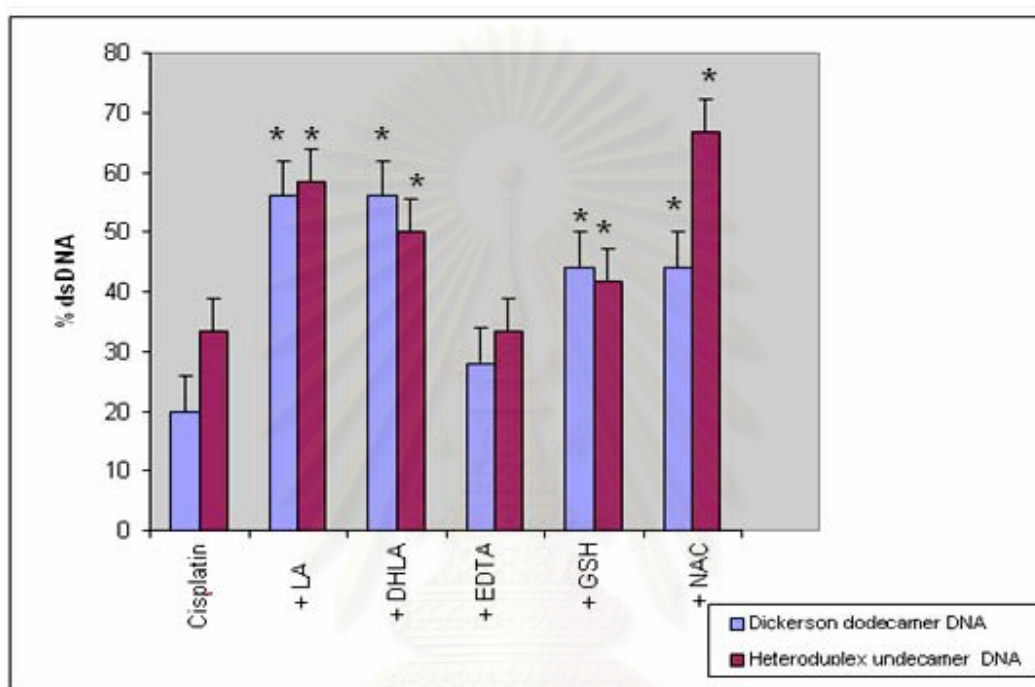


**Figure 34.** The recovery efficacies of different treatment in cisplatin induced DNA damage after 4 h ( $n=3$ , \*,  $p<0.05$  compare with treated control)

### 9.3 The effect of LA, LA-PRx complex and cholesterol modified LA-PRx complex on DNA damage protection

LA, and its delivery systems, LA-PRx complex and cholesterol modified LA-PRx complex, were investigated for the DNA damage protection using dHPLC. The damage of DNA was studied from 0-24 h. All of LA, and its delivery systems could protect the damage of DNA when compared with negative control. The LA-PRx complex and cholesterol modified LA-PRx showed could protect DNA as good as LA alone (data are shown in Figure 35). As a result, it showed that delivery systems of LA,



PRx and cholesterol modified PRx, did not reduce the protection efficacy of LA against DNA damage when compared with LA solution.

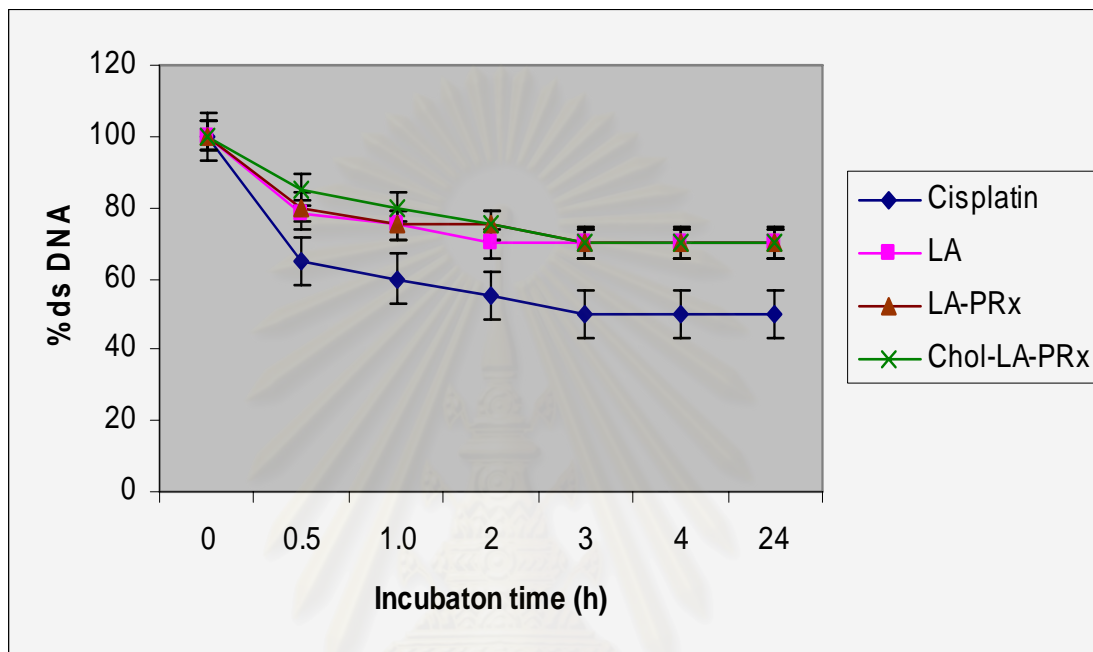


**Figure 35** The protection effect of LA solution, LA-PRx complex and cholesterol modified LA-PRx complex on DNA damage

## 10. The apoptosis assay of human epithelial lung cancer H-460 cells

### 10.1 Cisplatin (PT) induced apoptosis in H-460 cell line

Apoptosis, or programmed cell death, is one mechanism that induces cell death by cisplatin (PT) (Previati et al., 2006). In this experiment, apoptosis study was used to examine whether LA and DHLA could inhibit the effect of cisplatin (PT) or not. The completely confluent cultured human epithelial lung cancer H-460 cells were treated with various concentration of cisplatin (PT) (0-500  $\mu$ M) for a 12 h time period. The apoptotic cells exhibiting shrunken nuclei, chromatin condensation, and nuclear

fragmentation. The results showed that cisplatin (PT) induced cell apoptotic death in a concentration-dependent manner (Figure 36).

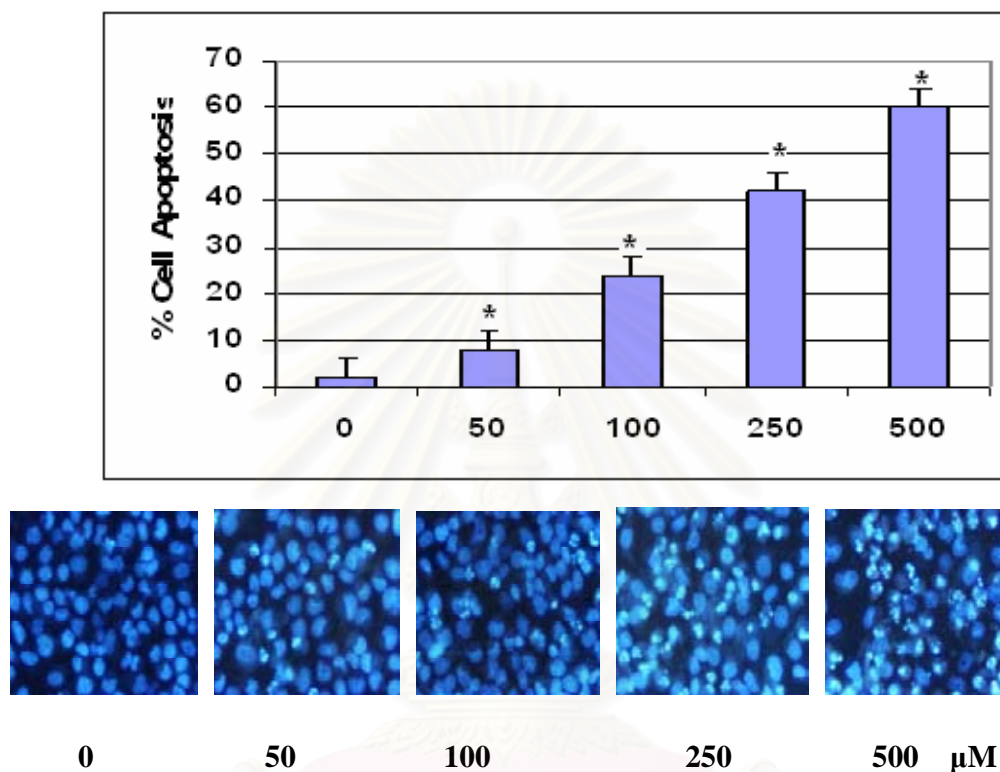
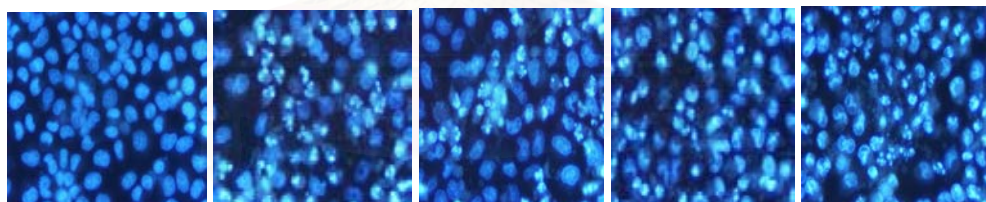
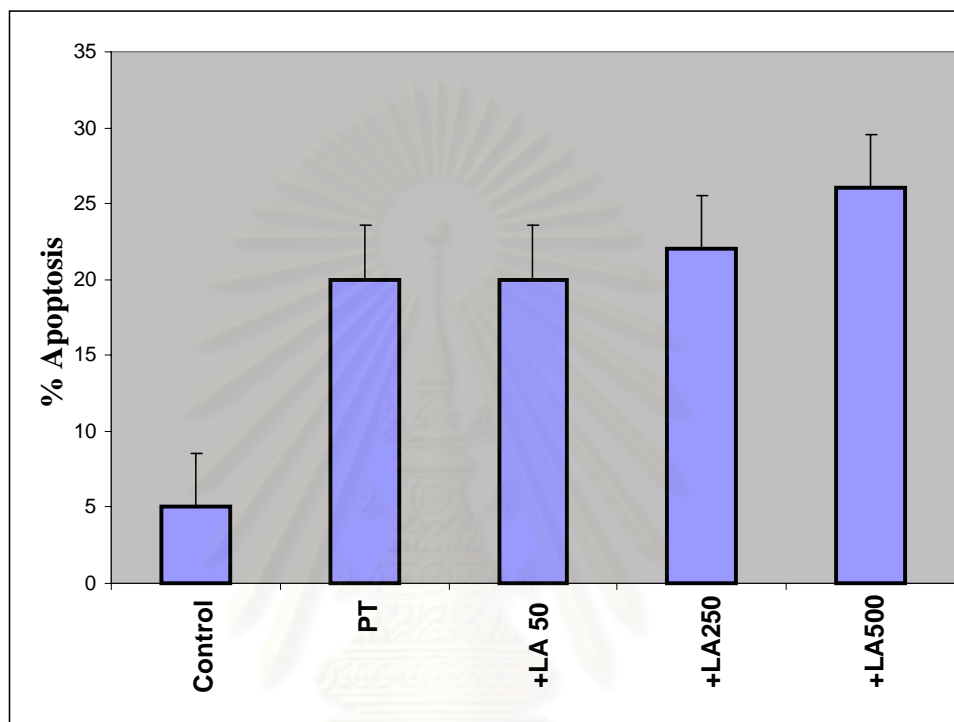


**Figure 36** Cisplatin (PT) induced H-460 cells apoptosis in dose-dependent manner. Cells were incubated with various doses of PT (0, 50, 100, 250, 500  $\mu\text{M}$ ). Apoptotic cells were analyzed by Hoechst 33342 staining method. Photographs of apoptotic cells detected by a fluorescent microscope (taken at X200 magnification) are shown.

### 10.2 The effect of LA and DHLA on cisplatin (PT) induced apoptosis in H-460 cells

It was found that LA and DHLA could not prevent cisplatin (PT) toxicity. H-460 was used as the model to study whether LA and DHLA could affect the anti-cancer properties of cisplatin (PT) or not. Apoptosis result showed that LA did not

significantly affect cisplatin (PT)-induced apoptosis (Figure 37). The result from DHLA was also the same as LA.



Control PT +LA 50 +LA250 +LA500  $\mu\text{M}$

**Figure 37** The effect of LA on cisplatin (PT) induced apoptosis in H-460 cells

### 10.3 LA and DHLA induce apoptosis in H-460 Cells

LA and DHLA have been reported to induce apoptosis in some cancer and transformed cell lines (Wenzel et al., 2005). However, their mechanisms of apoptosis induction are unclear. To determine the apoptosis mechanisms and to test whether these compounds can also induce apoptosis in human lung cancer epithelial cells, the apoptosis response to LA and DHLA treatment in H-460 cells was characterized. Figures 38A and 38B show that both LA and DHLA significantly induced cell apoptosis over control level with the effect of the former being more pronounced. The apoptotic cells exhibited shrunken nuclei, DNA fragmentation, and intense nuclear fluorescence.



สถาบันวิทยบริการ  
จุฬาลงกรณ์มหาวิทยาลัย

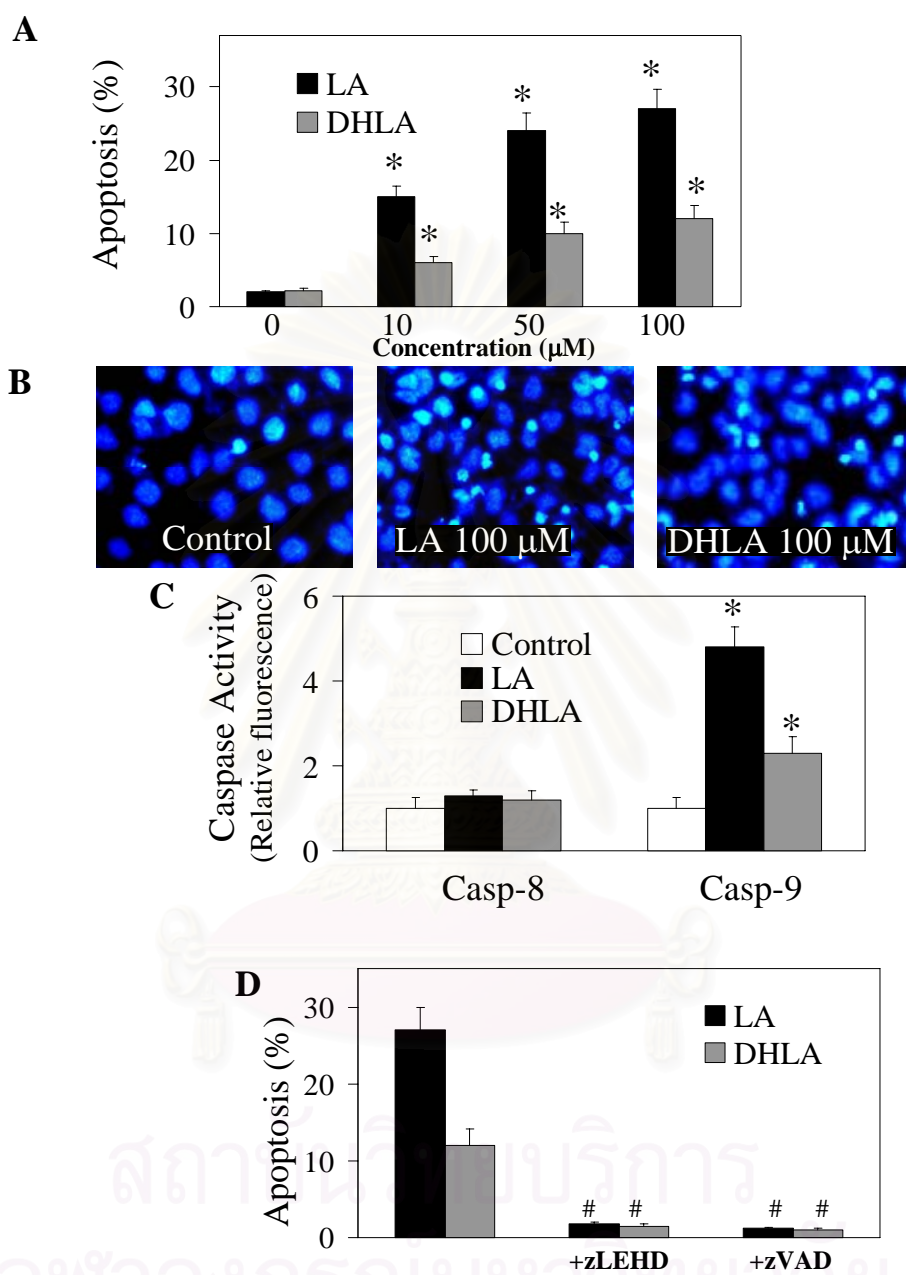


**Figure 38** LA and DHLA induce apoptosis in H460 cells (A). Fluorescence micrographs of treated cells stained with the Hoechst dye (B). LA and DHLA induced caspase activity in H460 cells (C). Caspase activity after cells were treated with LA or DHLA in the presence or absence of caspase-9 inhibitor or pan-caspase inhibitor (D) ( $n = 4$ , \*  $p < 0.05$  versus nontreated control; #,  $p < 0.05$  versus treated control)

#### 10.4 Effect of antioxidants on LA- and DHLA-induced apoptosis

H-460 cells were treated with LA or DHLA in the presence or absence of various known antioxidants, including NAC (general antioxidant), catalase ( $\text{H}_2\text{O}_2$  scavenger), MnTBAP ( $\text{O}_2^{\cdot-}$  scavenger), sodium formate ( $\text{OH}^{\cdot}$  scavenger) to test whether the apoptosis-inducing effect of LA and DHLA is associated with their pro-oxidant activity. The results showed that all tested antioxidants were able to inhibit apoptosis induced by LA or DHLA (Figure 39A), indicating that multiple ROS are involved in the apoptotic process. The potent inhibitory effects of catalase and MnTBAP further indicate that  $\text{H}_2\text{O}_2$  and  $\text{O}_2^{\cdot-}$  play an important role in the process. Subsequent studies using GPx and SOD overexpressed cells confirm this finding. These results also suggest that LA and DHLA induce apoptosis through a similar ROS-dependent mechanism.

#### 11. LA and DHLA induce caspase activation

LA and related short-chain fatty acids have been suggested to induce apoptosis through Fas death signaling pathway (Sen et al., 1999; Hara et al., 2000). Fas is a cell surface receptor which upon activation by Fas ligand or agonistic Fas antibody induces apoptosis via caspase-8 activation (Lenardo et al., 1999; Nagata, 1999). Caspase activity assays showed that LA, and to a lesser extent DHLA, induced caspase-9 activation but had no significant effect on caspase-8 activity (Figure 38C). Since caspase-9 serves as the apical caspase of the intrinsic (mitochondrial) pathway of apoptosis while caspase-8 represents the apical caspase of the extrinsic (death receptor) pathway (Salvesen and Dixit, 1997; Green and Reed, 1998; Wallach et al., 1999), the results suggest that the mitochondrial death pathway is the major pathway of apoptosis induction by LA and DHLA. Control experiments using pan-caspase inhibitor (z-VAD-fmk) and caspase-9-specific inhibitor (z-LEHD-fmk) showed complete inhibition of the apoptotic effect of LA and DHLA by the inhibitors (Figure 38D), supporting the role of caspases and in particular caspase-9 in the apoptotic process.



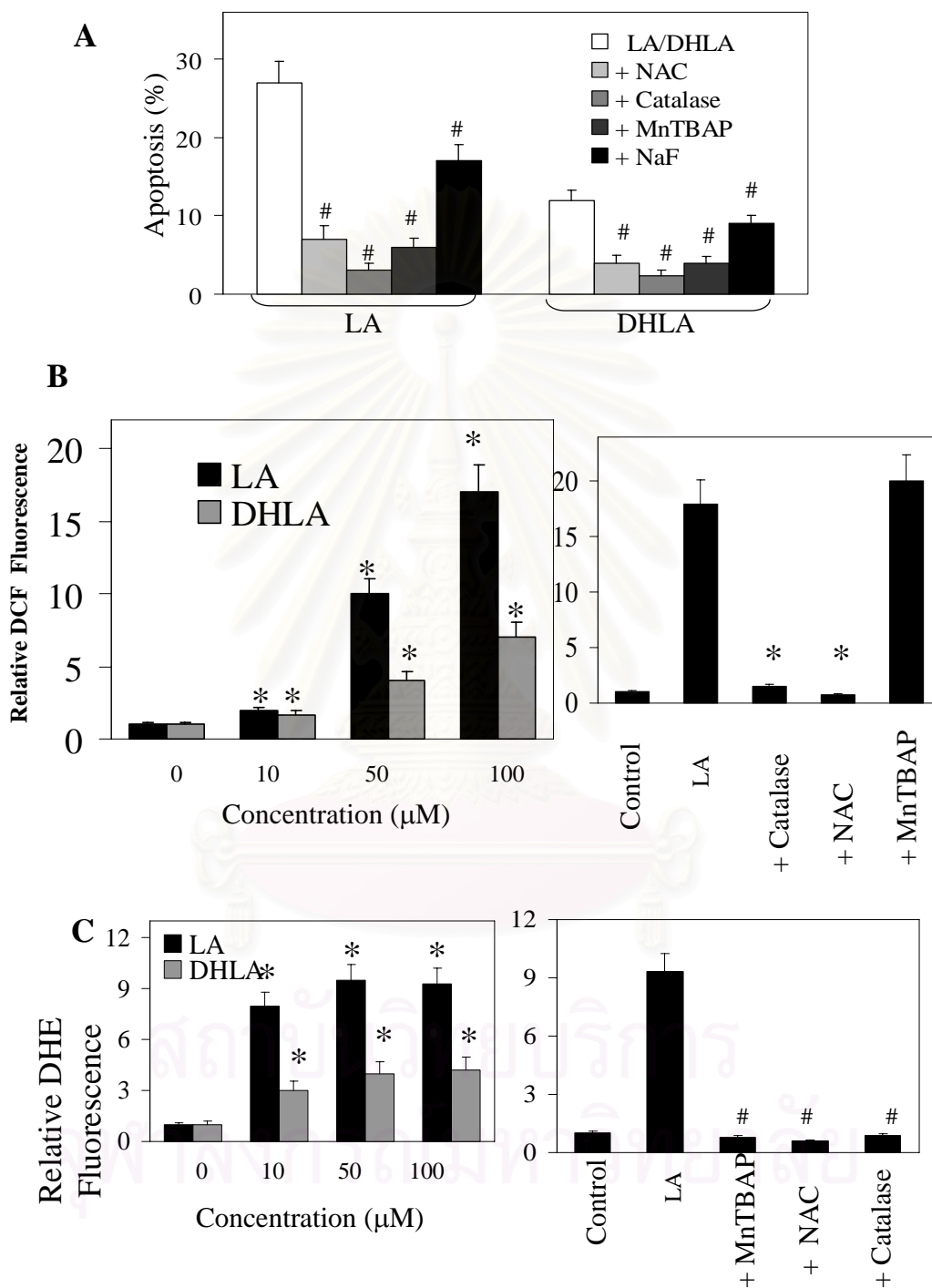


**Figure 39** Effects of antioxidants on LA- and DHLA-induced apoptosis (A). Flow cytometric analysis of ROS production in H-460 cells (B and C)

## 12. LA and DHLA induce ROS generation

LA and DHLA were able to induce intracellular peroxide production in a dose-dependent manner, as indicated by the increase in DCF fluorescence intensity (data was shown in Figure 39B). The effect of LA was more pronounced than DHLA and was inhibited by the addition of catalase, indicating the specificity of peroxide detection in the test system. Likewise, the general antioxidant NAC strongly inhibited the fluorescence signal, whereas the SOD mimetic MnTBAP showed minimal effect. DHE analysis of treated cells also indicates the formation of  $O_2^{\bullet-}$  by LA and DHLA treatment. The DHE signal was inhibited by the addition of MnTBAP and NAC (Figure. 39C). Interestingly, catalase also inhibited this signal, suggesting that LA-induced  $O_2^{\bullet-}$  generation may involve peroxide formation, possibly through the reaction of peroxide with cellular trace metals such as Fe(III), i.e.,  $H_2O_2 + Fe(III) \rightarrow Fe^{2+} + 2H^+ + O_2^{\bullet-}$  (Halliwell and Gutteridge 1990) or through the reaction of peroxide with thiols to form  $O_2^{\bullet-}$  via peroxidase-catalyzed reaction. Alternatively, DHE may detect some form of peroxides that can be blocked by catalase.

## 13. Responsibility of mitochondrial ROS on LA-induced apoptosis

The results showed that rotenone strongly inhibited LA-induced apoptosis and ROS generation, whereas DPI had weak effects (Figures. 40A-40C). These results indicate that mitochondria are the primary source of ROS production induced by LA and that these ROS are involved in the apoptotic process. The differential inhibitory effect of rotenone on superoxide and peroxide generation could reflect the non-specific effect of this compound on ROS and the varying rates of reaction between the ROS, their probes, and the compound. The role of specific ROS in LA-induced apoptosis could be more conclusively addressed using specific ROS inhibitors or antioxidant enzymes, as earlier demonstrated (Figure 39).

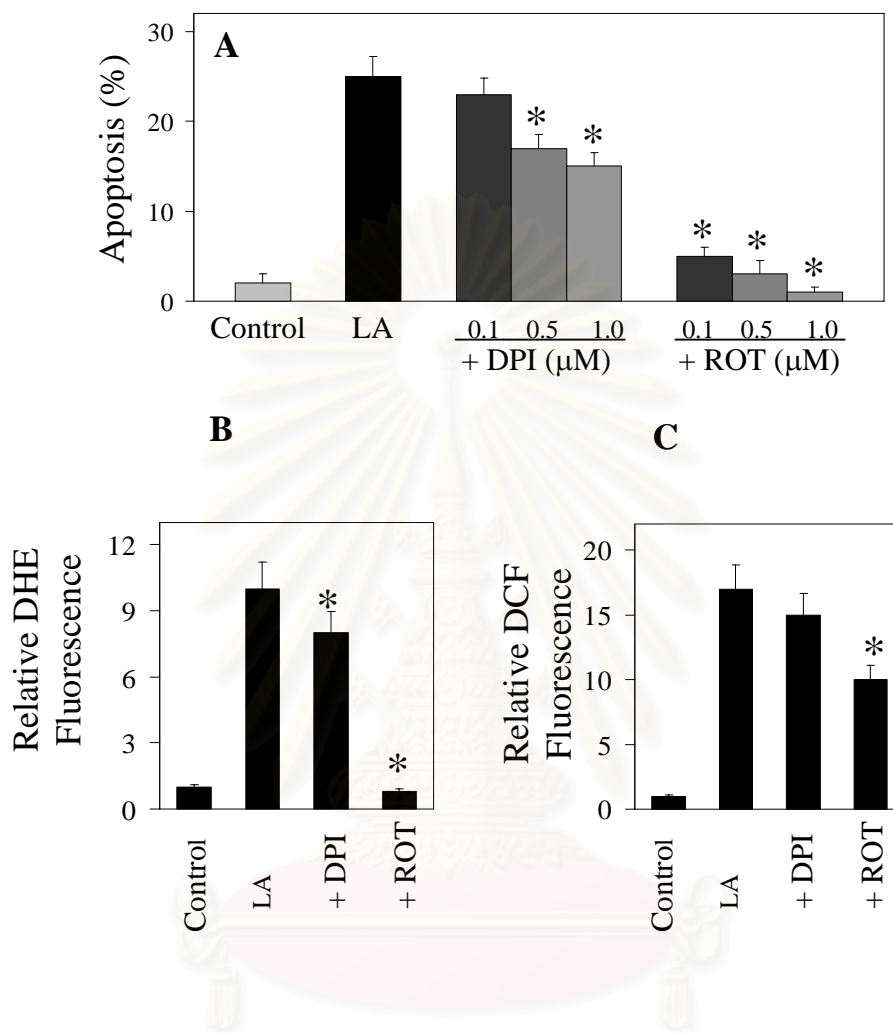


**Figure 40** Effects of DPI and ROT on LA-induced apoptosis detected by Hoechst dye (A). Effects of DPI and ROT on LA-induced ROS generation detected by flow cytometric measurements (B and C) ( $n = 3$ , \*  $p < 0.05$  versus nontreated control)

## **14. The effect of antioxidant and Bcl-2 overexpression on LA-Induced apoptosis and ROS generation**

### **14.1 Effect of ROS on LA induced apoptosis using GPx and SOD overexpression cells**

GPx, SOD stably transfected cells, or control plasmid was used to confirm the role of ROS in LA-induced apoptosis. Western blot analysis of the transfected cells showed an increase in antioxidant enzymes in the corresponding transfected cells as compared to mock transfected control (Figure 41A). Apoptosis assays showed a decrease in apoptotic response to LA treatment in GPx- and SOD-transfected cells but not in mock-transfected cells (Figure 41B). Flow cytometric analysis of ROS generation by DCF fluorescence also showed a substantial reduction in LA-induced fluorescence in GPx-transfected cells, as compared to mock and SOD-transfected cells (Figure 41C). DHE fluorescence measurements showed strong inhibition of LA-induced fluorescence in SOD and GPx-transfected cells relative to mock-transfected cells (Figure 41D), the results that were consistent with our earlier MnTBAP and catalase data.

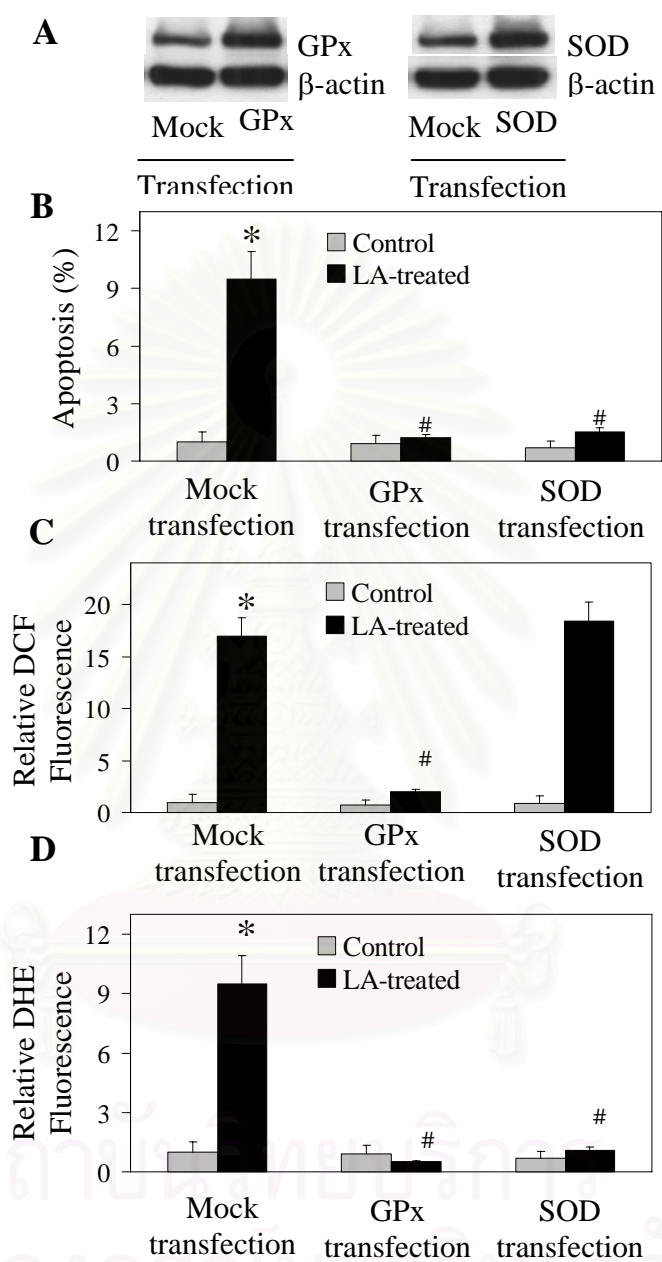


**Figure 41** Effects of GPx and SOD overexpression on LA-induced apoptosis and ROS generation (A). Transfected cells were treated with LA and analyzed for apoptosis (B) and analyzed for DCF and DHE fluorescence intensities (C and D) ( $n = 3$ , \*  $p < 0.05$  versus nontreated control; #,  $p < 0.05$  versus treated control)

### **14.2 Effect of Bcl-2 on LA induced apoptosis**

LA-induced apoptosis was earlier shown to be mediated through the mitochondrial caspase-9 activation pathway (Figure. 38). Since this pathway is known to be regulated by the anti-apoptotic Bcl-2 protein (Green and Reed, 1998), we evaluated whether this protein was involved in the regulation of apoptosis by LA. Western blot analysis of the transfected cells showed an increase in Bcl-2 expression in Bcl-2-transfected cells compared to mock-transfected control (Figure. 42A). Apoptosis assays showed a strong inhibition of LA-induced apoptosis by the Bcl-2 overexpression at various treatment concentrations of LA (Figure 42B). These results indicate the role of Bcl-2 as a negative regulator of LA-induced apoptosis and further support the role of mitochondria in the death signaling process.

### **14.3 Effect of LA treatment on Bcl-2 expression**

The Western blot results showed that the expression level of Bcl-2 responded to LA. Figures 43A and 43B showed that treatment of the cells with LA caused a dose- and time-dependent decrease in Bcl-2 expression levels. These data indicated a mechanistic insight into the regulation of LA-induced apoptosis regulated by Bcl-2 protein. Since previous studies have shown that Bcl-2 is downregulated primarily through proteasomal degradation pathway, we tested whether such degradation was involved in the downregulation of Bcl-2 by LA. Figure 41C showed that lactacystin (LAC) completely inhibited Bcl-2 downregulation induced by LA. This result was confirmed by the observation that another proteasome inhibitor, MG132, also inhibited LA-induced Bcl-2 downregulation. This finding indicated that proteasomal degradation was a key mechanism of LA-induced Bcl-2 downregulation.



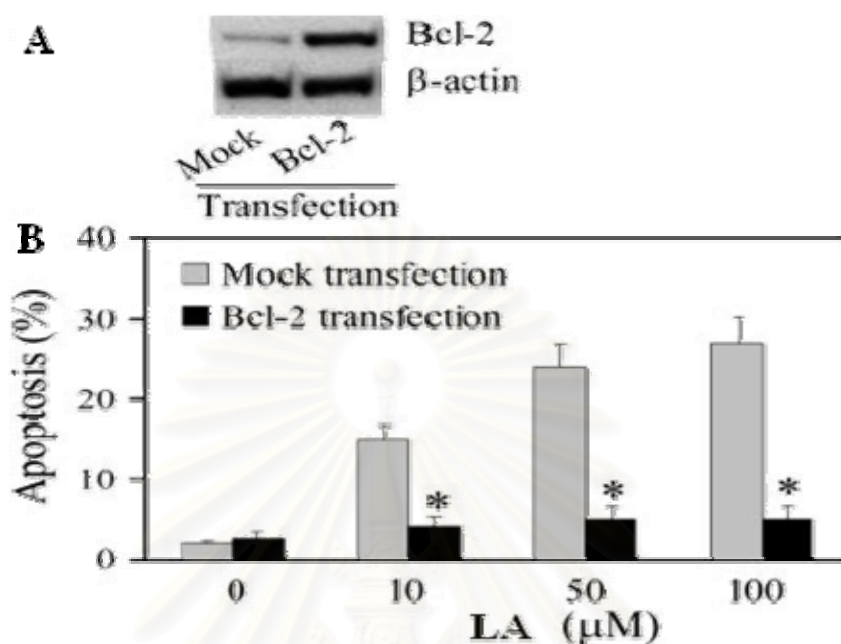


**Figure 42** Bcl-2 protein overexpression of Bcl-2 transfection cells compared with mock transfection cells (A). Transfected cells were treated with varying doses of LA before % apoptosis was determined (B) ( $n = 3$ , \*  $p < 0.05$  versus nontreated control)

#### 14.4 Effect of antioxidants on Bcl-2 expression

The role of Bcl-2 in LA-induced apoptosis was demonstrated on Figure 42 and 43. ROS have previously been shown to mediate TNF- $\alpha$ -induced proteasomal degradation of Bcl-2 in human umbilical vein endothelial cells (Breitschopf et al., 2000). H-460 cells were treated with LA in the presence or absence of antioxidants to test whether ROS might also mediate the effect of LA via Bcl-2 expression. Figure 44A showed that pre-treatment of the cells with NAC or catalase completely inhibited LA-induced Bcl-2 downregulation, whereas MnTBAP treatment showed no inhibitory effect. These results were confirmed in GPx- and SOD-overexpressed cells. Figure 44B showed that GPx overexpression completely inhibited LA-induced Bcl-2 downregulation, whereas SOD overexpression was ineffective. These results indicated that hydroperoxide was the primary ROS responsible for LA-induced Bcl-2 downregulation.

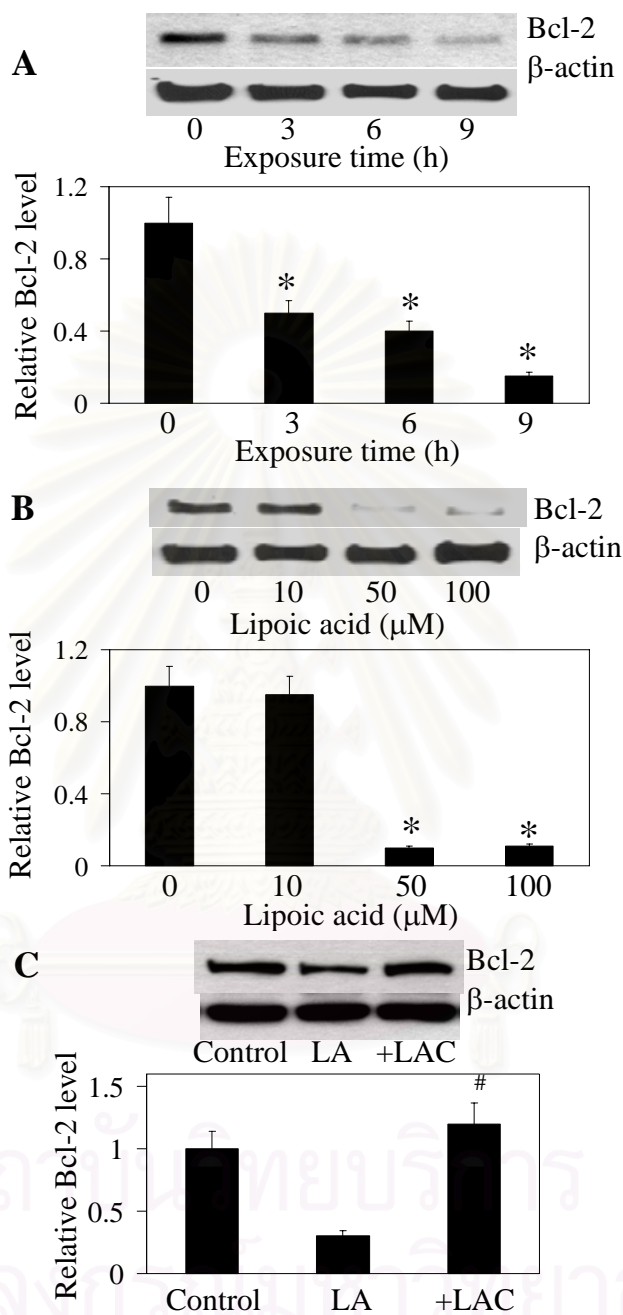


**Figure 43** Effect of LA exposure time on Bcl-2 expression level(A). Dose effect of LA on Bcl-2 expression determined at 9 h post-treatment (B). Effect of proteasome inhibitor (LAC) on LA-induced Bcl-2 down-regulation (C) ( $n = 3$  \*  $p < 0.05$  versus nontreated control; #,  $p < 0.05$  versus treated control)

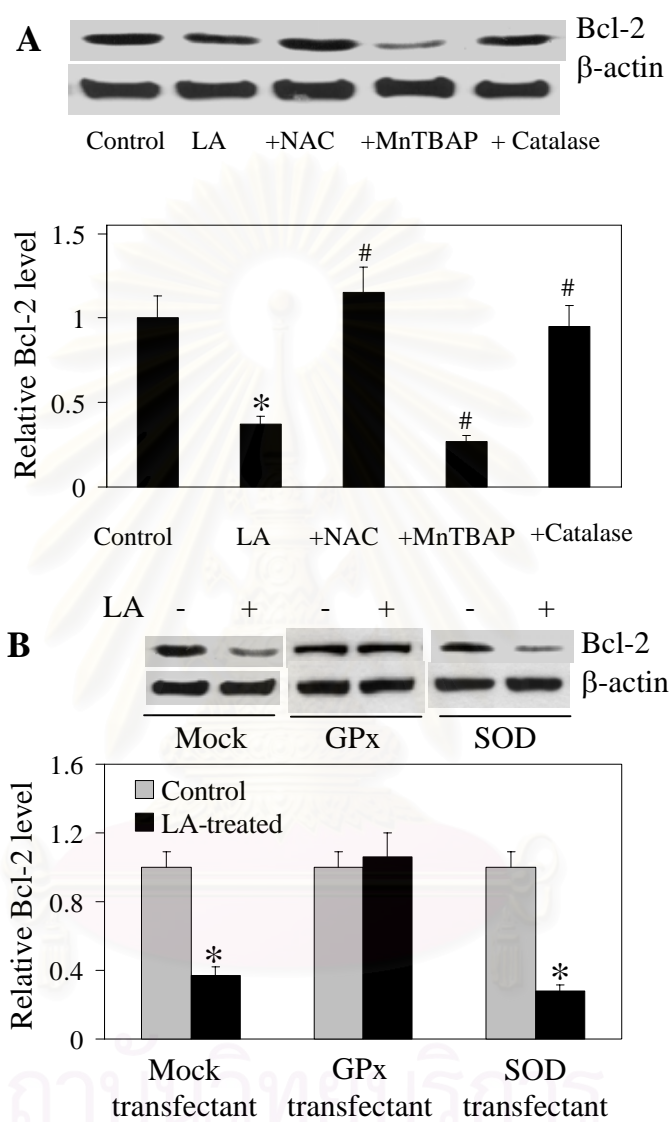


**Figure 44** Effect of antioxidants on Bcl-2 expression (A). Effect of overexpression cells (GPx-, SOD-, or mock-transfected cells) on Bcl-2 expression (B) ( $n = 3$  \*  $p < 0.05$  versus nontreated control; #,  $p < 0.05$  versus treated control)

## CHAPTER V

### CONCLUSION

#### 1. The extraction of LA from Thai spinach (*Spinacea oleracea*)

LA could be extracted from Thai spinach (*Spinacea oleracea*) leaves. It was found in alcoholic fraction. The simple solvent extraction might not be appropriate for extraction of the active ingredient that is tightly bound with protein. The extraction method might need to further development.

#### 2. The synthesis of DHLA

DHLA is a very unstable antioxidant and expensive. Therefore, in this investigation we freshly synthesized DHLA from LA for each experiment to prevent the oxidation of DHLA during storage. Yield of DHLA was very high and constant for each synthesis.

#### 3. Characterization of LA, DHLA and DNA-platinum adducts using ESI-MS and dHPLC

ESI-MS showed the sensitivity and specificity for characterization of the small molecule compounds i.e. LA extracted from *Spinacea oleracea* including DHLA that was synthesized from LA. It also is useful for studying DNA. The structures of DNA-platinum adducts could be characterized using ESI-MS. The amount of damaged DNA could be quantitated by dHPLC, which is the highly sensitive method for detecting the mutation or the damaged DNA.

#### **4. Novel biodegradable PRx and cholesterol modified PRx enhanced the penetration of LA**

PRx was selected as the delivery system of LA. PRx showed the sustain released effect for the penetration of LA through the SC. According to the result, free LA was detected after 2 h. This might imply that PRx needed the lag time for hydrolyzing LA before penetration. Interestingly, after 2 h LA could penetrate to receptor compartment and rate of penetration was higher than LA solution. The final concentration of LA from LA-PRx complex was higher than LA solution. The mechanisms of PRx to enhance the permeability of drugs through the skin have been extensively discussed in relation to the changing the structure or dissolving skin lipids, altering the conformation or denaturing skin proteins, disruption of water structure in skin and increasing membrane fluidity (Ooya et al., 1998). Because PRx composes of PEG threaded with CDs, the structure is not more flexible. It needed time to penetrate into the skin, but once it penetrated into the skin, it could improve the penetration of drugs. To improve the flexibility of PRx and improve the penetration of LA from PRx, cholesterol was introduced to PRx. The cholesterol was introduced to RPx by cross-linking with PEG to prepare cholesterol modified PRx. Each mole of PRx contained cholesterol 1 mole. Cholesterol modified PRx improved the penetration of LA with short lag time. Cholesterol makes the structure of SC more flexible so PRx can penetrate into the skin easier. LA-PRx complex and cholesterol modified LA-PRx also enhanced cell proliferation in human skin fibroblast cells. These results agree with Tachaboonyakiat et.al. (Tachaboonyakiat et al., 2004). They studied the cholesterol modified PRx in chondrocyte. Cholesterol modified PRx improved the chondrocyte proliferation and GAG production. Likewise, the modification of cholesterols to PRx also control the degradation time of cholesterol modified PRx. Time to complete degradation was shortened by increasing the degree of substitution to PRx through hydrophobic interaction of cholesterol groups (Tachaboonyakiat et al., 2004).The toxicities of PRx and cholesterol modified PRx were studied in normal human dermal fibroblast cells. The results showed that both of them were not toxic to cells. In addition, they seemed to be stimulating the growth of fibroblast cells. Therefore cholesterol modified LA-PRx might be a good

approach for creating new biodegradable systems for topical application in terms of enhancing the penetration and improving cell proliferation of the skin. While LA-PRx complex might be used for sustained release of LA.

### **5. LA and DHLA protect against DNA damage inducing by cisplatin**

For studying the protection of LA to DNA, non self-complementary DNA, (heteroduplex undecamer), and self-complementary oligonucleotide DNA (Dickerson dodecamer) were used as the model for investigation. The data from this study showed that cisplatin (PT) formed different adducts between non self-complementary DNA (heteroduplex undecamer) and self-complementary DNA (Dickerson dodecamer). Undecamer DNA composes of 5'-GGC GCG CGC GG-3' which is containing two adjacent guanine and 5' CCG CGC GCG CC-3'. Another DNA, Dickerson dodecamer, composed of d(5'- CGCGAATTTCGCG-3'), does not have adjacent guanine but it contains 1,3 d- (GXG). The undecamer DNA formed only mono adduct with Pt(NH<sub>3</sub>)<sub>2</sub>. Interestingly, Dickerson dodecamer DNA formed many types of adduct with cisplatin (PT) which characterized by ESI-MS. The DNA-platinum adduct formation of adjacent guanine, 1,2-d(GGX), occurred very quickly and reach steady state within 1 h and it form only one adduct species. But DNA-platinum adducts of 1,3-d(GXG) occurred slower and it formed many types of platinum-adducts.

This report describes the efficacy of LA and DHLA as an inhibitor of DNA damage *in vitro* model. According to our results, dHPLC showed the rescued effect of both LA and DHLA. LA and DHLA protected DNA from the formation of platinum-DNA adduct. The data of ESI-MS also showed the reduction of adduct formation both intrastrand 1,2-d(GGX) and 1,3-d(GXG) in the systems that contain LA or DHLA. ESI-MS analysis of LA or DHLA and cisplatin (PT) suggested that platinum from cisplatin inserted in between 2-sulfur group and from the stable heterocyclic ring. In addition, when compared with carboxylic acid and EDTA, the results also showed that the protection efficacy of LA and DHLA did not come from carboxylic group or the chelating efficacy. Moreover, the dHPLC results showed that LA and DHLA could reverse nucleotide from the platinum-adducts if



LA or DHLA was added within 4 h. This result implies that, if LA or DHLA was administered after the platinum had accumulated and bound in DNA before irreversible damage had occurred, then the nephrotoxicity, ototoxicity and other side effects that come from cytotoxicity of platinum-DNA adducts might be inhibited.

The mechanisms to damage DNA of cisplatin not only directly formed adduct to DNA, but also generated some oxidants to damage DNA. The adding of other antioxidants, GSH and NAC, also protect the damage of DNA from cisplatin. LA and DHLA which are strongly antioxidant could efficiently protect DNA with 2 mechanisms, formed complex with cisplatin directly and acted as antioxidant. LA is the small molecule and it is easily absorbed and penetrated inside cells so it can be the potential substance exhibited high efficacy to protect the damage of DNA from cisplatin and reduce its side effect.

#### **6. The effect of LA and DHLA on PT induced apoptosis in H-460 cells**

The apoptosis data showed that LA and DHLA did not significantly disturb the efficacy of cisplatin in H-460 cancer cells. Additionally, according to dHPLC results, even LA and DHLA were added after the platinum adducts formation 4 h, they still could recover dsDNA. The result from these experiments suggested the time course and doses of LA and DHLA for chemoprotection after cisplatin matches provided an opportunity to manipulate route and timing to maintain cisplatin antitumor efficacy while protecting against chemotherapy side effects.

#### **7. The efficacy of LA, LA-PRx complex and cholesterol modified LA-PRx complex on DNA damage protection**

The result from the study showed that LA, LA-PRx complex and cholesterol modified LA-PRx complex could protect the damage of DNA inducing from cisplatin. All of them had the same efficacy for the protection. These results demonstrated that LA-PRx complex and cholesterol modified LA-PRx complex had the same protection effect as LA solution. Whilst the penetration results as mention earlier, LA from cholesterol modified LA-PRx complex enhanced the

penetration through the SC which is the rate limiting step for the topical application better than LA solution and LA-PRx complex. We might conclude that cholesterol modified LA-PRx had greater ability to protect the damage of DNA when compare with LA solution and LA-PRx complex.

### **8. ROS mediate caspase activation and apoptosis induced by LA in human lung epithelial cancer cells through Bcl-2 down-regulation**

This study showed that LA induced peroxide generation in H-460 cells. Similar ROS-inducing effects were observed with DHLA. Inhibition of ROS generation by the antioxidant NAC, catalase, and MnTBAP effectively inhibited apoptosis induced by LA and DHLA, indicating the role of ROS, especially  $\text{H}_2\text{O}_2$  and  $\text{O}_2^{\cdot-}$ , in this process. The results also suggest a similar ROS-dependent apoptogenic mechanism of LA and DHLA. The role of  $\text{H}_2\text{O}_2$  and  $\text{O}_2^{\cdot-}$  was confirmed in cells overexpressing GPx and SOD, both of which showed strongly reduced apoptotic responses to LA treatment.

The mechanism by which ROS mediate the apoptotic effect of LA and DHLA also be studied. The results showed LA and DHLA were unable to induce caspase-8 activation in H460 cells. The previous study showed that H-460 cells are susceptible to Fas-mediated apoptosis through caspase-8 activation (Chanvorachote et al., 2005). Therefore, the inability of LA and DHLA to activate caspase-8 suggests that their apoptotic effect is not mediated through the Fas signaling pathway. These results are consistent with a previous report showing that Fas-deficient Jurkat cells retained their sensitivity to LA-induced apoptosis (van de Mark et al., 2003). LA and DHLA induce apoptosis through the mitochondrial death pathway also was shown in this study. This induction of apoptosis involves mitochondrion-dependent activation of caspase-9, which can be inhibited by caspase-9-specific inhibitor (z-LEHD-fmk) or pan-caspase inhibitor (z-VAD-fmk). LA- and DHLA-induced caspase-9 activation was also found to be inhibited by the ROS scavenger NAC. These results are consistent with previous reports showing the presence of procaspase-9 in the mitochondria which is released and subsequently activated in the cytoplasm during apoptosis (Salvesen and Dixit, 1997; Green and Reed, 1998)

The generation of ROS induced by LA occurs primarily in the mitochondria since the mitochondrial respiratory chain inhibitor rotenone effectively inhibited this generation. Rotenone has previously been shown to inhibit mitochondrial ROS in other cell systems (Chen et al., 2003). DPI, a known inhibitor of cellular NADPH oxidase (Freeman and Crapo, 1982), showed a weak effect on LA-induced ROS generation, indicating the less important role of this enzyme system in the ROS production.

Bcl-2 is a key regulator of the mitochondrial pathway that prevents apoptosis by preserving mitochondrial permeability transition (Fiers et al., 1999). The result showed that overexpression of Bcl-2 strongly inhibited LA-induced apoptosis, further supporting the role of mitochondria in LA-induced cell death. Exposure of the cells to LA caused a dose- and time-dependent downregulation of Bcl-2. Such downregulation is mediated by the proteasomal pathway since inhibition of this pathway by the proteasome inhibitor lactacystin completely inhibited the effect of LA on Bcl-2. This study also showed that this downregulation is ROS-dependent since co-treatment of the cells with antioxidant NAC or catalase completely inhibited the downregulation effect of LA on Bcl-2. The  $O_2^{\bullet-}$  scavenger MnTBAP failed to inhibit this effect, indicating that peroxide, but not  $O_2^{\bullet-}$ , is the primary ROS responsible for LA-induced Bcl-2 downregulation. Gene transfection studies using GPx and SOD overexpressed cells confirmed these results and indicate the critical role of peroxide in this process. The observation that MnTBAP and SOD failed to inhibit Bcl-2 downregulation while exhibiting a protective effect on LA-induced apoptosis suggests that other  $O_2^{\bullet-}$ -mediated Bcl-2-independent mechanisms may be involved in the apoptotic effect of LA.

Signal transduction leading to apoptotic cell death has been of great interest in biomedical and pharmaceutical research mainly because successful apoptotic agents could be used to treat cancer. The therapeutic potential of LA in cancer treatment has been demonstrated in several studies (Sen et al., 1999; van de Mark et al., 2003; Wenzel et al., 2005). Previously, chemotherapeutic agents such as doxorubicin, cisplatin, vincristine, and the alkaloid taxol have commonly been used as anti-tumor agents. However, at high concentrations these drugs are toxic to cells and cause adverse side-effects. In contrast, LA is an endogenous agent that has been widely

used as a dietary supplement. It is known to increase cellular glutathione levels, regulate cellular redox balance and help protect against diabetic complications (Sen et al., 1997; Kocak and Karasu, 2002; Jesudason et al., 2005). The finding on the apoptotic effect of LA in human lung cancer cells supports its potential utility as an agent for the treatment of lung cancer.

In summary, these researches provide evidence that natural LA extracted from Thai spinach (*Spinacea oleracea*) and its reduced form, DHLA, could protect the damage of DNA and recover damaged DNA. The delivery system in this research, cholesterol modified LA-PRx complex improved the penetration of LA. Therefore, they could improve the DNA damage protection effect of LA. The finding on the apoptotic effect of LA could be use for the treatment of the diseases and the pathology involved in the apoptosis disorder.



สถาบันวิทยบริการ  
จุฬาลงกรณ์มหาวิทยาลัย

## REFERENCES

- Alexandre, J., Batteux, F. et al. (2006). "Accumulation of hydrogen peroxide is an early and crucial step for paclitaxel-induced cancer cell death both in vitro and in vivo." Int J Cancer **119**(1): 41-8.
- Arner, E. S., Nordberg, J. et al. (1996). "Efficient reduction of lipoamide and lipoic acid by mammalian thioredoxin reductase." Biochem Biophys Res Commun **225**(1): 268-74.
- Ashkenazi, A. and Dixit, V. M. (1998). "Death receptors: signaling and modulation." Science **281**(5381): 1305-8.
- Ashkenazi, A. and Dixit, V. M. (1999). "Apoptosis control by death and decoy receptors." Curr Opin Cell Biol **11**(2): 255-60.
- Baik, M. H., Friesner, R. A. et al. (2003). "Theoretical study of cisplatin binding to purine bases: why does cisplatin prefer guanine over adenine?" J Am Chem Soc **125**(46): 14082-92.
- Balayssac, D., Cayre, A. et al. (2006). "Involvement of the multidrug resistance transporters in cisplatin-induced neuropathy in rats. Comparison with the chronic constriction injury model and monoarthritic rats." Eur J Pharmacol **544**(1-3): 49-57.
- Bartsch, H. and Nair, J. (2006). "Chronic inflammation and oxidative stress in the genesis and perpetuation of cancer: role of lipid peroxidation, DNA damage, and repair." Langenbecks Arch Surg **391**(5): 499-510.
- Bast, A. and Haenen, G. R. (1988). "Interplay between lipoic acid and glutathione in the protection against microsomal lipid peroxidation." Biochim Biophys Acta **963**(3): 558-61.
- Bernkop-Schnurch, A., Schuhbauer, H. et al. (2004). "Development of a sustained release dosage form for alpha-lipoic acid. I. Design and in vitro evaluation." Drug Dev Ind Pharm **30**(1): 27-34.
- Biewenga, G. P., Haenen, G. R. et al. (1997). "The pharmacology of the antioxidant lipoic acid." Gen Pharmacol **29**(3): 315-31.



- Biewenga, G. P., Veening-Griffioen, D. H. et al. (1998). "Effects of dihydrolipoic acid on peptide methionine sulfoxide reductase. Implications for antioxidant drugs." Arzneimittelforschung **48**(2): 144-8.
- Bilska, A. and Wlodek, L. (2005). "Lipoic acid - the drug of the future?" Pharmacol Rep **57**(5): 570-7.
- Bodmer, J. L., Burns, K. et al. (1997). "TRAMP, a novel apoptosis-mediating receptor with sequence homology to tumor necrosis factor receptor 1 and Fas(Apo-1/CD95)." Immunity **6**(1): 79-88.
- Borch, R. F. and Pleasants, M. E. (1979). "Inhibition of cis-platinum nephrotoxicity by diethyldithiocarbamate rescue in a rat model." Proc Natl Acad Sci U S A **76**(12): 6611-4.
- Breitschopf, K., Haendeler, J. et al. (2000). "Posttranslational modification of Bcl-2 facilitates its proteasome-dependent degradation: molecular characterization of the involved signaling pathway." Mol Cell Biol **20**(5): 1886-96.
- Cadet, J., Delatour, T., et al. (1999). "Hydroxyl radicals and DNA base damage." Mutat Res **424**(1-2): 9-21.
- Cakatay, U. (2006). "Pro-oxidant actions of alpha-lipoic acid and dihydrolipoic acid." Med Hypotheses **66**(1): 110-7.
- Cakatay, U. and Kayali, R. (2005). "Plasma protein oxidation in aging rats after alpha-lipoic acid administration." Biogerontology **6**(2): 87-93.
- Cakatay, U., Kayali R., et al. (2005). "Prooxidant activities of alpha-lipoic acid on oxidative protein damage in the aging rat heart muscle." Arch Gerontol Geriatr **40**(3): 231-40.
- Carreau, J. P. (1979). "Biosynthesis of lipoic acid via unsaturated fatty acids." Methods Enzymol **62**: 152-8.
- Cathcart, R., Schwiers, E. et al. (1984). "Thymine glycol and thymidine glycol in human and rat urine: a possible assay for oxidative DNA damage." Proc Natl Acad Sci U S A **81**(18): 5633-7.
- Chanvorachote, P., Nimmannit, U. et al. (2005). "Nitric oxide negatively regulates Fas CD95-induced apoptosis through inhibition of ubiquitin-proteasome-mediated degradation of FLICE inhibitory protein." J Biol Chem **280**(51): 42044-50.



- Chen, Q., Vazquez, E. J. et al. (2003). "Production of reactive oxygen species by mitochondria: central role of complex III." J Biol Chem **278**(38): 36027-31.
- Cohen, S. M. and Lippard, S. J. (2001). "Cisplatin: from DNA damage to cancer chemotherapy." Prog Nucleic Acid Res Mol Biol **67**: 93-130.
- Coleman, M. D., Williams, C. et al. (2006). "Effects of Lipoic Acid and Dihydrolipoic Acid on 4-Aminophenol-Mediated Erythrocytic Toxicity in vitro\*." Basic Clin Pharmacol Toxicol **99**(3): 225-229.
- Coombes, J. S., Powers, S. K. et al. (2000). "Effect of combined supplementation with vitamin E and alpha-lipoic acid on myocardial performance during in vivo ischaemia-reperfusion." Acta Physiol Scand **169**(4): 261-9.
- Correa, J. G. and Stoppani, A. O. (1996). "Catecholamines enhance dihydrolipoamide dehydrogenase inactivation by the copper Fenton system. Enzyme protection by copper chelators." Free Radic Res **24**(4): 311-22.
- Crompton, M. (1999). "The mitochondrial permeability transition pore and its role in cell death." Biochem J **341** (Pt 2): 233-49.
- Curran, W. J. (2002). "New chemotherapeutic agents: update of major chemoradiation trials in solid tumors." Oncology **63 Suppl 2**: 29-38.
- Demir, U., Demir, T. et al. (2005). "The protective effect of alpha-lipoic acid against oxidative damage in rabbit conjunctiva and cornea exposed to ultraviolet radiation." Ophthalmologica **219**(1): 49-53.
- Dene, B. A., Maritim, A. C. et al. (2005). "Effects of antioxidant treatment on normal and diabetic rat retinal enzyme activities." J Ocul Pharmacol Ther **21**(1): 28-35.
- Deubel, D. V. (2004). "Factors governing the kinetic competition of nitrogen and sulfur ligands in cisplatin binding to biological targets." J Am Chem Soc **126**(19): 5999-6004.
- Dhein, J., Walczak, H. et al. (1995). "Autocrine T-cell suicide mediated by APO-1/(Fas/CD95)." Nature **373**(6513): 438-41.
- Dhein, J., Walczak, H. et al. (1995). "Molecular mechanisms of APO-1/Fas(CD95)-mediated apoptosis in tolerance and AIDS." Behring Inst Mitt(96): 13-20.

- Dicter, N., Madar, Z. et al. (2002). "Alpha-lipoic acid inhibits glycogen synthesis in rat soleus muscle via its oxidative activity and the uncoupling of mitochondria." J Nutr **132**(10): 3001-6.
- Dogru-Abbasoglu, S., Aykac-Toker G., et al. (2007). "The Arg194Trp polymorphism in DNA repair gene XRCC1 and the risk for sporadic late-onset Alzheimer's disease." Neurol Sci **28**(1): 31-4.
- Douki, T., Reynaud-Angelin, A. et al. (2003). "Bipyrimidine photoproducts rather than oxidative lesions are the main type of DNA damage involved in the genotoxic effect of solar UVA radiation." Biochemistry **42**(30): 9221-6.
- Edenharder, R., Keller, G. et al. (2001). "Isolation and characterization of structurally novel antimutagenic flavonoids from spinach (*Spinacia oleracea*)." J Agric Food Chem **49**(6): 2767-73.
- El Midaoui, A. and de Champlain, J. (2002). "Prevention of hypertension, insulin resistance, and oxidative stress by alpha-lipoic acid." Hypertension **39**(2): 303-7.
- Fiers, W., Beyaert R., et al. (1999). "More than one way to die: apoptosis, necrosis and reactive oxygen damage." Oncogene **18**(54): 7719-30.
- Freeman, B. A. and Crapo, J. D. (1982). "Biology of disease: free radicals and tissue injury." Lab Invest **47**(5): 412-26.
- Fujiwara, K., Okamura-Ikeda, K. et al. (1996). "Lipoylation of acyltransferase components of alpha-ketoacid dehydrogenase complexes." J Biol Chem **271**(22): 12932-6.
- Glantzounis, G. K., Yang, W. et al. (2006). "The role of thiols in liver ischemia-reperfusion injury." Curr Pharm Des **12**(23): 2891-901.
- Gonzalez, V. M., Fuertes, M. A. et al. (2001). "Is cisplatin-induced cell death always produced by apoptosis?" Mol Pharmacol **59**(4): 657-63.
- Goodlett, D. R., Camp, D. G. 2nd, et al. (1993). "Direct observation of a DNA quadruplex by electrospray ionization mass spectrometry." Biol Mass Spectrom **22**(3): 181-3.
- Green, D. R. and Kroemer, G. (2004). "The pathophysiology of mitochondrial cell death." Science **305**(5684): 626-9.

- Green, D. R. and Reed, J. C. (1998). "Mitochondria and apoptosis." Science **281**(5381): 1309-12.
- Gut, J., Christen, U. et al. (1995). "Molecular mimicry in halothane hepatitis: biochemical and structural characterization of lipoylated autoantigens." Toxicology **97**(1-3): 199-224.
- Hacker, G. and Weber, A. (2007). "BH3-only proteins trigger cytochrome c release, but how?" Arch Biochem Biophys.
- Hah, S. S., Stivers, K. M. et al. (2006). "Kinetics of carboplatin-DNA binding in genomic DNA and bladder cancer cells as determined by accelerator mass spectrometry." Chem Res Toxicol **19**(5): 622-6.
- Halliwell, B. and Gutteridge, J. M. (1990). "Role of free radicals and catalytic metal ions in human disease: an overview." Methods Enzymol **186**: 1-85.
- Handelman, G. J., Han, D. et al. (1994). "Alpha-lipoic acid reduction by mammalian cells to the dithiol form, and release into the culture medium." Biochem Pharmacol **47**(10): 1725-30.
- Hara, I., Miyake, H. et al. (2000). "Differential involvement of the Fas receptor/ligand system in p53-dependent apoptosis in human prostate cancer cells." Prostate **45**(4): 341-9.
- Herbert, A. A. and Guest, J. R. (1975). "Lipoic acid content of Escherichia coli and other microorganisms." Arch Microbiol **106**(3): 259-66.
- Hyppolito, M. A., de Oliveira, J. A. et al. (2006). "Cisplatin ototoxicity and otoprotection with sodium salicylate." Eur Arch Otorhinolaryngol **263**(9): 798-803.
- Irmeler, M., Thome, M. et al. (1997). "Inhibition of death receptor signals by cellular FLIP." Nature **388**(6638): 190-5.
- Jesudason, E. P., Masilamoni, J. G. et al. (2005). "The protective role of DL-alpha-lipoic acid in biogenic amines catabolism triggered by Abeta amyloid vaccination in mice." Brain Res Bull **65**(4): 361-7.
- Jones, M. M., Basinger, M. A. et al. (1992). "Control of the nephrotoxicity of cisplatin by clinically used sulfur-containing compounds." Fundam Appl Toxicol **18**(2): 181-8.

- Kam, P. C. and Ferch, N. I. (2000). "Apoptosis: mechanisms and clinical implications." Anaesthesia **55**(11): 1081-93.
- Kang, S. G., Jeong, H. K. et al. (2007). "Characterization of a lipoate-protein ligase A gene of rice (*Oryza sativa* L.)." Gene.
- Katta, V. and Chait, B. T. (1991). "Conformational changes in proteins probed by hydrogen-exchange electrospray-ionization mass spectrometry." Rapid Commun Mass Spectrom **5**(4): 214-7.
- Kaufmann, S. H. and Gores, G. J. (2000). "Apoptosis in cancer: cause and cure." Bioessays **22**(11): 1007-17.
- Koc, A., Duru, M. et al. (2005). "Protective agent, erdosteine, against cisplatin-induced hepatic oxidant injury in rats." Mol Cell Biochem **278**(1-2): 79-84.
- Kocak, G. and Karasu, C. (2002). "Elimination of \*O(2)(-)/H(2)O(2) by alpha-lipoic acid mediates the recovery of basal EDRF/NO availability and the reversal of superoxide dismutase-induced relaxation in diabetic rat aorta." Diabetes Obes Metab **4**(1): 69-74.
- Konrad, D. (2005). "Utilization of the insulin-signaling network in the metabolic actions of alpha-lipoic acid-reduction or oxidation?" Antioxid Redox Signal **7**(7-8): 1032-9.
- Korsmeyer, S. J., Wei, M. C. et al. (2000). "Pro-apoptotic cascade activates BID, which oligomerizes BAK or BAX into pores that result in the release of cytochrome c." Cell Death Differ **7**(12): 1166-73.
- Korst, A. E., Boven, E. et al. (1998). "Pharmacokinetics of cisplatin with and without amifostine in tumour-bearing nude mice." Eur J Cancer **34**(3): 412-6.
- Kuwana, T., Mackey, M. R. et al. (2002). "Bid, Bax, and lipids cooperate to form supramolecular openings in the outer mitochondrial membrane." Cell **111**(3): 331-42.
- Lapenna, D., Ciofani, G. et al. (2003). "Dihydrolipoic acid inhibits 15-lipoxygenase-dependent lipid peroxidation." Free Radic Biol Med **35**(10): 1203-9.
- Lenardo, M., Chan, K. M. et al. (1999). "Mature T lymphocyte apoptosis--immune regulation in a dynamic and unpredictable antigenic environment." Annu Rev Immunol **17**: 221-53.

- Lester, G. E., Hodges, D. M. et al. (2004). "Pre-extraction preparation (fresh, frozen, freeze-dried, or acetone powdered) and long-term storage of fruit and vegetable tissues: effects on antioxidant enzyme activity." J Agric Food Chem **52**(8): 2167-73.
- Letai, A., Bassik, M. C. et al. (2002). "Distinct BH3 domains either sensitize or activate mitochondrial apoptosis, serving as prototype cancer therapeutics." Cancer Cell **2**(3): 183-92.
- Loginov, A. S., Nilova, T. V. et al. (1989). "[Pharmacokinetics of preparations of lipoic acid and their effect on ATP synthesis, processes of microsomal and cytosol oxidation in hepatocytes in liver damage in man]." Farmakol Toksikol **52**(4): 78-82.
- Lorenzo, H. K., Susin, S. A. et al. (1999). "Apoptosis inducing factor (AIF): a phylogenetically old, caspase-independent effector of cell death." Cell Death Differ **6**(6): 516-24.
- Luo, X., Budihardjo, I. et al. (1998). "Bid, a Bcl2 interacting protein, mediates cytochrome c release from mitochondria in response to activation of cell surface death receptors." Cell **94**(4): 481-90.
- MacFarlane, M., Ahmad, M. et al. (1997). "Identification and molecular cloning of two novel receptors for the cytotoxic ligand TRAIL." J Biol Chem **272**(41): 25417-20.
- Malet, G., Martin A. G., et al. (2006). "Small molecule inhibitors of Apaf-1-related caspase- 3/-9 activation that control mitochondrial-dependent apoptosis." Cell Death Differ **13**(9): 1523-32.
- Mattulat, A. and Baltes, W. (1992). "Determination of lipoic acid in meat of commercial quality." Z Lebensm Unters Forsch **194**(4): 326-9.
- McDonald, E. S., Randon, K. R. et al. (2005). "Cisplatin preferentially binds to DNA in dorsal root ganglion neurons in vitro and in vivo: a potential mechanism for neurotoxicity." Neurobiol Dis **18**(2): 305-13.
- Midaoui, A. E., Elimadi, A. et al. (2003). "Lipoic acid prevents hypertension, hyperglycemia, and the increase in heart mitochondrial superoxide production." Am J Hypertens **16**(3): 173-9.



- Mikadze, E. and Mamatsashvili, T. (2006). "Early contact stage of apoptosis: its morphological features and function." ScientificWorldJournal **6**: 1783-804.
- Moini, H., Packer, L. et al. (2002). "Antioxidant and prooxidant activities of alpha-lipoic acid and dihydrolipoic acid." Toxicol Appl Pharmacol **182**(1): 84-90.
- Morris, T. W., Reed, K. E. et al. (1994). "Identification of the gene encoding lipoate-protein ligase A of Escherichia coli. Molecular cloning and characterization of the lplA gene and gene product." J Biol Chem **269**(23): 16091-100.
- Morris, T. W., Reed, K. E. et al. (1995). "Lipoic acid metabolism in Escherichia coli: the lplA and lipB genes define redundant pathways for ligation of lipoyl groups to apoprotein." J Bacteriol **177**(1): 1-10.
- Muldoon, L. L., Walker-Rosenfeld, S. L. et al. (2001). "Rescue from enhanced alkylator-induced cell death with low molecular weight sulfur-containing chemoprotectants." J Pharmacol Exp Ther **296**(3): 797-805.
- Muller, L. and Menzel, H. (1990). "Studies on the efficacy of lipoate and dihydrolipoate in the alteration of cadmium<sup>2+</sup> toxicity in isolated hepatocytes." Biochim Biophys Acta **1052**(3): 386-91.
- Nagata, S. (1999). "Fas ligand-induced apoptosis." Annu Rev Genet **33**: 29-55.
- Nechushtan, A., Smith, C. L. et al. (2001). "Bax and Bak coalesce into novel mitochondria-associated clusters during apoptosis." J Cell Biol **153**(6): 1265-76.
- Oancea, M., S. Mazumder, et al. (2006). "Apoptosis assays." Methods Mol Med **129**: 279-90.
- Ooya, T., Eguchi, M. et al. (2001). "Enhanced accessibility of peptide substrate toward membrane-bound metalloexopeptidase by supramolecular structure of polyrotaxane." Biomacromolecules **2**(1): 200-3.
- Ooya, T., Kumeno, T. et al. (1998). "Regulation of intracellular metabolism by biodegradable polyrotaxanes." J Biomater Sci Polym Ed **9**(4): 313-26.
- Ooya, T. and Yui, N. (1999). "Polyrotaxanes: synthesis, structure, and potential in drug delivery." Crit Rev Ther Drug Carrier Syst **16**(3): 289-330.
- Osman, A. M., El-Sayed, E. M. et al. (2000). "Prevention of cisplatin-induced nephrotoxicity by methimazole." Pharmacol Res **41**(1): 115-21.



- Ou, P., Tritschler, H. J. et al. (1995). "Thioctic (lipoic) acid: a therapeutic metal-chelating antioxidant?" Biochem Pharmacol **50**(1): 123-6.
- Packer, L., Roy, S. et al. (1997). "Alpha-lipoic acid: a metabolic antioxidant and potential redox modulator of transcription." Adv Pharmacol **38**: 79-101.
- Packer, L., Witt, E. H. et al. (1995). "alpha-Lipoic acid as a biological antioxidant." Free Radic Biol Med **19**(2): 227-50.
- Pan, G., Ni, J. et al. (1997). "An antagonist decoy receptor and a death domain-containing receptor for TRAIL." Science **277**(5327): 815-8.
- Pan, G., O'Rourke, K. et al. (1997). "The receptor for the cytotoxic ligand TRAIL." Science **276**(5309): 111-3.
- Patrick, L. (2000). "Nutrients and HIV: part three - N-acetylcysteine, alpha-lipoic acid, L-glutamine, and L-carnitine." Altern Med Rev **5**(4): 290-305.
- Petros, A. M., Olejniczak, E. T. et al. (2004). "Structural biology of the Bcl-2 family of proteins." Biochim Biophys Acta **1644**(2-3): 83-94.
- Pirlich, M., Kiok, K. et al. (2002). "Alpha-lipoic acid prevents ethanol-induced protein oxidation in mouse hippocampal HT22 cells." Neurosci Lett **328**(2): 93-6.
- Prausnitz, M. R. (1997). "Reversible skin permeabilization for transdermal delivery of macromolecules." Crit Rev Ther Drug Carrier Syst **14**(4): 455-83.
- Previati, M., Lanzoni, I. et al. (2006). "Cisplatin-induced apoptosis in human promyelocytic leukemia cells." Int J Mol Med **18**(3): 511-6.
- Reedijk, J. (1987). "Bioinorganic chemistry. Inorganic chemistry in a perspective of biology, medicine and the environment." Naturwissenschaften **74**(2): 71-7.
- Reedijk, J. and Lohman, P. H. (1985). "Cisplatin: synthesis, antitumour activity and mechanism of action." Pharm Weekbl Sci **7**(5): 173-80.
- Rose, R. C. and Bode, A. M. (1995). "Comments on the glutathione-ascorbic acid redox couple." Free Radic Biol Med **18**(5): 955-6.
- Salvesen, G. S. and Dixit, V. M. (1997). "Caspases: intracellular signaling by proteolysis." Cell **91**(4): 443-6.
- Sastry, J. and Kellie, S. J. (2005). "Severe neurotoxicity, ototoxicity and nephrotoxicity following high-dose cisplatin and amifostine." Pediatr Hematol Oncol **22**(5): 441-5.

- Schreibelt, G., Musters, R. J. et al. (2006). "Lipoic acid affects cellular migration into the central nervous system and stabilizes blood-brain barrier integrity." J Immunol **177**(4): 2630-7.
- Sen, C. K., Roy, S. et al. (1997). "Regulation of cellular thiols in human lymphocytes by alpha-lipoic acid: a flow cytometric analysis." Free Radic Biol Med **22**(7): 1241-57.
- Sen, C. K., Sashwati, R. et al. (1999). "Fas mediated apoptosis of human Jurkat T-cells: intracellular events and potentiation by redox-active alpha-lipoic acid." Cell Death Differ **6**(5): 481-91.
- Sharpe, J. C., Arnoult, D. et al. (2004). "Control of mitochondrial permeability by Bcl-2 family members." Biochim Biophys Acta **1644**(2-3): 107-13.
- Shigenaga, M. K., Gimeno, C. J. et al. (1989). "Urinary 8-hydroxy-2'-deoxyguanosine as a biological marker of in vivo oxidative DNA damage." Proc Natl Acad Sci U S A **86**(24): 9697-701.
- Sigalov, A. B. and Stern, L. J. (1998). "Enzymatic repair of oxidative damage to human apolipoprotein A-I." FEBS Lett **433**(3): 196-200.
- Sigalov, A. B. and Stern, L. J. (2002). "Dihydrolipoic acid as an effective cofactor for peptide methionine sulfoxide reductase in enzymatic repair of oxidative damage to both lipid-free and lipid-bound apolipoprotein a-I." Antioxid Redox Signal **4**(3): 553-7.
- Sigel, H., Prijs, B. et al. (1978). "Stability and structure of binary and ternary complexes of alpha-lipoate and lipoate derivatives with Mn<sup>2+</sup>, Cu<sup>2+</sup>, and Zn<sup>2+</sup> in solution." Arch Biochem Biophys **187**(1): 208-14.
- Smith, P. B., Snyder, A. P. et al. (1995). "Characterization of bacterial phospholipids by electrospray ionization tandem mass spectrometry." Anal Chem **67**(11): 1824-30.
- Souto, E. B., Muller, R. H. et al. (2005). "A novel approach based on lipid nanoparticles (SLN) for topical delivery of alpha-lipoic acid." J Microencapsul **22**(6): 581-92.
- Storz, P. (2005). "Reactive oxygen species in tumor progression." Front Biosci **10**: 1881-96.

- Susin, S. A., Lorenzo, H. K. et al. (1999). "Mitochondrial release of caspase-2 and -9 during the apoptotic process." J Exp Med **189**(2): 381-94.
- Susin, S. A., Lorenzo, H. K. et al. (1999). "Molecular characterization of mitochondrial apoptosis-inducing factor." Nature **397**(6718): 441-6.
- Suzuki, Y. J., Tsuchiya, M. et al. (1991). "Thioctic acid and dihydrolipoic acid are novel antioxidants which interact with reactive oxygen species." Free Radic Res Commun **15**(5): 255-63.
- Tachaboonyakiat, W., Furubayashi, T. et al. (2004). "Novel biodegradable cholesterol-modified polyrotaxane hydrogels for cartilage regeneration." J Biomater Sci Polym Ed **15**(11): 1389-404.
- Takahashi, A., Masuda, A. et al. (2004). "Oxidative stress-induced apoptosis is associated with alterations in mitochondrial caspase activity and Bcl-2-dependent alterations in mitochondrial pH (pH<sub>m</sub>)." Brain Res Bull **62**(6): 497-504.
- Tartaglia, L. A., Ayres, T. M. et al. (1993). "A novel domain within the 55 kd TNF receptor signals cell death." Cell **74**(5): 845-53.
- Tartaglia, L. A., Goeddel, D. V. et al. (1993). "Stimulation of human T-cell proliferation by specific activation of the 75-kDa tumor necrosis factor receptor." J Immunol **151**(9): 4637-41.
- Tartaglia, L. A., Pennica, D. et al. (1993). "Ligand passing: the 75-kDa tumor necrosis factor (TNF) receptor recruits TNF for signaling by the 55-kDa TNF receptor." J Biol Chem **268**(25): 18542-8.
- Tartaglia, L. A., Rothe, M. et al. (1993). "Tumor necrosis factor's cytotoxic activity is signaled by the p55 TNF receptor." Cell **73**(2): 213-6.
- Taylor, N. L., Heazlewood J. L., et al. (2004). "Lipoic acid-dependent oxidative catabolism of alpha-keto acids in mitochondria provides evidence for branched-chain amino acid catabolism in Arabidopsis." Plant Physiol **134**(2): 838-48.
- Teichert, J. and Preiss, R. (1995). "Determination of lipoic acid in human plasma by high-performance liquid chromatography with electrochemical detection." J Chromatogr B Biomed Appl **672**(2): 277-81.

- Teuben, J. M., Bauer, C. et al. (1999). "Solution structure of a DNA duplex containing a cis-diammineplatinum(II) 1,3-d(GTG) intrastrand cross-link, a major adduct in cells treated with the anticancer drug carboplatin." Biochemistry **38**(38): 12305-12.
- Toutou, E., Junginger, H. E. et al. (1994). "Liposomes as carriers for topical and transdermal delivery." J Pharm Sci **83**(9): 1189-203.
- Touyz, R. M. and Schiffrin, E. L. (2004). "Reactive oxygen species in vascular biology: implications in hypertension." Histochem Cell Biol **122**(4): 339-52.
- Tuaille, N., Andre, C. et al. (1992). "A lipoyl synthetic octadecapeptide of dihydrolipoamide acetyltransferase specifically recognized by anti-M2 autoantibodies in primary biliary cirrhosis." J Immunol **148**(2): 445-50.
- Valerie, K. and Povirk, L. F. (2003). "Regulation and mechanisms of mammalian double-strand break repair." Oncogene **22**(37): 5792-812.
- Valko, M., Leibfritz, D. et al. (2007). "Free radicals and antioxidants in normal physiological functions and human disease." Int J Biochem Cell Biol **39**(1): 44-84.
- Valko, M., Rhodes, C. J. et al. (2006). "Free radicals, metals and antioxidants in oxidative stress-induced cancer." Chem Biol Interact **160**(1): 1-40.
- van de Mark, K., Chen, J. S. et al. (2003). "Alpha-lipoic acid induces p27Kip-dependent cell cycle arrest in non-transformed cell lines and apoptosis in tumor cell lines." J Cell Physiol **194**(3): 325-40.
- van Schooten, F. J., Knaapen, A. M. et al. (2007). "DNA damage, mutagenesis and cardiovascular disease." Mutat Res.
- Veenstra, T. D. (1999). "Electrospray ionization mass spectrometry in the study of biomolecular non-covalent interactions." Biophys Chem **79**(2): 63-79.
- Vickers, A. E., Rose, K. et al. (2004). "Kidney slices of human and rat to characterize cisplatin-induced injury on cellular pathways and morphology." Toxicol Pathol **32**(5): 577-90.
- Vincent, A. M., McLean, L. L. et al. (2005). "Short-term hyperglycemia produces oxidative damage and apoptosis in neurons." Faseb J **19**(6): 638-40.

- Vincent, A. M., Stevens, M. J. et al. (2005). "Cell culture modeling to test therapies against hyperglycemia-mediated oxidative stress and injury." Antioxid Redox Signal **7**(11-12): 1494-506.
- Wallach, D., Varfolomeev, E. E. et al. (1999). "Tumor necrosis factor receptor and Fas signaling mechanisms." Annu Rev Immunol **17**: 331-67.
- Watanabe, J., Ooya, T. et al. (2002). "Fibroblast adhesion and proliferation on poly(ethylene glycol) hydrogels crosslinked by hydrolyzable polyrotaxane." Biomaterials **23**(20): 4041-8.
- Wei, M. C., Lindsten, T. et al. (2000). "tBID, a membrane-targeted death ligand, oligomerizes BAK to release cytochrome c." Genes Dev **14**(16): 2060-71.
- Wenzel, U., Nickel, A. et al. (2005). "alpha-Lipoic acid induces apoptosis in human colon cancer cells by increasing mitochondrial respiration with a concomitant O<sub>2</sub>-\*-generation." Apoptosis **10**(2): 359-68.
- Wu, X., F. Kassie, et al. (2005). "Induction of apoptosis in tumor cells by naturally occurring sulfur-containing compounds." Mutat Res **589**(2): 81-102.
- Yang, J. C. and Cortopassi, G. A. (1998). "Induction of the mitochondrial permeability transition causes release of the apoptogenic factor cytochrome c." Free Radic Biol Med **24**(4): 624-31.
- Yee, S., Fazekas-May, M. et al. (1994). "Inhibition of cisplatin toxicity without decreasing antitumor efficacy. Use of a dithiocarbamate." Arch Otolaryngol Head Neck Surg **120**(11): 1248-52.
- Yui, N. and Ooya, T. (2004). "Design of polyrotaxanes as supramolecular conjugates for cells and tissues." J Artif Organs **7**(2): 62-8.
- Zeiss, C. J. (2003). "The apoptosis-necrosis continuum: insights from genetically altered mice." Vet Pathol **40**(5): 481-95.
- Zhang, L., Cooper, A. J. et al. (2006). "Cisplatin-induced toxicity is associated with platinum deposition in mouse kidney mitochondria in vivo and with selective inactivation of the alpha-ketoglutarate dehydrogenase complex in LLC-PK1 cells." Biochemistry **45**(29): 8959-71.
- Zimmermann, K. C. and Green, D. R. (2001). "How cells die: apoptosis pathways." J Allergy Clin Immunol **108**(4 Suppl): S99-103.



Zou, H., Li, Y. et al. (1999). "An APAF-1.cytochrome c multimeric complex is a functional apoptosome that activates procaspase-9." J Biol Chem **274**(17): 11549-56.



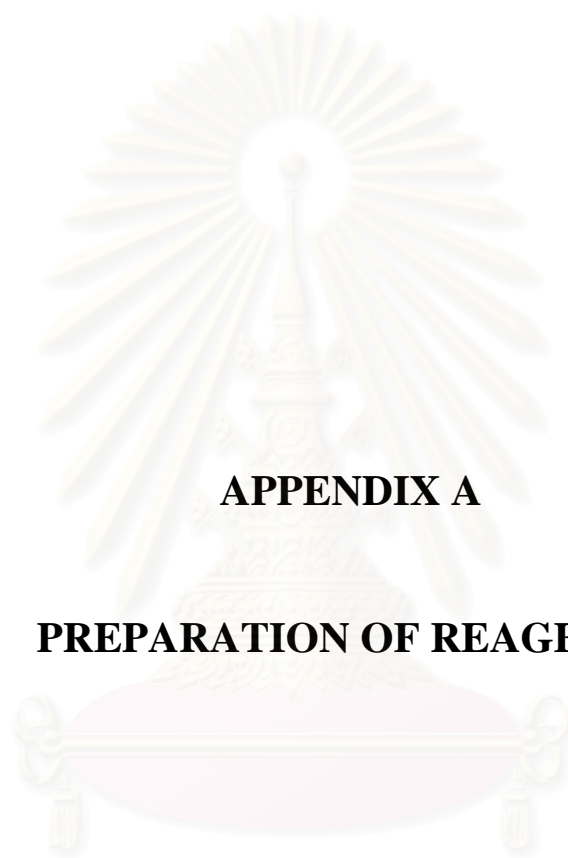
สถาบันวิทยบริการ  
จุฬาลงกรณ์มหาวิทยาลัย





## APPENDICES

สถาบันวิทยบริการ  
จุฬาลงกรณ์มหาวิทยาลัย



## **APPENDIX A**

### **PREPARATION OF REAGENTS**

สถาบันวิทยบริการ  
จุฬาลงกรณ์มหาวิทยาลัย

## Acrylamide gel

Solution A	0.8% methylene bis acrylamide, 30% acrylamide
Solution B	1.5 M Tris HCl (pH 8.8)
Solution C	10% SDS
Solution D	0.5 M Tris HCl (pH 6.8)
APS (ammonium persulfate)	10% APS in DDW
TEMED (N, N, N', N'- tetramethylenediamine)	
Solution A, B, APS, and TEMED	stored at 4 °C
Solution C	stored at room temperature
APS	freshly prepared

The gel apparatus and spacers (1.5 mm thick) were assembly.

### 1. Preparation of separating gel

To make two plates of 10% acrylamide gel, the ingredients of separating gel are

solution A	6.7 mL
solution B	5.0 mL
solution C	0.2 mL
DDW	7.9 mL

All of the ingredients were thoroughly mixed. The mixture was supplemented with 200  $\mu$ L APS and 8  $\mu$ L TEMED, then gentle mixed, and immediately pour the gel between the glass plates. Before gel polymerization was complete, 0.1% SDS in DDW was layered on the top of the separating gel (5 mm thick). Wait until the gel completely polymerized (approximately 20-30 min).

### 2. Preparation of stacking gel

Once the separating gel has completely polymerized, 0.1% SDS was removed from the top of the gel. To make stacking gel, the ingredients are

solution A	1.3 mL
------------	--------

solution C	34 $\mu$ L
solution D	2.5 mL
DDW	6.1 mL

All of the ingredients were thoroughly mixed. The mixture was supplemented with 50  $\mu$ L APS and 10  $\mu$ L TEMED, then thoroughly mixed, and immediately pour the gel between the glass plates. The combs were inserted between the two glass plates of two sets of gel apparatus. The gels were leaved for approximately 30-40 min to polymerize.

### 3. Application of samples

Once the stacking gel has completely solidated, the combs were gently removed. The wells were flushed out thoroughly with running buffer. The clips and sealing tapes were removed and set up the gel chamber. The air bubbles between layers were removed by gently rolling the chamber.

### Running buffer

To make 1 liter of 5X running buffer (250 mM Tris, 1.92 M glycine, and 0.5 % SDS) for stock solution, the ingredients are

Tris	30.2 g
Glycine	144.13 g
SDS	5 g

All ingredients were dissolved in DDW with continuously stirring. The solution was adjusted volume to 1000 mL. Before use, the solution was diluted to 1X running buffer (50 mM Tris, 0.384 M glycine, and 0.1 % SDS) with DDW, 5X running buffer: DDW = 4: 1.

## Transfer buffer

To make 1 liter of 10 X transfer buffer (1 M Tris, and 1.92 M glycine) for stock solution, the ingredients are

Tris	121.14 g
Glycine	144.13 g

All ingredients were dissolved in DDW with continuously stirring. The solution was adjusted volume to 1000 mL. Before use, the solution was diluted to 1000 mL of 1X running buffer ( 0.1 M Tris, 0.192 M glycine) supplemented with 5% methanol, 10X transfer buffer : methanol : DDW = 100 mL : 50 mL : 850 mL.

## Tris-buffered saline, 0.1 % Tween 20 (TBST)

To make 1 liter of 10 X TBST (100 mM Tris, 1 M NaCl, and 0.1 % Tween 20) for stock solution, the ingredients are

Tris	12.114 g
NaCl	58.44 g
Tween 20	10 mL

All ingredients were dissolved in DDW with continuously stirring. The solution was adjusted volume to 1000 ml. Before use, the solution was diluted to 1 X TBST (10 mM Tris, 100 mM NaCl, and 0.01 % Tween 20) with DDW, 10X TBST : DDW = 9 : 1.

## Sample buffer

To make 50 ml of 3X sample buffer (225 mM Tris HCl (pH 6.8), 6 % SDS, 30% glycerol, 9 % 2-mercaptoethanol, and 0.009 % bromphenol blue) for stock solution, the ingredients are

Tris HCl	22.5 of 0.5 M
SDS	3 g
Glycerol	10 mL
2-mercaptoethanol	4.5 mL
bromphenol blue	225 $\mu$ L of 2 %

All ingredients were dissolved in DDW with continuously stirring. The solution was adjusted volume to 50 mL. 3X sample buffer was aliquot into 1 mL/tube and stored at  $-20^{\circ}\text{C}$ . Before use, the solution was diluted to 1 X sample buffer (75 mM Tris HCl, 2% SDS, 10 % glycerol, 3 % 2-mercaptoethanol, and 0.003 % bromphenol blue) with DDW, 3X sample buffer : DDW = 2 : 1.

### **Lysis buffer**

To make 50 ml of lysis buffer (50 mM Tris HCl (pH 7.5), 150 mM NaCl, 20 mM EDTA, 50 mM NaF, 1 % Triton X-100, 1 mM phenylmethanesulfonyl fluoride (PMSF) and a commercial protease inhibitor mixture (Roche)) the ingredients are

Tris HCl	2.5 ml of 1M (pH 7.5)
NaCl	0.4383 g
EDTA	0.3722 g
NaF	2.5 ml of 1 M
Triton X-100	0.51 mL

All ingredients were dissolved in DDW 40 mL. The lysis buffer was aliquot into 1 mL/tube and stored at  $4^{\circ}\text{C}$ . Before use, the solution was supplemented with 200  $\mu$ L of 50 mM PMSF and a commercial protease inhibitor mixture (1 tablet/50mL) and the volume was adjusted to 10 mL.





**APPENDIX B**

**THE CHROMATROGRAMS AND STATISTIC DATA**

สถาบันวิทยบริการ  
จุฬาลงกรณ์มหาวิทยาลัย

**Table 9** Accuracy data of LA assayed by HPLC method

<b>Samples</b>	<b>Theoretical Conc. (µg/mL)</b>	<b>Measured Conc. (µg/mL)</b>	<b>Average Measure Conc. (µg/mL)</b>	<b>Recovery (%)</b>	<b>Average (Range)</b>	<b>CV (%)</b>	<b>SD</b>
1A	0.5300	0.5227	0.5272	98.62	99.47	0.7465	0.0039
1B	0.5300	0.5289		99.79	(94.36-100.00)		
1C	0.5300	0.5300		100.00			
2A	1.0032	0.9806	0.9817	97.75	97.85	0.8102	0.0080
2B	1.0032	0.9743		97.12	(94.98-97.75)		
2C	1.0032	0.9901		98.69			
3A	1.5206	1.5150	1.5089	99.63	99.23	0.4843	0.0073
3B	1.5206	1.5109		99.36	(97.34-99.36)		
3C	1.5206	1.5008		98.70			
4A	2.0104	2.0004	1.9922	99.50	99.10	0.4672	0.0093
4B	2.0104	1.9821		98.59	(97.16-99.50)		
4C	2.0104	1.9942		99.19			
5A	2.5507	2.5010	2.5059	98.05	98.24	0.9685	0.0243
5B	2.5507	2.5322		99.27	(97.40-99.27)		
5C	2.5507	2.4844		97.40			
6A	3.0103	2.9614	2.9682	98.38	98.60	0.6522	0.0194
6B	3.0103	2.9900		99.33	(98.10-99.33)		
6C	3.0103	2.9531		98.10			

**Table 10** Precision data of LA by HPLC method

Samples	Theoretical Conc. (µg/mL)	Measured Conc. (µg/mL)	Average Measure Conc. (µg/mL)	Recovery (%)	Average (Range)	CV (%)	SD
A	2.0104	2.0004	1.9975	99.5026	99.36	0.4289	0.0086
B	2.0104	1.9821		98.5923	(98.97-99.77)		
C	2.0104	1.9942		99.1942			
D	2.0104	2.0058		99.7712			
E	2.0104	1.9983		99.3981			
F	2.0104	2.0039		99.6767			

สถาบันวิทยบริการ  
จุฬาลงกรณ์มหาวิทยาลัย

**Table 11** Linearity data of LA assayed by HPLC method

<b>Samples</b>	<b>Theoretical Conc. (<math>\mu\text{g/mL}</math>)</b>	<b>Average Theoretical Conc. (<math>\mu\text{g/mL}</math>)</b>	<b>Measured Conc. (<math>\mu\text{g/mL}</math>)</b>	<b>Average Measured Conc. (<math>\mu\text{g/mL}</math>)</b>
1A	0.5300	0.5300	0.5227	0.5272
1B	0.5300		0.5289	
1C	0.5300		0.5300	
2A	1.0032	1.0032	0.9806	0.9817
2B	1.0032		0.9743	
2C	1.0032		0.9901	
3A	1.5206	1.5206	1.5150	1.5089
3B	1.5206		1.5109	
3C	1.5206		1.5008	
4A	2.0104	2.0104	2.0004	1.9922
4B	2.0104		1.9821	
4C	2.0104		1.9942	
5A	2.5507	2.5507	2.5010	2.5059
5B	2.5507		2.5322	
5C	2.5507		2.4844	
6A	3.0103	3.0103	2.9614	2.9682
6B	3.0103		2.9900	
6C	3.0103		2.9531	

**Table 12** LOD and LOQ data of LA assayed by the HPLC method

<b>Theoretical Conc. (µg/mL)</b>	<b>Peak Area</b>	<b>Regression</b>	<b>Parameters</b>	<b>LOD (µg/mL)</b>	<b>LOQ ((µg/mL)</b>
0.5300	16597	Slope	35218.71354	0.28	0.87
1.0032	28114	Intercept	-3661.979186		
1.5206	51423	r <sup>2</sup>	0.99660803		
2.0104	68000				
2.5507	86269				
3.0103	101831				

**Table 13** Linearity data of LA assayed by UV/VIS spectrometer at 208 nm

<b>Weight (mg)</b>	<b>Absorbance</b>				<b>SD</b>	<b>r2</b>	<b>SLOP</b>	<b>Y-Intercept</b>
	<b>A1</b>	<b>A2</b>	<b>A3</b>	<b>Average</b>				
0.0000	0.00000	0.00000	0.00000	0.00000	0	0.9994	7.3015	-0.00077
0.0072	0.04740	0.04740	0.04740	0.04740	0			
0.0196	0.13109	0.13701	0.13690	0.13500	0.003387			
0.0433	0.32563	0.32476	0.32491	0.32510	0.000465			
0.0520	0.36772	0.37835	0.37893	0.37500	0.006311			
0.0577	0.43188	0.42212	0.40540	0.41980	0.013392			
0.0862	0.59770	0.69267	0.64115	0.64384	0.047542			
0.1404	0.89439	0.14766	1.00295	1.01500	0.465638			

**Table 14** The amount of LA in PRx or cholesterol modified PRx analyzed by UV/VIS spectrometer at 208 nm

Delivery form	Absorbance				SD
	A1	A2	A3	Average	
LA-PRx	0.29307	0.27679	0.29535	0.28840	0.010122
Cho-LA-PRx	0.29335	0.27713	0.30102	0.29050	0.012197

**Table 15** The cumulative amount of LA from LA solution ( $n = 4$ )

Sample	Peak area	Conc ( $\mu\text{g}/\text{mL}$ )	Cumulative amount ( $\mu\text{g}$ )	Average amount ( $\mu\text{g}$ )
0.5 h				
1	0	0.00	0.00	0.00
2	0	0.00	0.00	
3	0	0.00	0.00	
4	0	0.00	0.00	
1 h				
1	16597	0.53	5.25	5.26
2	16284	0.52	5.22	
3	16600	0.53	5.30	
4	16590	0.53	5.28	
2 h				
1	27833	0.99	9.91	9.92
2	28114	1.00	9.97	
3	27800	0.99	9.90	
4	27824	0.99	9.90	
3 h				
1	39922	1.42	14.21	14.24
2	40203	1.43	14.30	
3	39930	1.42	14.24	
4	39915	1.42	14.20	
4 h				
1	53791	1.59	15.85	15.84
2	53453	1.58	15.83	
3	53460	1.58	15.81	
4	53800	1.59	15.88	



**Table 15** The cumulative amount of LA from LA solution ( $n = 4$ )(Continued)

Sample	Peak area	Conc ( $\mu\text{g}/\text{mL}$ )	Cumulative amount ( $\mu\text{g}$ )	Average amount ( $\mu\text{g}$ )
5 h				
1	60219	1.78	17.75	17.75
2	60225	1.78	17.80	
3	59881	1.77	17.73	
4	59870	1.77	17.71	
6 h				
1	64955	1.92	19.21	19.21
2	64888	1.92	19.18	
3	65091	1.92	19.24	
4	64955	1.92	19.20	
12 h				
1	86641	2.56	25.62	25.61
2	86573	2.56	25.60	
3	86472	2.56	25.57	
4	86776	2.57	25.66	
24 h				
1	87926	2.60	26.00	26.06
2	88332	2.61	26.12	
3	88095	2.61	26.05	
4	88163	2.61	26.07	

**Table 16** The cumulative amount, flux and rate constant ( $k$ ) of LA from LA solution

Time (h)	Cumulative amount ( $\mu\text{g}$ )	Flux ( $\mu\text{g}/\text{h}/\text{cm}^2$ )	$k$ ( $\mu\text{g}/\text{h}$ )
0.5	$0 \pm 0.00$	0	0.9283
1.0	$5.26 \pm 0.035$	0.13	
2.0	$9.92 \pm 0.034$	0.12	
3.0	$14.24 \pm 0.045$	0.11	
4.0	$15.84 \pm 0.030$	0.09	
5.0	$17.75 \pm 0.039$	0.08	
6.0	$19.21 \pm 0.025$	0.08	
12.0	$25.61 \pm 0.038$	0.05	
24.0	$26.06 \pm 0.050$	0.02	

**Table 17** The cumulative amount of LA from LA-PRx complex ( $n = 4$ )

Sample	Peak area	Conc ( $\mu\text{g}/\text{mL}$ )	Cumulative amount ( $\mu\text{g}$ )	Average amount ( $\mu\text{g}$ )
0.5 h				
1	0	0.00	0.00	0.00
2	0	0.00	0.00	
3	0	0.00	0.00	
4	0	0.00	0.00	
1 h				
1	0	0.00	0.00	0.00
2	0	0.00	0.00	
3	0	0.00	0.00	
4	0	0.00	0.00	
2 h				
1	51423	0.15	1.52	1.51
2	50070	0.15	1.48	
3	50746	0.15	1.50	
4	52099	0.15	1.54	
3 h				
1	100139	2.96	29.62	29.67
2	100478	2.97	29.70	
3	125174	3.70	29.65	
4	100478	2.97	29.71	
4 h				
1	121792	3.60	36.02	36.03
2	122129	3.61	36.07	
3	121790	3.60	36.00	
4	122197	3.60	36.04	
5 h				
1	126865	3.75	37.49	37.52
2	127204	3.76	37.63	
3	126528	3.74	37.44	
4	126900	3.75	37.52	
6 h				
1	140398	4.15	41.52	41.52
2	140737	4.16	41.55	
3	140364	4.15	41.49	
4	140499	4.15	41.53	
12 h				
1	149533	4.42	44.20	44.20
2	149634	4.42	44.23	
3	149465	4.42	44.18	
4	149534	4.42	44.20	

**Table 17** The cumulative amount of LA from LA-PRx complex ( $n = 4$ )(Continued)

Sample	Peak area	Conc ( $\mu\text{g}/\text{mL}$ )	Cumulative amount ( $\mu\text{g}$ )	Average amount ( $\mu\text{g}$ )
24 h				
1	149702	4.43	44.25	44.22
2	149499	4.42	44.19	
3	149634	4.42	44.23	
4	148425	4.42	44.22	

**Table 18** The cumulative amount, flux and rate constant (k) of LA from LA-PRx complex

Time (h)	Cumulative amount ( $\mu\text{g}$ )	Flux ( $\mu\text{g}/\text{h}/\text{cm}^2$ )	k ( $\mu\text{g}/\text{h}$ )
0.5	$0 \pm 0.00$	0	k1 = 1.0789
1.0	$0 \pm 0.00$	0	
2.0	$1.51 \pm 0.026$	0.01	k2 = 28.16
3.0	$29.67 \pm 0.042$	0.24	
4.0	$36.03 \pm 0.030$	0.22	
5.0	$37.52 \pm 0.080$	0.18	k3 = 0.5003
6.0	$41.52 \pm 0.025$	0.17	
12.0	$44.20 \pm 0.021$	0.09	
24.0	$44.22 \pm 0.025$	0.04	

**Table 19** The cumulative amount of LA from cholesterol modified LA-PRx complex ( $n = 4$ )

Sample	Peak area	Conc ( $\mu\text{g}/\text{mL}$ )	Cumulative amount ( $\mu\text{g}$ )	Average amount ( $\mu\text{g}$ )
0.5 h				
1	14562	0.47	4.65	4.65
2	14499	0.46	4.63	
3	14530	0.46	4.64	
4	14624	0.47	4.67	
1 h				
1	31713	1.13	11.28	11.30
2	31769	1.13	11.30	
3	31909	1.14	11.35	
4	31656	1.13	11.26	
2 h				
1	84679	2.50	25.04	25.05
2	84612	2.50	25.02	
3	84781	2.51	25.07	
4	84713	2.51	25.05	
3 h				
1	90681	2.72	27.15	27.18
2	91984	2.72	27.20	
3	91849	2.72	27.16	
4	91950	2.72	27.19	
4 h				
1	96824	2.86	28.62	28.63
2	96959	2.87	28.66	
3	96723	2.86	28.59	
4	96926	2.87	28.65	
5 h				
1	105958	3.13	31.32	31.36
2	106128	3.14	31.37	
3	106229	3.14	31.40	
4	105992	3.13	31.33	
6 h				
1	119491	3.53	35.32	35.34
2	119423	3.53	35.30	
3	119694	3.54	35.38	
4	119592	3.54	35.35	
12 h				
1	129741	3.84	38.35	38.40
2	129944	3.84	38.41	
3	130012	3.84	38.43	
4	129877	3.84	38.39	

**Table 19** The cumulative amount of LA from cholesterol modified LA-PRx complex ( $n = 4$ )(Continue)

Sample	Peak area	Conc ( $\mu\text{g}/\text{mL}$ )	Cumulative amount ( $\mu\text{g}$ )	Average amount ( $\mu\text{g}$ )
24 h				
1	148856	4.40	44.00	44.09
2	149262	4.41	44.12	
3	149363	4.42	44.15	
4	149093	4.41	44.07	

**Table 20** The cumulative amount, flux and rate constant (k) of LA from cholesterol modified LA-PRx complex

Time (h)	Cumulative amount	Flux	k
	( $\mu\text{g}$ )	( $\mu\text{g}/\text{h}/\text{cm}^2$ )	( $\mu\text{g}/\text{h}$ )
0.5	$4.65 \pm 0.017$	0.22	k1 = 13.30
1.0	$11.30 \pm 0.039$	0.28	
2.0	$25.05 \pm 0.021$	0.31	k2 = 13.75
3.0	$27.18 \pm 0.024$	0.22	
4.0	$28.63 \pm 0.032$	0.17	k3 = 0.8109
5.0	$31.36 \pm 0.037$	0.15	
6.0	$35.34 \pm 0.035$	0.14	
12.0	$38.40 \pm 0.034$	0.08	
24.0	$44.09 \pm 0.066$	0.04	

**Table 21** The cytotoxicity of LA ,PRx-LA and cholesterol modified LA-PRx complex to human skin fibroblast.

Concentration ( $\mu\text{M}$ )	% Cell viability		
	LA	LA-PRx	LA-PRx-Cho
0	95.1 $\pm$ 3.0	99.0 $\pm$ 2.3	92.3 $\pm$ 2.3
10	93.0 $\pm$ 5.1	97.2 $\pm$ 2.5	97.2 $\pm$ 4.2
50	90.7 $\pm$ 2.7	98.1 $\pm$ 3.0	97.3 $\pm$ 3.6
100	93.5 $\pm$ 2.3	99.1 $\pm$ 5.8	95.6 $\pm$ 5.0
500	98.8 $\pm$ 5.1	95.5 $\pm$ 1.3	97.2 $\pm$ 5.2
1000	99.0 $\pm$ 1.9	99.3 $\pm$ 3.2	93.1 $\pm$ 3.4

Each value represents the mean  $\pm$  S.D. of the experiments ( $n=3$ ). \*  $P < 0.05$  versus non-treated cells determined by student t-test

**Table 22** The effect of LA, PRx-LA and cholesterol modified LA-PRx to cell growth.

Conc ( $\mu\text{M}$ )	% Cell Growth		
	LA	LA-PRx	LA-PRx-Cho
0	100 $\pm$ 2.0	100 $\pm$ 2.0	100 $\pm$ 2.0
10	330 $\pm$ 2.0	295 $\pm$ 1.0	311 $\pm$ 0.2
50	172 $\pm$ 2.1	246 $\pm$ 1.0	298 $\pm$ 0.7
100	59 $\pm$ 1.4	130 $\pm$ 0.7	77 $\pm$ 0.1
500	145 $\pm$ 2.3	100 $\pm$ 0.9	279 $\pm$ 1.2
1000	60 $\pm$ 1.9	120 $\pm$ 0.5	134 $\pm$ 0.3

Each value represents the mean  $\pm$  S.D. of the experiments ( $n=3$ ).



**Table 23** The percentage of apoptotic H460 cells at 12 h, detected by Hoechst 33342 assay induced by LA and DHLA treatment at various concentration

Treatment ( $\mu\text{M}$ )	%Apoptosis	
	LA	DHLA
0	$2 \pm 1.02$	$2 \pm 0.99^*$
10	$21 \pm 3.04^*$	$13 \pm 1.15^*$
50	$22 \pm 2.58^*$	$15 \pm 1.29^*$
100	$25 \pm 3.15^*$	$16 \pm 1.42^*$

Each value represents the mean  $\pm$  S.D. of the experiments. Asterisks refer significant difference from the control group (non-treated control): \*  $P < 0.05$  versus non-treated H460 cells determined by student t-test ( $n=4$ ).

**Table 24** Caspase activities of H460 cells after treatment with LA or DHLA analyzed by fluorometric assays

Treatment	Caspase activity	
	Caspase 8	Caspase 9
Control	$1.0 \pm 0.2$	$1.0 \pm 0.1$
LA100uM	$1.3 \pm 0.3$	$4.8 \pm 0.3^*$
DHLA 100uM	$1.2 \pm 0.2$	$2.3 \pm 0.2^*$

Each value represents the mean  $\pm$  S.D. of the experiments. Asterisks refer significant difference from the control group (non-treated control): \*  $P < 0.05$  versus non-treated H460 cells determined by student t-test ( $n=4$ ).

**Table 25** The percentage of apoptotic H460 cells at 12 h, detected by Hoechst 33342 assay, cells were treated with LA or DHLA in the presence or absence of caspase-9 inhibitor z-LEHD-FMK (10 $\mu$ M) or pan-caspase inhibitor z-VAD-FMK (10  $\mu$ M).

Treatment	% Apoptosis	
	LA	DHLA
Control	27 $\pm$ 1.02	12 $\pm$ 0.99
zLEHD-FMK	1.8 $\pm$ 0.15 <sup>#</sup>	1.5 $\pm$ 0.18 <sup>#</sup>
zVAD-FMK	1.2 $\pm$ 0.23 <sup>#</sup>	1.0 $\pm$ 0.07 <sup>#</sup>

Each value represents the mean  $\pm$  S.D. of the experiments. Asterisks refer significant difference from the control group (non-treated control): #,  $p < 0.05$  versus treated control H460 cells determined by student t-test ( $n=4$ ).

**Table 26** Effects of antioxidants on LA- and DHLA-induced apoptosis and ROS generation analyzed by Hoechst assay.

Treatment	% Apoptosis	
	LA	DHLA
Control	27 $\pm$ 1.02	12 $\pm$ 0.99
NAC	8 $\pm$ 1.23 <sup>#</sup>	3 $\pm$ 1.18 <sup>#</sup>
Catalase	3 $\pm$ 0.45 <sup>#</sup>	2 $\pm$ 0.98 <sup>#</sup>
MnTBAP	7 $\pm$ 1.15 <sup>#</sup>	3 $\pm$ 1.12 <sup>#</sup>
NaF	11 $\pm$ 1.46 <sup>#</sup>	7 $\pm$ 1.08 <sup>#</sup>

Values are mean  $\pm$ S.D. ( $n = 3$ ), #,  $p < 0.05$  versus treated control.

**Table 27** The relative fluorescence intensity of DCF and DHE over nontreated control at the peak response time of 1 h after treatment of LA or DHLA.

Dose	Relative fluorescence intensity			
	DCF		DHE	
	LA	DHLA	LA	DHLA
0	1.06 ± 0.25	1.03 ± 0.16	1.00 ± 0.02	1.05 ± 0.07
10	3.01 ± 0.11 <sup>*</sup>	1.30 ± 0.32 <sup>*</sup>	8.07 ± 0.25 <sup>*</sup>	3.02 ± 0.18 <sup>*</sup>
50	12.05 ± 0.45 <sup>*</sup>	4.17 ± 0.58 <sup>*</sup>	9.51 ± 0.83 <sup>*</sup>	4.45 ± 1.00 <sup>*</sup>
100	18.10 ± 1.25 <sup>*</sup>	7.50 ± 0.89 <sup>*</sup>	4.04 ± 0.16 <sup>*</sup>	4.21 ± 1.00 <sup>*</sup>

Values are mean ±S.D. ( $n = 3$ ). \*  $p < 0.05$  versus nontreated control

**Table 28** Effects of antioxidants on LA- and DHLA-induced DCF and DHE fluorescence intensities.

Treatment	Relative fluorescence intensity	
	DCF	DHE
Control	0.5 ± 0.02	1 ± 0.03
LA	18 ± 1.08	9.3 ± 0.21 <sup>#</sup>
LA+Catalase	1.5 ± 0.15 <sup>*</sup>	0.9 ± 0.18 <sup>#</sup>
LA+NAC	0.3 ± 0.01 <sup>*</sup>	0.6 ± 0.14 <sup>#</sup>
LA+MnTBAP	20 ± 2.04	0.8 ± 0.11 <sup>#</sup>

Values are mean ±S.D. ( $n = 3$ ). \*  $p < 0.05$  versus nontreated control; #,  $p < 0.05$  versus treated control.

**Table 29** Effects of DPI and ROT on LA-induced apoptosis in H460 cells .

Treatment	% Apoptosis
Control	2 ± 1.02
LA	27 ± 1.02
LA+DPI 0.1 µM	23 ± 2.15
LA+DPI 0.5 µM	17 ± 1.64*
LA +DPI 1.0 µM	15 ± 1.55*
LA + ROT 0.1 µM	5 ± 0.68*
LA + ROT 0.5 µM	3 ± 1.00*
LA + ROT 1.0 µM	1 ± 0.25*

Values are mean ± S.D. ( $n = 3$ ). \*  $p < 0.05$  versus LA-treated control.

**Table 30** Effects of DPI and ROT on LA-induced ROS in H460 cells analyzed by flow cytometric measurements of DHE and DCF fluorescence intensities.

Treatment	Relative fluorescence intensity	
	DCF	DHE
Control	0.5 ± 0.02	1 ± 0.03
LA	18 ± 1.08	9.3 ± 0.21
LA+ ROT	15 ± 0.58 *	0.8 ± 0.21*
LA+ DPI	9.2 ± 1.22	8 ± 1.53*

Values are mean ± S.D. ( $n = 3$ ). \*  $p < 0.05$  versus LA-treated control.

**Table 31** Effects of GPx and SOD overexpression on LA-induced apoptosis in H460 cells analyzed by Hoechst 33342 assays.

Cell type	% Apoptosis	
	Control	LA
Mock Transfection	1.0 ± 0.05	9.5 ± 0.19 *
SOD overexpress	0.9 ± 0.15	1.2 ± 0.23 #
GPx overexpress	0.7 ± 0.08	1.5 ± 0.10 #

Values are mean ± S.D. ( $n = 3$ ). \*  $p < 0.05$  versus nontreated control; #,  $p < 0.05$  versus LA-treated control.

**Table 32** Effects of GPx and SOD overexpression on LA-induced ROS generation in H460 cells analyzed for DCF and DHE fluorescence intensities by flow cytometry at 1 h post-treatment.

Treatment	DCF		DHE	
	Control	LA	Control	LA
Mock Transfection	1.0 ± 0.05	17.0 ± 1.36 *	1.0 ± 0.13	9.5 ± 0.52*
SOD overexpress	0.7 ± 0.18	2.0 ± 0.23	0.9 ± 0.02	0.5 ± 0.05#
GPx overexpress	0.9 ± 0.24	18.4 ± 1.56 #	0.7 ± 0.03	1.1 ± 0.01#

Values are mean ± S.D. ( $n = 3$ ). \*  $p < 0.05$  versus nontreated control; #,  $p < 0.05$  versus LA-treated control.

**Table 33** Bcl-2 overexpression inhibits LA-induced apoptosis in H460 cells determined by Hoechst 33342 assay.

LA ( $\mu\text{M}$ )	% Apoptosis	
	Mock Transfection	Bcl-2 Transfection
0	$2 \pm 0.05$	$2.5 \pm 0.21$
10	$15 \pm 1.28$	$4 \pm 0.15^*$
50	$24 \pm 2.03$	$5 \pm 0.22^*$
100	$27 \pm 3.01$	$5 \pm 1.08^*$

Values are mean  $\pm$  S.D. ( $n = 4$ ). \*  $p < 0.05$  versus mock-transfected controls.

**Table 34** Effect of LA on Bcl-2 expression in H460 cells after treated with LA (100  $\mu\text{M}$ ) for various times and analyzed for Bcl-2 expression by Western blots using anti-Bcl-2 antibody and immunoblot signals were quantified by densitometry.

LA treatment (h)	Relative Bcl-2 Level
0	$1 \pm 0.04$
3	$0.5 \pm 0.01^*$
6	$0.4 \pm 0.02^*$
9	$0.15 \pm 0.01^*$

Values are mean  $\pm$  S.D. ( $n = 4$ ). \*,  $p < 0.05$  versus nontreated control; #,  $p < 0.05$  versus LA-treated control.



**Table 35** Effect of LA on Bcl-2 expression in H460 cells after treated with LA for various doses and analyzed for Bcl-2 expression by Western blots using anti-Bcl-2 antibody and immunoblot signals were quantified by densitometry.

LA treatment ( $\mu\text{M}$ )	Relative Bcl-2 Level
0	$1 \pm 0.04$
10	$0.95 \pm 0.09$
50	$0.1 \pm 0.02^*$
100	$0.11 \pm 0.01^*$

Values are mean  $\pm$  S.D. ( $n = 4$ ). \*,  $p < 0.05$  versus nontreated control.

**Table 36** Effect of LA on Bcl-2 expression of H460 cells in the presence or absence of LAC analyzed for Bcl-2 expression by Western blots using anti-Bcl-2 antibody and immunoblot signals were quantified by densitometry.

Treatment	Relative Bcl-2 Level
Control	$1 \pm 0.04$
LA	$0.37 \pm 0.02^*$
LA+LAC	$1.2 \pm 0.15^\#$

Values are mean  $\pm$  S.D. ( $n = 4$ ). \*,  $p < 0.05$  versus nontreated control; #,  $p < 0.05$  versus LA-treated control.

**Table 37** Effect of antioxidants on Bcl-2 expression in H460 cells analyzed for Bcl-2 expression by Western blotting and determined the relative expression of Bcl-2 by densitometry.

Treatment	Relative Bcl-2 Level
Control	1 ± 0.04
LA	0.37 ± 0.02*
LA + NAC	1.15 ± 0.14 <sup>#</sup>
LA + MnTBAP	0.27 ± 0.06 <sup>#</sup>
LA + Catalase	0.95 ± 0.11 <sup>#</sup>

Values are mean ± S.D. ( $n = 4$ ). \*,  $p < 0.05$  versus nontreated control; #,  $p < 0.05$  versus LA-treated control.

**Table 38** Effect of GPx and SOD overexpression on Bcl-2 expression. in H460 cells analyzed by Western blotting and determined the relative expression of Bcl-2 by densitometry.

Cell type	Relative Bcl-2 Level	
	Control	LA -treatment
Mock transfection	1 ± 0.07	0.37 ± 0.01*
SOD transfection	1.02 ± 0.05	1.06 ± 0.11
GPx transfection	1.01 ± 0.02	0.28 ± 0.03*

Values are mean ± S.D. ( $n = 4$ ). \*,  $p < 0.05$  versus nontreated control.

**Table 39** The protective effect of LA and DHLA to prevent the damage of DNA from cisplatin determined by dHPLC

Time(h)	% Peak Area		
	DD-PT	DD-PT-DHLA	DD-PT-LA
0	100 ± 1.64	100 ± 2.03	100 ± 2.15
0.5	75 ± 1.05	83.33 ± 1.67	50 ± 1.32
1	50 ± 1.12	58.33 ± 1.18	50 ± 1.16
2	41.67 ± 1.13	83.33 ± 1.37	50 ± 1.51
3	41.67 ± 1.54	91.67 ± 2.51	50 ± 1.21
4	33.33 ± 1.41	91.67 ± 1.62	50 ± 2.07
24	33.33 ± 1.23	91.67 ± 1.41	50 ± 1.38

Values are mean ± S.D. ( $n = 3$ )

**Table 40** The protective effect of LA at the different concentration to prevent the damage of DNA from cisplatin analyzed by dHPLC

Time (h)	% DNA double strand					
	DD	D-PT	D-PT-LA10	D-PT-LA20	D-PT-LA30	D-PT-LA40
0.5	100.00± 1.57	68.42± 2.58	67.83± 1.96	69.57± 2.43	73.91± 2.48	76.52± 1.93
1.0	100.00±1.45	63.16± 2.07	52.17±2.13	65.22± 1.54	69.57± 3.02	73.91± 1.48
2.0	100.00±1.36	57.89± 1.98	65.22± 2.11	65.22± 1.91	65.22± 1.05	73.91±2.68
3.0	100.00±2.08	52.63±1.65	60.87± 1.98	60.87± 1.18	60.87± 1.82	60.87±2.59
4.0	98.00± 1.94	52.63 ± 2.16	60.87± 1.12	60.87± 2.55	60.87±2.34	60.87±2.37
24.0	98.00±3.01	52.63± 2.16	60.87± 1.68	60.87± 3.02	60.87±1.71	60.87±1.96

Values are mean ± S.D. ( $n = 3$ )

**Table 41** The protective effect of DHLA at the different concentration to prevent the damage of DNA from cisplatin analyzed by dHPLC

% of DNA double strand						
Time (h)	DD	D-PT	D-PT-DHLA10	D-PT-DHLA20	D-PT-DHLA30	D-PT-DHLA40
0	100.00±1.57	68.42±2.58	100.00±3.08	100.00±2.57	100.00±1.55	100.00±0.06
0.5	100.00±1.45	63.16±2.07	77.78±1.55	91.40±1.28	94.74±1.84	100.00±1.15
1.0	100.00±1.36	57.89±1.98	77.78±2.96	86.02±1.63	89.47±1.51	93.75±0.75
2.0	100.00±2.08	52.63±1.65	66.67±1.17	75.27±1.53	84.21±1.19	87.50±1.32
3.0	98.00±1.94	52.63±2.16	66.67±1.57	75.27±2.07	84.21±2.24	87.50±2.15
4.0	98.00±3.01	52.63±2.16	66.67±2.00	75.27±2.18	78.95±2.30	87.50±2.14
24.0	100.00±1.57	68.42±2.58	66.67±3.19	75.27±1.16	78.95±1.06	87.50±2.29

Values are mean ± S.D. ( $n = 3$ )

**Table 42** The protective effect of LA, LA-PRx complex and cholesterol modified LA-PRx complex to prevent the damage of DNA from cisplatin analyzed by dHPLC

%DNA				
Time (h)	Cisplatin	LA	LA-PRx	Chol-LA-PRx
0	100.0±5.0	100.0±3.2	100.0±4.2	100.0±1.7
0.5	65.3±2.4	78.3±2.5	80.0±3.1	85.7±2.3
1.0	60.8±2.7	75.6±1.9	75.5±2.8	80.4±1.5
2	55.9±3.1	70.3±2.0	75.1±2.4	75.5±2.0
3	50.4±1.5	70.1±1.6	70.2±1.3	70.4±0.8
4	50.0±1.8	70.0±2.0	70.0±1.7	70.1±0.5
24	50.0±1.3	70.0±1.1	70.0±0.5	70.0±1

Values are mean ± S.D. ( $n = 3$ )



**APPENDIX C**

**WESTERN BLOT RESULTS AND MASS SPECTRUMS**

สถาบันวิทยบริการ  
จุฬาลงกรณ์มหาวิทยาลัย



**Figure 45** GPx and SOD overexpression of H460 cells. H460 cells were stably transfected with GPx, SOD, or control pcDNA3 plasmid as described under *Materials and Methods*. Cell extracts were prepared and separated on 10% polyacrylamide-SDS gels, transferred, and probed with GPx or SOD antibody.  $\beta$ -actin was used as a loading control.

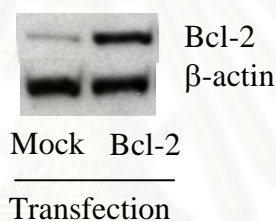


**Figure 46** Bcl-2 overexpression of H460 cells. H460 cells were stably transfected with Bcl-2 or control pcDNA3 plasmid as described under *Materials and Methods*. Cell extracts were prepared and separated on a 10% polyacrylamide-SDS gel, transferred, and probed with Bcl-2 antibody. Blots were reprobed with  $\beta$ -actin antibody to confirm equal loading of samples.



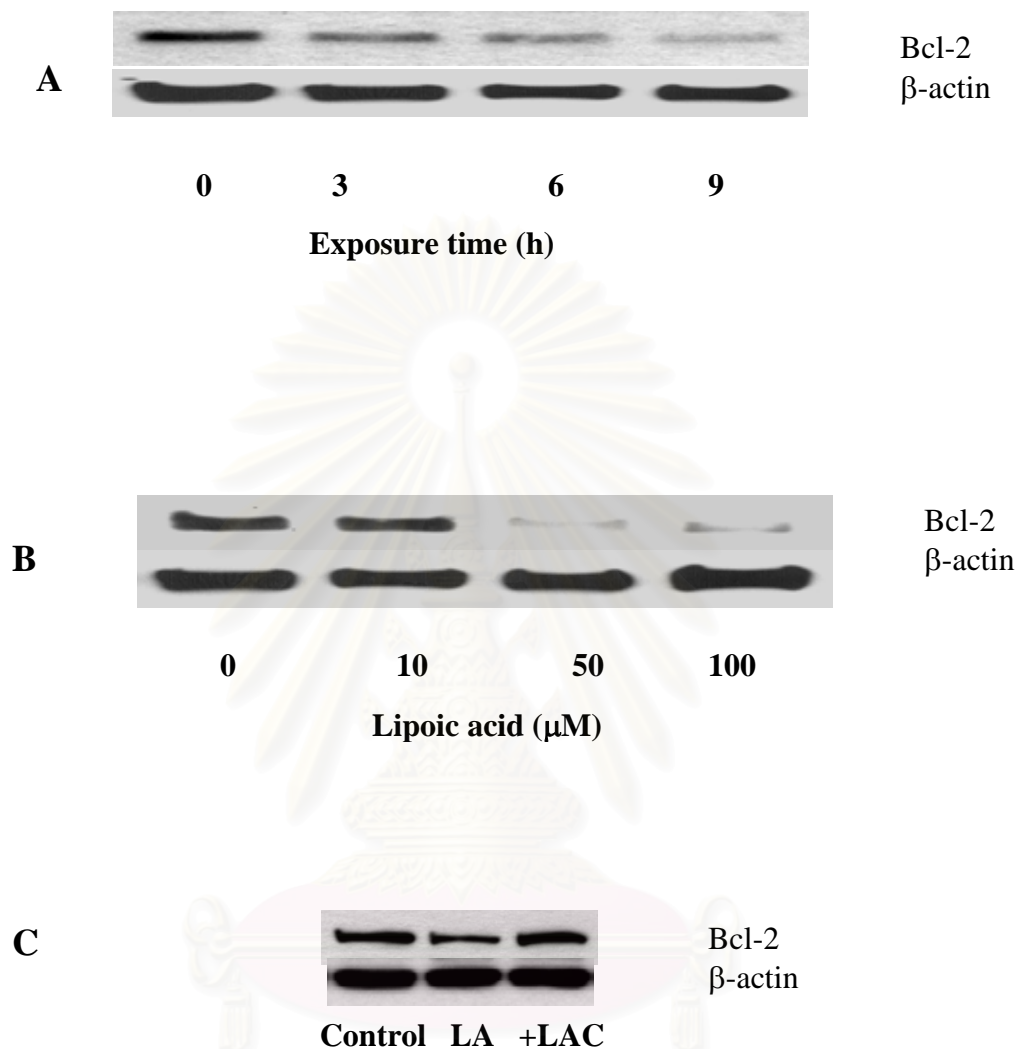


**Figure 47** Effect of LA on Bcl-2 expression. A, H460 cells were treated with LA (100 μM) for various times and analyzed for Bcl-2 expression by Western blots using anti-Bcl-2 antibody. B, Dose effect of LA (0-100 μM) on Bcl-2 expression determined at 9 h post-treatment. C, Effect of proteasome inhibitor on LA-induced Bcl-2 downregulation. Cells were treated LA (100 μM) in the presence or absence of lactacystin (LAC) (10 μM) and Bcl-2 expression was determined.

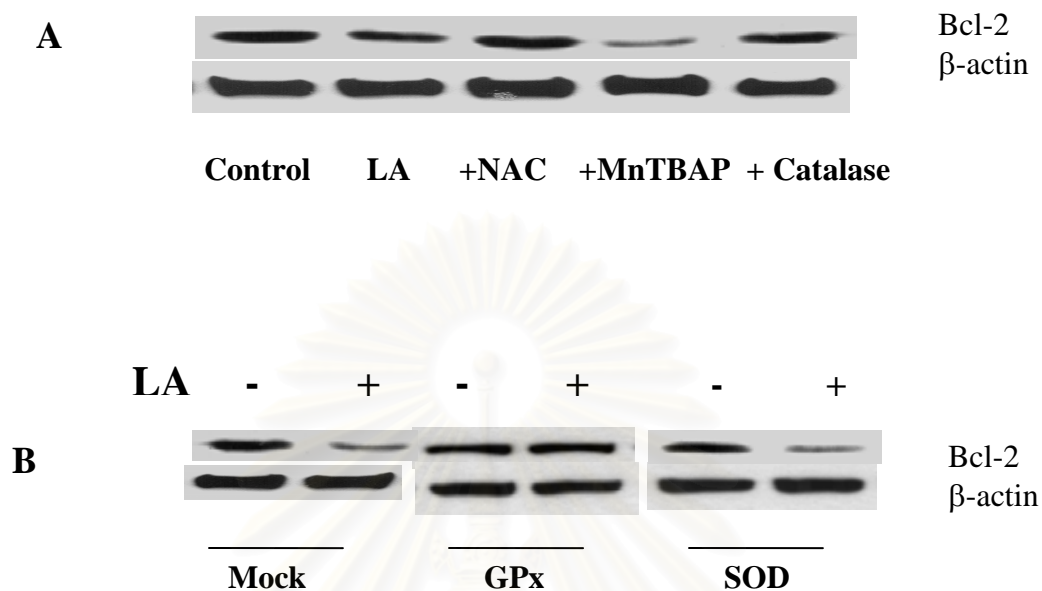


**Figure 48** Effect of antioxidants on Bcl-2 expression. A, H460 cells were either left untreated or pretreated with NAC (100  $\mu$ M), catalase (1,000 U/ml), or MnTBAP (100  $\mu$ M) for 1 h, followed by LA treatment (100  $\mu$ M) for 9 h. Cell lysates were then prepared and analyzed for Bcl-2 expression by Western blotting. B, GPx, SOD, or mock transfected cells were treated with LA (100  $\mu$ M) for 9 h and Bcl-2 expression was similarly determined. Blots were reprobbed with  $\beta$ -actin antibody to confirm equal loading of samples.

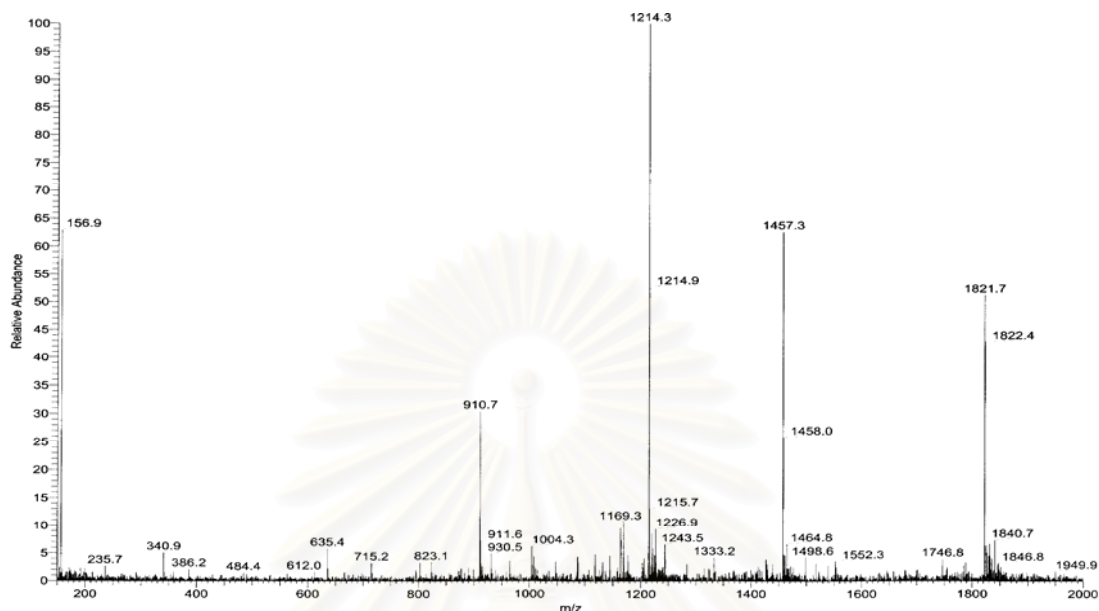


**Figure 49** The mass spectra of dsDNA (Dickerson dodecamer). The ions were found at m/z 910.7, 1214.3, 1457.3 and 1821.7 for charge -8, -3/-6, -5, and -2/-4 in the order.

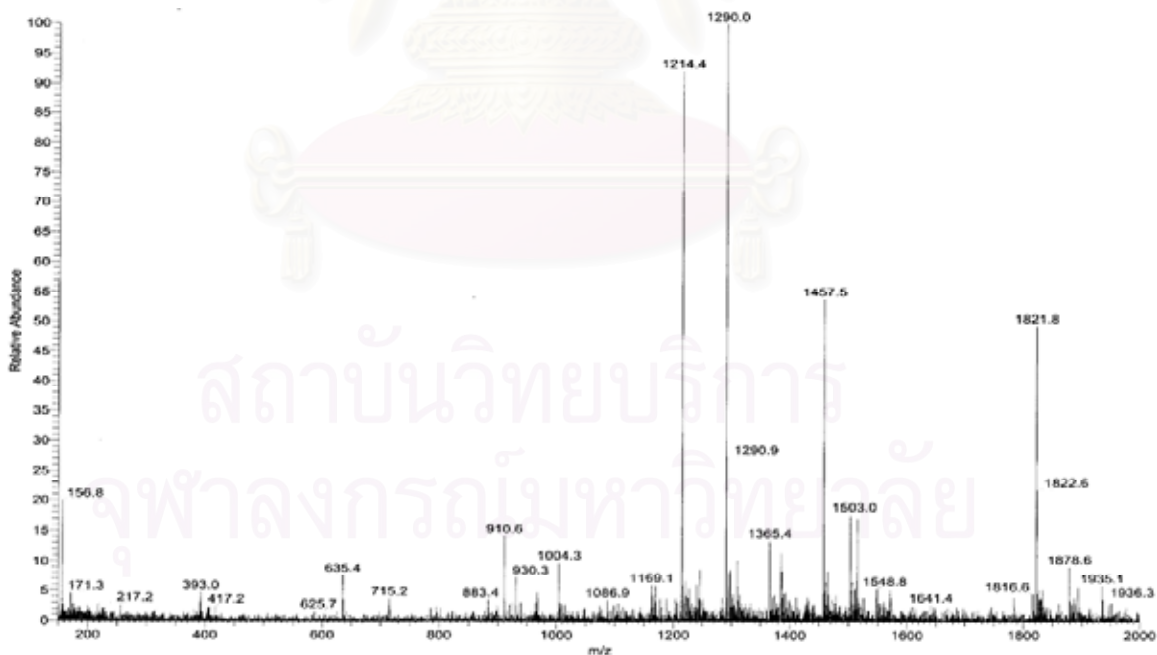
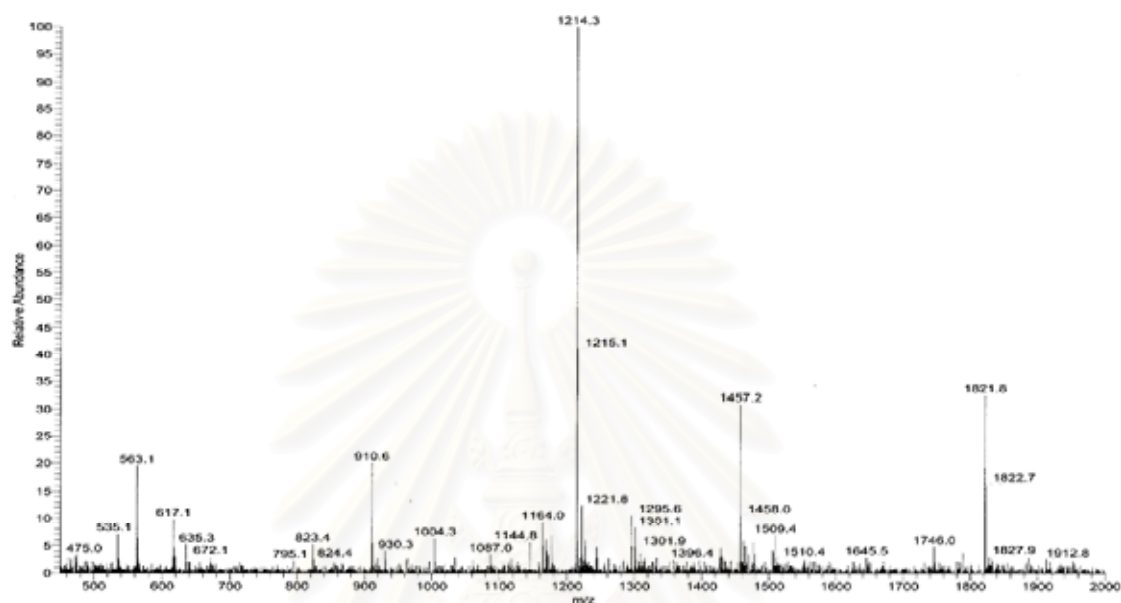


**Figure 50** MS spectra of ds DNA-platinum adducts DNA-platinum adducts were found at m/z 1290, 1365.4, 1503, 1548.8, 1936.3.

A



B

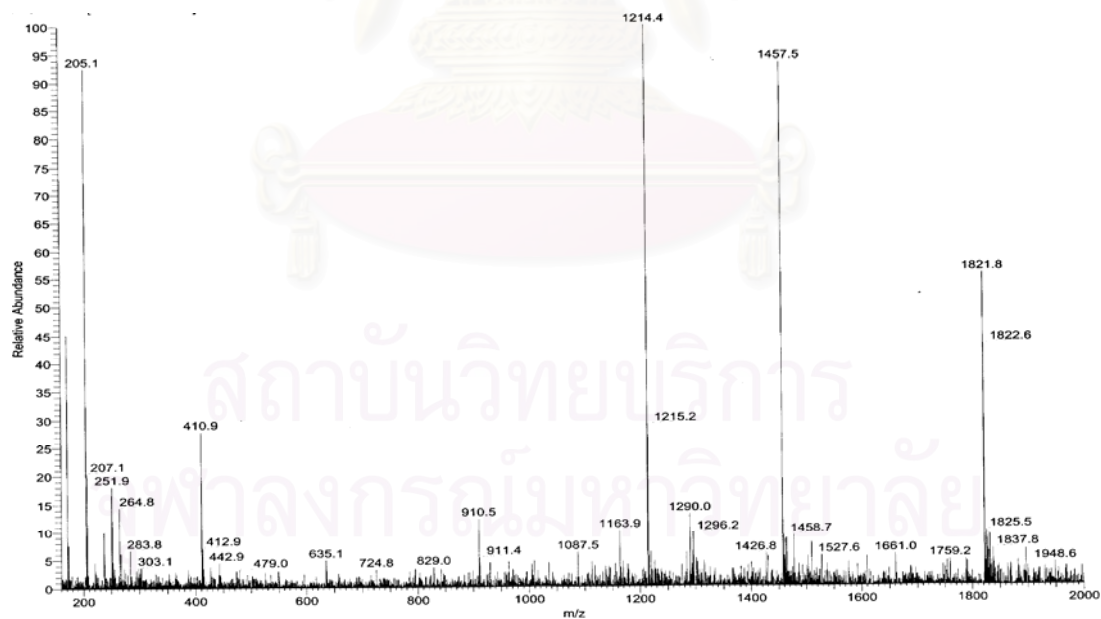


**Figure 51** Mass spectra of dsDNA and adducts of system containing dsDNA, cisplatin and LA (A) or DHLA (B) after incubated at 37 °C for 24 h.

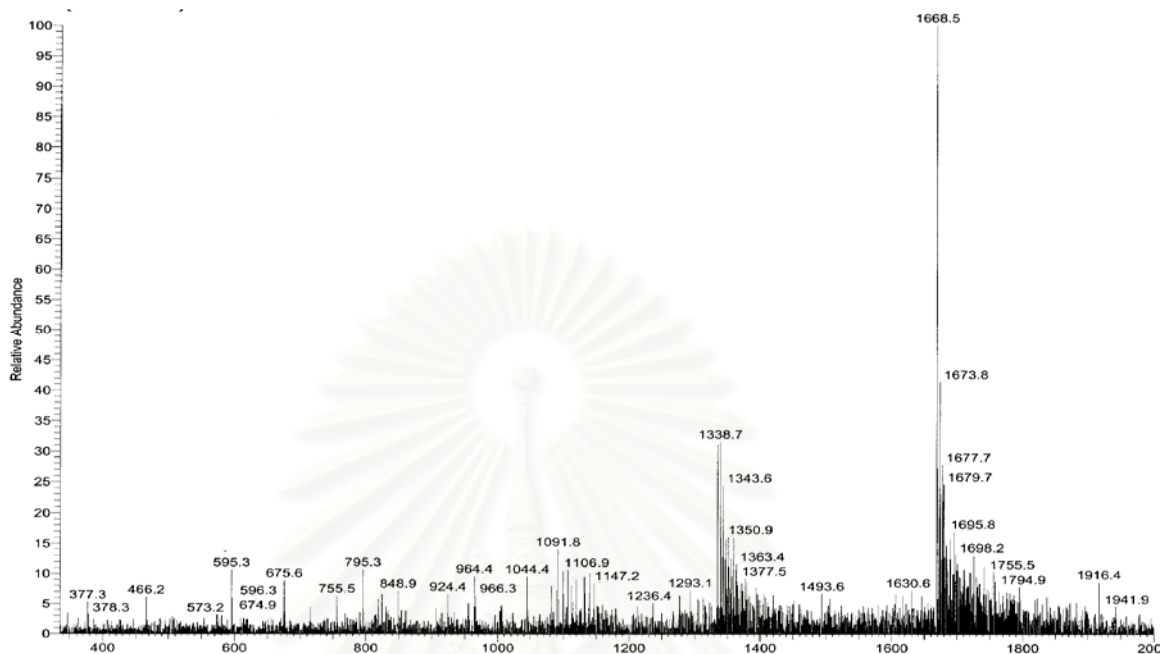


**Figure 52** Mass spectra of duplex undecamer DNA MW 6678 recorded at  $m/z$  1668.5 and 1336.7 for  $-4$  and  $-5$  ion .

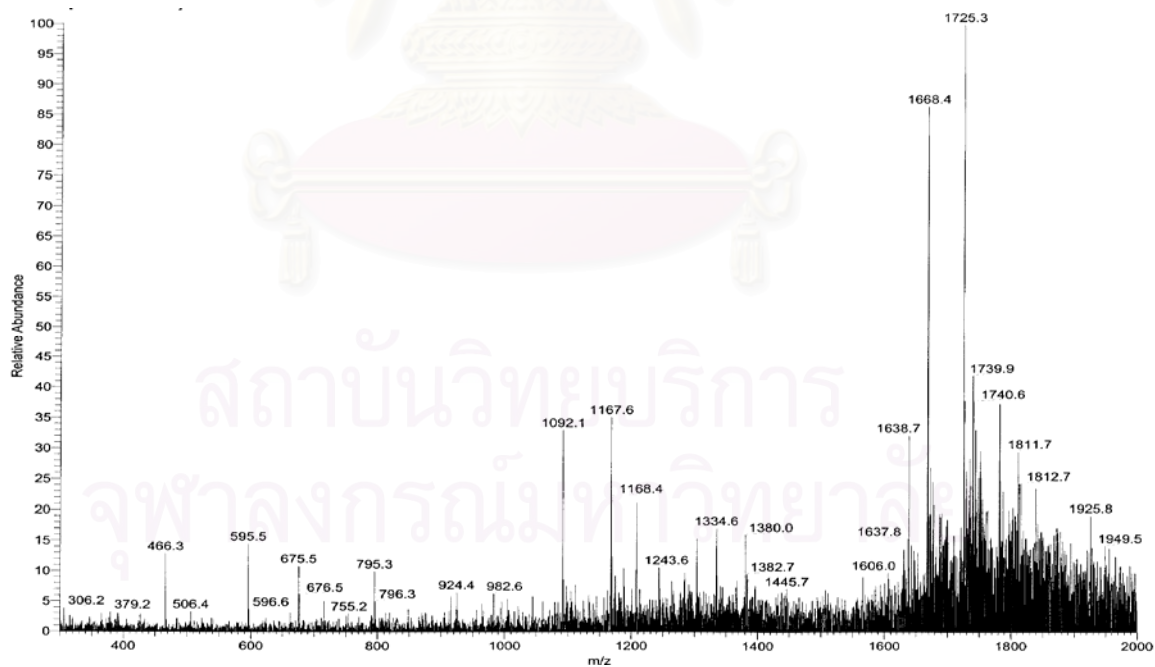


**Figure 53** Mass spectra of duplex undecamer DNA-platinum adduct. After adding cisplatin, the DNA-platinum adduct's ion was recorded. The  $ms/ms$  spectra of 1740 and 1725 ion.

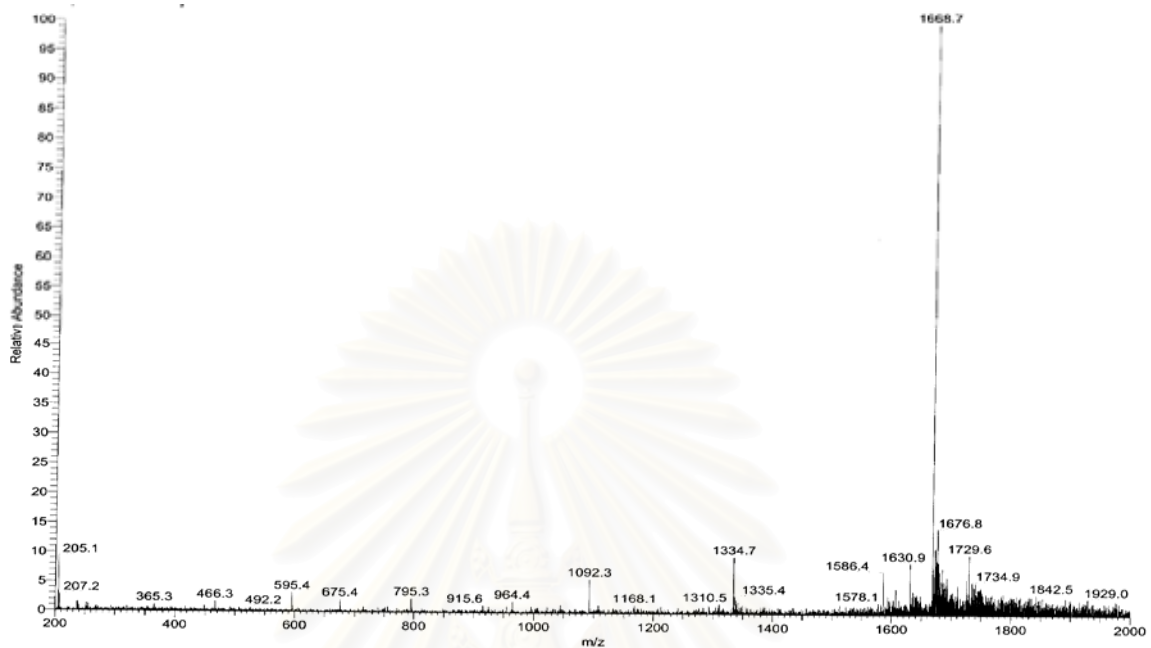


**Figure 54** Full scan mass spectra of undecamer DNA showed the DNA-adduct formation protection efficacy of LA.

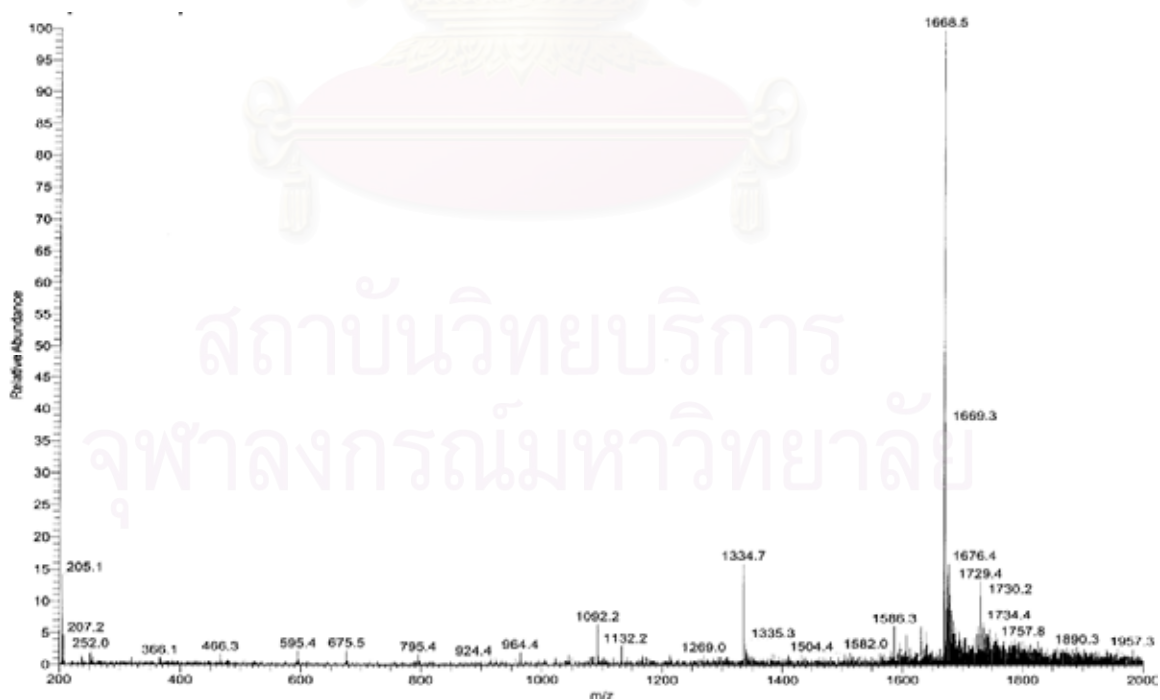


**Figure 55** Full scan mass spectra of undecamer DNA showed the DNA-adduct formation protection efficacy of DHLA.



## Vita

Ms. Jirapan Mounjaroen was born on July 22, 1976 in Nonthaburi. She received her B.Sc. in Pharmacy (2<sup>nd</sup> honor) from the Faculty of Pharmacy, Mahidol University in 1998. After graduated she worked as a research and development manager in Namsiang Trading company for 3 years.



สถาบันวิทยบริการ  
จุฬาลงกรณ์มหาวิทยาลัย